

DEVELOPMENT OF POST-TRAUMATIC OSTEOARTHRITIS MODELS
TO EVALUATE EFFECTS OF IMPACT INJURY ON JOINT HEALTH
FOR CLINICAL DISEASE TREATMENT AND PREVENTION

A Dissertation presented to
the Faculty of the Graduate School
at the University of Missouri - Columbia

In Partial Fulfillment
of the Requirements for the Degree

Doctor of Philosophy

by

NICOLE POYTHRESS WATERS

Dr. James L. Cook, Dissertation Supervisor

DECEMBER 2013

The Undersigned, appointed by the Dean of the Graduate School, have examined the dissertation entitled

DEVELOPMENT OF POST-TRAUMATIC OSTEOARTHRITIS MODELS
TO EVALUATE THE EFFECTS OF IMPACT INJURY ON JOINT HEALTH
FOR CLINICAL DISEASE TREATMENT AND PREVENTION

Presented by Nicole Poythress Waters,

A candidate for the degree of Doctor of Philosophy

And hereby certify that, in their opinion, it is worthy of acceptance.

Dr. James Cook

Dr. Aaron Stoker

Dr. Ferris Pfeiffer

Dr. Keiichi Kuroki

Dr. Derek Fox

Dr. Clark Hung

DEDICATION

For my loving parents, Roger and Bonnie, and many others who suffer from osteoarthritis. Before the age of 50, my parents underwent total hip replacement surgery so I have witnessed how significant osteoarthritis research is for improving the quality of life for those afflicted by this disease. I thank my parents and -in-laws for supporting me throughout life and encouraging me to always do my best.

For my loving husband, Cody, who encourages me to be all that I can be, and does everything in his power to make this happen. Thank you so much for understanding my passion for orthopaedic research. I realize it has been very difficult at times, but I greatly appreciate your steadfast love, patience, kindness, and limitless strength. You are my life!

For my loving children, Tommy and Cole. Although we wish that our children will always be healthy, I hope that the work I do today and in the future will somehow help my children, my siblings' children, and other children in the world that are at-risk for developing osteoarthritis.

With God all things are possible, and I truly believe with His guidance we will someday be able to help the lame walk again.

ACKNOWLEDGEMENTS

I feel very blessed that I have had the opportunity to conduct this multidisciplinary research and have many people to thank for it; Dr. Jimi Cook, for reading the initial e-mail I sent from Smith & Nephew Orthopaedics inquiring about graduate research opportunities in the MU Comparative Orthopaedic Laboratory (COL). You could have easily deleted that e-mail, but I appreciate you taking the time to give me a chance. Thank you again for all the research autonomy and support that you have provided. I hope I have been able to contribute to the COL team through this work; Dr. Aaron Stoker, for all the hours he spent training me in the biologics lab; Drs. Ferris Pfeiffer, Keiichi Kuroki, Derek Fox, and Clark Hung for their help and advice; Dr. Bill Carson for all the hours he spent training me in the biomechanics lab; Mr. Logan Stockman for his help fabricating and validating the final impactor in this dissertation; Ms. Mary Romesburg for all the technical assistance and Ms. Linda Salmon for the emotional support these ladies provided in the lab. You guys made this journey achievable for me and I greatly appreciate it.

TABLE OF CONTENTS

ACKNOWLEDGEMENTS	ii
LIST OF FIGURES	iii
LIST OF TABLES	vii
ABSTRACT	ix
Chapter	
1. Introduction.....	1
2. Literature review	15
3. Optimization of an in vitro mechanical injury device	65
4. Biomarkers affected by impact velocity and maximum strain during cartilage injury	84
5. Biomarkers affected by impact severity during osteochondral injury	111
6. Biomarkers affected by osteochondral impact with post-injury loading	137
7. Biomarkers affected by humeral head impact injury	154
8. Development of an impactor to deliver impact injury for pre-clinical models of osteoarthritis.....	161
CONCLUSION.....	177
APPENDIX.....	179
VITA.....	194

LIST OF FIGURES

Figure	Page
1-1. Comparison of healthy and osteoarthritic knee joints	6
1-2. Factors involved in the development of post-traumatic arthritis after injury	7
1-3. Moderate physical activity prevents injury and fosters optimal healing	8
2-1. Views of a diarthroidal joint.	39
2-2. Ultrastructure of articular cartilage.....	40
2-3. Unconfined, confined, and indentation test set-up.	41
2-4. Molecular factors involved in osteoarthritis	42
2-5. Signaling cascades activated following a single impact load, leading to apoptosis-like cell death. RyR = ryanodine receptor, CaMKII = calcium/calmodulin-regulated kinase II.....	43
2-6. Proposed signal transduction pathway that leads to the induction of COX-2, mPGES-1 and 15-PGDH by compressive stress in cartilage.....	44
2-7. A model of Toll-like Receptor (a) and complement activation (b) in the joint leading to synovitis and potentiation of cartilage erosion in OA.....	45
2-8. Molecular cross-talk at the osteochondral junction. A vascular channel is shown breaching from the subchondral bone (SCB), through the calcified cartilage (CC) into the non-calcified cartilage (NCC).....	46
2-9. Immediate cellular responses within 14 days after acute joint trauma	47
2-10. Cell membrane phospholipids pathway involving PGE2.....	48
2-11. Instron 8821s servo-hydraulic testing machine in the biomechanics lab of the Comparative Orthopaedic Laboratory (COL).....	49

3-1. Custom designed stainless steel fixtures used to measure thickness and deliver impact load to ex vivo cartilage explants.....	73
3-2. Impact parameter terminology and actual response generated using given parameter values for Instron computer software program and PID values 40, 0, 0.	74
3-3. 100 mm/sec set velocity v1 no load impact ram displacement.....	75
3-4. 50 mm/sec set velocity v1 no load impact ram displacement.....	76
3-5. 25 mm/sec set velocity v1 no load impact ram displacement.....	77
3-6. 10 mm/sec set velocity v1 no load impact ram displacement.....	78
3-7. 1 mm/sec set velocity v1 no load impact ram displacement.....	79
3-8. Visual representation of relationship between absolute ram position AP and ram displacement P	80
3-9. Indicated force, F, from impacting to 50% ϵ	81
3-10. Ram displacement from impacting rubber to 50% ϵ	82
4-1. Test cell configuration and non-porous stainless steel fixtures	97
4-2. Effect of impact velocity and maximum strain on cell viability at day 0 and 12	98
4-3. Effect of impact velocity and maximum strain on glycosaminoglycan (A) and Prostaglandin E2 (B) released from the articular cartilage explant post-injury into the culture media.....	99
4-4. Thickness of cartilage explants at day 0 (pre-injury), and the effect of impact velocity and maximum strain on cartilage thickness at days 6 and 12 (post-injury).	100
5-1. Custom made stainless steel fixtures consisting of the impactor ($\phi = 3.9\text{mm}$) attached to test machine ram (A), well ($\phi = 6.01\text{mm}$) (B), and base fixture (C) attached to test machine table used to measure the thickness and deliver impact injury of an osteochondral explant ($\phi = 6\text{mm}$, thickness= $3.6\pm 0.29\text{mm}$) (D).	124

5-2. Energy absorbed by integrating the area under the force-displacement curve during 100mm/sec impact resulting in max compression of 0.25mm (Low), 0.5mm (Low-Mod), 0.75mm (Moderate), 1mm (Mod-High), or 1.25mm(High) of the osteochondral explant.	125
5-3. Representative fluorescent images of live (green) and dead (red) cells within cartilage of osteochondral explants from Control – no impact (A), Low Impact – 0.25mm max compression (B), Moderate Impact – 0.75mm max compression (C), and High Impact – 1.25mm max compression groups after impact on day 0 and day 12 after culture (D).....	126
5-4. Prostaglandin E2 (PGE2) released by the osteochondral explants into the media.	127
6-1. Harvest of osteochondral explants using a 6mm-diameter coring reamer and jig to stabilize humeral head (A). Trimming of bone using a diamond blade saw to ~3.6mm total thickness of explant (B). Delivery of impact ($v = 100\text{mm/sec}$) injury using a 3.9mm-diameter impactor attached to ram of test machine (C). Dynamic compressive loading ($P=1\text{MPa}$, $f=1\text{Hz}$, $d=30\text{min}$, 3x/day for 7 days) of explants in four, 6-well plates using a bioreactor device (D).....	146
6-2. Representative images of fluorescent live (green) and dead (red) cells from test groups after 7 days of culture (A). Total percent cell viability (live/total cells x 100) and area percent cell viability (live area/total area x 100) of chondrocytes within explants after 7 days of culture (B).....	147
6-3. Prostaglandin E ₂ , PGE ₂ , (A) and Glycosaminoglycan, GAG, (B) release from osteochondral explants into culture media. Groups within each time point sharing a letter are significantly different ($p<0.05$).	148
7-1. Custom-made impactor used to deliver impact injury on humeral head.	157
7-2. Gross observation using india ink staining of humeral heads at Day 0 and Day 12 post-injury.	158
7-3. Cartilage analysis: A) Glycosaminoglycan (GAG), B) Hydroxyproline (HP), C) DNA content.	159
7-4. Media analysis: A) Glycosaminoglycan (GAG), B) Prostaglandin E2 (PGE2), C) Nitric oxide (NO) released into culture media from humeral head during 12 days of culture.	160

8-1. Arthroscopic impactor.	166
8-2. Pendulum device.	167
8-3. Impactor calibration.	168
8-4. Impactor placed upon the lateral femoral condyle prior to impact.	169
8-5. Maximum stress applied from 5, 10, 15, and 20 turns of the impactor.	170
8-6. India ink staining of cadaveric rabbit femoral condyles.	171

LIST OF TABLES

Table	Page
1-1. Types of physical activity based on intensity, velocity, and duration of loading. ...	9
2-1. Biologic processes and mediators responsible for joint tissue destruction in osteoarthritis and potential therapeutic interventions.....	50
2-2. Reported roles of prostaglandin E2 (PGE2) on cartilage and bone.	51
2-3. Work by others studying the effect of impact load conditions on cartilage.....	52
3-1. Effect of set impact velocity v_1 on observed impact velocity v_1 and overshoot T_o	83
4-1. Summary of investigations into effect of impact magnitude and/or rate on tissue parameters and constituents released to culture media.	101
4-2. Study 1 and study 2 test groups and protocols.....	101
4-3. Illustration of 25 kN test machine capabilities-results	104
4-4. Summary of tissue biomarker results at day 12 (mean \pm standard deviation). ...	105
5-1. Biomechanical properties during day 0 testing of osteochondral explants.	128
5-2. Cell viability of chondrocytes within osteochondral explants.	129
5-3. Cartilage double-stranded DNA, glycosaminoglycan (GAG), and hydroxyproline (HP) concentration of osteochondral explants.	130
5-4. Biomarkers released by osteochondral explants into the media.....	131
6-1. Biomarkers released by osteochondral explants into the media.....	149
8-1. Calibration results from 5, 10, 15, and 20 turns of the impactor striking the weight at the end of the pendulum device.....	172
8-2. Comparison of impactor devices used with various animal species, impact location, impactor type, and calibration developed for pre-clinical OA models.	173

8-2 (continued). Comparison of impactor devices used at various time points, outcome measures, and results for pre-clinical OA models.....	174
8-2 (continued). Comparison of advantages and disadvantages of impactor devices for pre-clinical OA models.	175

DEVELOPMENT OF POST-TRAUMATIC OSTEOARTHRITIS MODELS
TO EVALUATE THE EFFECTS OF IMPACT INJURY ON JOINT HEALTH
FOR CLINICAL DISEASE TREATMENT AND PREVENTION

Nicole Poythress Waters

Dr. James Cook, Dissertation Supervisor

ABSTRACT

Osteoarthritis is one of the most common, debilitating, musculoskeletal diseases in the world. Currently, there is no cure. It is well-known that a traumatic, joint injury increases the risk of developing post-traumatic osteoarthritis (PTOA). Therefore, in order to improve clinical treatment and prevention strategies for post-traumatic osteoarthritis (PTOA), a series of translational studies were conducted to develop research models to evaluate the effects of impact injury.

The first section of this dissertation (Ch. 1-2) provides a comprehensive introduction and literature review related to both clinical PTOA as well as previous research investigations of PTOA. The second section of this dissertation (Ch. 3-6) describes the methodology of optimizing a servo-hydraulic test machine to deliver a controlled impact injury (Ch. 3) as well as subsequent studies using this device to injure articular cartilage (Ch. 4) and cartilage-bone explants (Ch. 5-6). Further, the effects of dynamic, compressive loading to mimic walking after impact injury of cartilage-bone explants was

investigated (Ch. 6). The third section of this dissertation (Ch. 7-8) details the development of an impactor device that may be used for pre-clinical, animal models.

Many significant findings were discovered through this dissertation work. Specifically, by using the proportional-integral-derivative (40, 0, 0) values, a large (25kN) servo-hydraulic test machine may be used to deliver a controlled impact injury to explants (Ch. 3). Biomarkers glycosaminoglycan (GAG) and prostaglandin E₂ (PGE₂) were elevated after cartilage impact injury with PGE₂ having the highest mechanosensitivity than any other biomarker (Ch. 4). Energy absorbed during cartilage-bone injury is dependent upon trauma severity; PGE₂ and monocyte attractant protein (MCP-1) were elevated following cartilage-bone injury (Ch. 5). Dynamic, compressive loading retained cell viability in non-impacted cartilage-bone explants and mitigated GAG release in impacted explants; GAG and PGE₂ were elevated due to cartilage-bone injury whereas matrix metalloproteinase-2 (MMP-2) and interleukin-8 (IL-8) were elevated due to injury plus dynamic, compressive loading (Ch. 6). The development of a 8mm diameter impactor does create articular cartilage damage (Ch. 7), albeit a smaller, 2mm diameter impactor creates higher impact stresses and may be used arthroscopically for pre-clinical animal models (Ch. 8).

CHAPTER 1

INTRODUCTION

Osteoarthritis: An Epidemic Joint Disease

Osteoarthritis (OA) is a debilitating disease that affects musculoskeletal joints (Fig. 1-1) which is anticipated to affect 59 million Americans by 2020.¹ A classic hallmark of OA is cartilage degradation; however, hypertrophy and spurring of bone (osteophyte formation), and synovitis are additional features of late-stage OA. These joint conditions cause pain and stiffness in the affected joint, leading to decreases in range of motion as well as overall mobility. Ultimately, this disease endangers people's quality of life.

A common treatment for late-stage OA is total joint replacement. There are major risks involved with this surgery including implant loosening and/or infection which may lead to implant failure requiring revisional surgery.² The intense rehabilitation process after total joint replacement surgery may be physically painful, and/or psychologically taxing for the individual.³ Currently, there is no cure for OA or disease modifying osteoarthritis drugs available. Thus, a better understanding of what causes this disastrous disease is warranted and the impetus for this dissertation work.

Post-Traumatic Osteoarthritis (PTOA): Are Physically-Active Children At-Risk?

As the last few seconds of the high school championship basketball game dwindle, the recently-signed NCAA recruit sprints towards the goal after stealing the ball. She has an uncanny sense that a defender is right behind her as she approaches the basket. Making a nanosecond decision to alter her right-handed layup, she abruptly stops hard—with a little too much knee extension and internal rotation—and hears a loud POP and

immediately collapses underneath the goal. A swirl of thoughts pass through her mind: Did my shot go in the basket? Did we win? Quickly followed by a swarm of emotions: Help me! My knee feels like it's crushed! Please make the pain go away. Will I still be able to play ball in college?

Immediately, the coach, trainer, and player's parents rush onto the court to help her cope with the injury. Within a day or so, the player is examined by a physician and imaging may be used to confirm the diagnosis of an anterior cruciate ligament (ACL) injury. Most likely, there is also additional articular cartilage injury. Depending on the severity of these injuries, an appropriate treatment strategy will be implemented. Nevertheless, for this girl, the risk of developing post-traumatic osteoarthritis (PTOA) has significantly increased.

It has been well-established that people who sustain ligament and meniscal injuries have a 10-fold⁴ increase risk for PTOA whereas articular fractures of the hip, knee, and ankle increase the risk of OA to 25%,⁵ 23-44%,⁶ and >50%,⁷ respectively resulting in a >20-fold risk for most articular fractures⁸ as compared to non-injured joints. Injury severity has been suggested to increase the risk for PTOA since the outcomes of intraarticular fractures are relatively poor.⁹ Similarly, joint malalignment, incongruity, and instability can increase the risk of PTOA.¹⁰ Also, another risk factor is chronic repetitive loading, or polytrauma as indicated in Fig. 1-2.⁸ For example, among all OA cases, hip (1.6%), knee (9.8%), and ankle (79.5%) had a verified history of one or more joint injuries.¹¹ Similarly, additional loading due to high body mass index or physically-demanding activities increases the risk of PTOA.¹²⁻¹⁴

Although many joint injuries occur in young adults (age<50), older adults may have an increased risk of developing OA after joint injury. For example, patients 50+ years old have a 2-4 fold greater risk of developing OA due to knee intraarticular fractures than younger patients.¹⁵⁻¹⁷ This aging trend is similar for ankle intraarticular fractures¹⁸ as well as ligament injuries.¹⁹

Lastly, genetic mutations in syndecan-4,²⁰ runt-related transcription factor 2 (Runx2),²¹ Aggrecan cleavage by a disintegrin and metalloproteinase with a thrombospondin type 1 motif, member 5 (ADAMTS5),^{20,22} matrix metalloproteinase (MMP13),²³ Hedgehog activation,²⁴ CCAAT/enhancer-binding protein (C/EBP β),²⁵ ADAMTS-mediated cleavage of aggrecan²⁶ have been shown to be involved in mouse models of PTOA.

Although there have been great advancements in ACL reconstructive surgery and rehabilitation programs there is still a high chance that cartilage degradation resulting in PTOA after a common ACL injury will occur. With increased participation in athletics, we must increase our efforts in providing better treatments for PTOA otherwise these numbers will subsequently increase. Specifically, we must develop early treatments after injury to prevent further cell death, suppress catabolic mediators, and boost anabolic processes. With the average age of ACL injury for American females being 16 years old, how do we improve current medical practices in order to prevent OA from developing as these children mature throughout life?

Ideally, optimal joint health will mitigate the risk of developing PTOA. The modifiable ways of improving joint health rely on diet and exercise. For instance, moderate physical activity will condition the joint to be less susceptible to sudden injury

as well as promote healing in the recovery/rehabilitation phase as indicated in Fig. 1-3. In contrast, high excessive loading and low minimal loading will be detrimental for prevention and/or rehabilitation from joint injury.

What constitutes high, moderate, or low loading? Is it possible to design an ideal loading or exercise program that is patient-specific? One approach for this would be to consider exercise as a specific “mechanical loading” activity that has a definable intensity, frequency/velocity, and duration.

Cartilage responds (anabolically/catabolically) to internal forces. Since internal forces are influenced by external joint moments, then it may be possible to promote cartilage health by optimizing joint moments during physical activity. The largest external moments tend to flex the joint, thus a comparison of maximum flexion moments or the magnitude of loading ($I = \% \text{ body weight} \times \text{height}$) at the hip, knee, and ankle joint during common activities have been summarized in Table 1-1.

The majority of musculoskeletal injuries do not require surgery. Also, the majority of people who suffer a traumatic, joint injury will not develop post-traumatic osteoarthritis OA. However, it is still unknown what causes and perpetuates OA. By the year 2020, the Centers of Disease Control estimates that there will be a larger increase in new cases of arthritis than any other disease in the United States. It is crucial that we closely evaluate through translational research ways of diagnosing, treating, and preventing OA.

Translational PTOA Research to Improve Evidence-Based Medicine

As later discussed, the amount of cartilage damaged during injury is dependent on the rate and magnitude of impact loads²⁷⁻³⁰ and may elicit immediate cell (chondrocyte) death^{27,29-38} breakdown of cell membrane phospholipids into arachidonic acid ultimately

resulting in inflammation³⁹ and physical disruption of the extracellular matrix (ECM) of the cartilage.^{27,28,36,38,40-47} Destruction of the ECM correlates to glycosaminoglycan (GAG) release^{31,37,43,48-53} from the tissue consequently leading to increases in tissue water content (swelling).^{35,45} Delayed pathologic effects of mechanical injury to articular cartilage include additional cell death and decreased tissue mechanical stiffness.³² In order to further elucidate the effects of impact injury on joint health and develop an optimal post-traumatic osteoarthritis model, a series of studies was conducted in this dissertation. Hopefully, this work will enable a greater understanding of the mechanisms following joint injury that may be translated for clinical treatment or prevention of osteoarthritis.

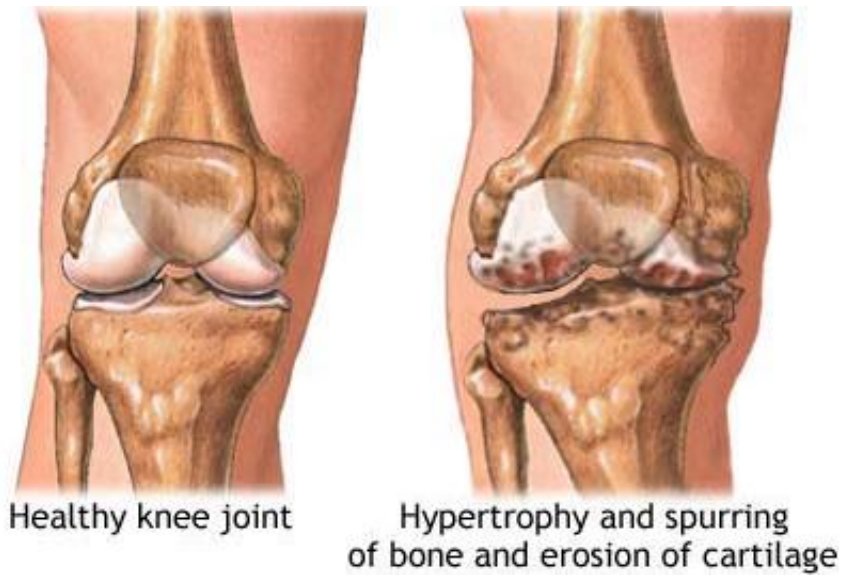


Figure 1-1. Comparison of healthy and osteoarthritic knee joints
(<http://www.nlm.nih.gov/medlineplus/ency/imagepages/17103.htm>)

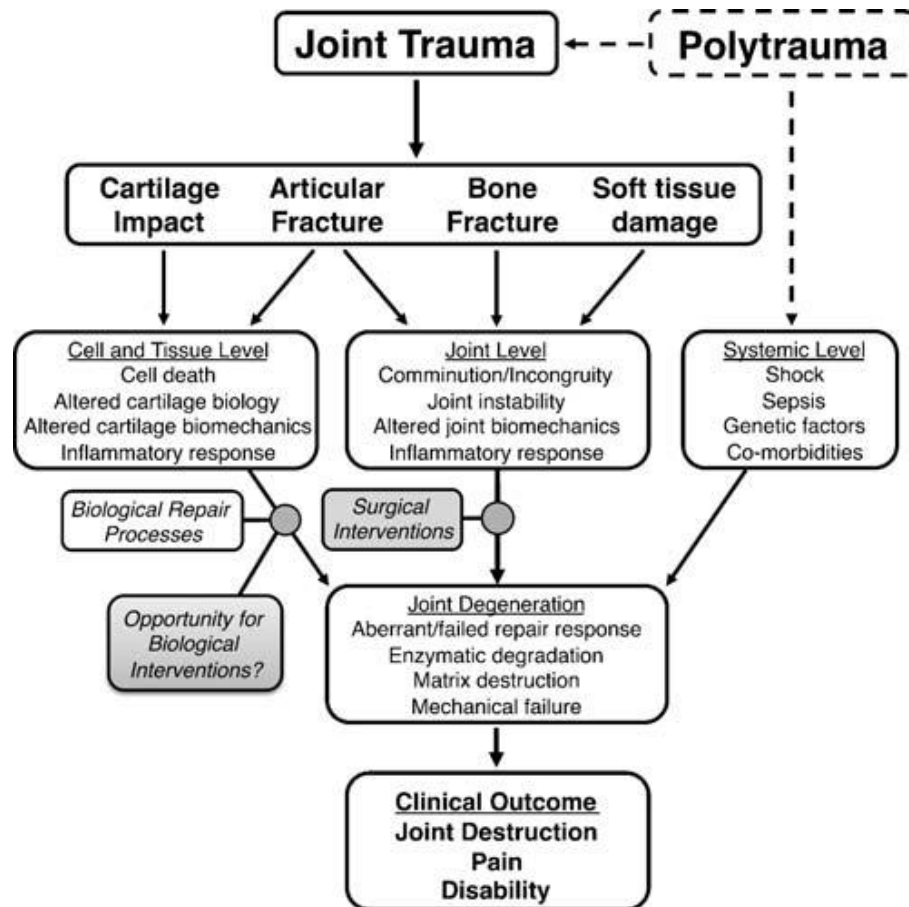


Figure 1-2. Factors involved in the development of post-traumatic arthritis after injury.⁸

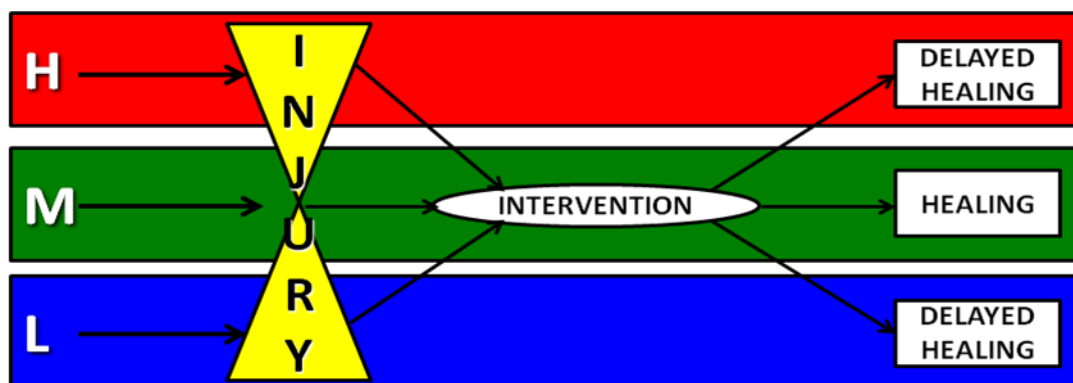


Figure 1-3. Moderate physical activity prevents injury and fosters optimal healing. In contrast, too high or too low physical activity increases risk of injury, delays healing, and potentially increases risk of post-traumatic osteoarthritis.

Table 1-1. Types of physical activity based on intensity, velocity, and duration of loading.

Table 1a. HIGH activity with excessive loading for lower extremity joints									
Type of Physical Activity	Hip			Knee			Ankle		
	I	V	D	I	V	D	I	V	D
WALKING	12% ⁵⁴	1.5 ⁵⁴	>30	5% ⁵⁴	1.5 ⁵⁴	>30	11% ⁵⁴	1.5 ⁵⁴	>30
RUNNING	>12%	>3	>30	>12%	>3	>30	>15%	>3	>30
CYCLING	>34.3	>60rpm	>30	>28.8	>60rpm	>30	>30.9	>60rpm	>30

Table 1b. MODERATE activity with beneficial loading for lower extremity joints									
OPTIMAL JOINT HEALTH									
Type of Physical Activity	Hip			Knee			Ankle		
	I	V	D	I	V	D	I	V	D
WALKING	9% ⁵⁴	1.2 ⁵⁴	30	3.5% ⁵⁴	1.2 ⁵⁴	30	9.5% ⁵⁴	1.2 ⁵⁴	30
RUNNING	12% ⁵⁴	3 ⁵⁴	30	12% ⁵⁴	3 ⁵⁴	30	15% ⁵⁴	3 ⁵⁴	30
CYCLING	34.3 ⁵⁵	60rpm	30	28.8 ⁵⁵	60rpm	30	30.9 ⁵⁶	60rpm	30

Table 1c. LOW activity with minimal loading for lower extremity joints									
Type of Physical Activity	Hip			Knee			Ankle		
	I	V	D	I	V	D	I	V	D
WALKING	6% ⁵⁴	0.8 ⁵⁴	<30	2.5% ⁵⁴	0.8 ⁵⁴	<30	8.5% ⁵⁴	0.8 ⁵⁴	<30
RUNNING	<12%	<3	<30	<12%	<3	<30	<15%	<3	<30
CYCLING	<34.3	<60rpm	<30	<28.8	<60rpm	<30	<30.9	<60rpm	<30

I = Intensity or magnitude of loading (Nm or %bw*ht), V = velocity or rate of loading (m/s), D = Duration of time of loading (min) for 3x per week, Thick = Thickness of cartilage (mm). Values are estimates if not indicated by a specific reference.

References

1. Lawrence RC, Helmick CG, Arnett FC, et al. Estimates of the prevalence of arthritis and selected musculoskeletal disorders in the United States. *Arthritis Rheum.* 1998;41:778-799.
2. Parratte S, Pagnano MW. Instability after total knee arthroplasty. *Instr Course Lect.* 2008;57:295-304.
3. Wylde V, Dieppe P, Hewlett S, et al. Total knee replacement: is it really an effective procedure for all? *Knee.* 2007;14:417-423.
4. Gillquist J, Messner K. Anterior cruciate ligament reconstruction and the long-term incidence of gonarthrosis. *Sports Med.* 1999;27:143-156.
5. Laird A, Keating JF. Acetabular fractures: a 16-year prospective epidemiological study. *J Bone Joint Surg Br.* 2005;87:969-973.
6. Weigel DP, Marsh JL. High-energy fractures of the tibial plateau. Knee function after longer follow-up. *J Bone Joint Surg Am.* 2002;84-A:1541-1551.
7. Marsh JL, Weigel DP, Dirschl DR. Tibial plafond fractures. How do these ankles function over time? *J Bone Joint Surg Am.* 2003;85-A:287-295.
8. Anderson DD, Chubinskaya S, Guilak F, et al. Post-traumatic osteoarthritis: improved understanding and opportunities for early intervention. *J Orthop Res.* 2011;29:802-809.
9. Marsh JL, Buckwalter J, Gelberman R, et al. Articular fractures: does an anatomic reduction really change the result? *J Bone Joint Surg Am.* 2002;84-A:1259-1271.
10. Buckwalter JA, Brown TD. Joint injury, repair, and remodeling: roles in post-traumatic osteoarthritis. *Clin Orthop Relat Res.* 2004;423:7-16.
11. Brown TD, Johnston RC, Saltzman CL, et al. Posttraumatic osteoarthritis: a first estimate of incidence, prevalence, and burden of disease. *J Orthop Trauma.* 2006;20:739-744.
12. Buckwalter JA, Lane NE. Athletics and osteoarthritis. *Am J Sports Med.* 1997;25:873-881.
13. Roach KE, Persky V, Miles T, et al. Biomechanical aspects of occupation and osteoarthritis of the hip: a case-control study. *J Rheumatol.* 1994;21:2334-2340.
14. Yoshimura N, Sasaki S, Iwasaki K, et al. Occupational lifting is associated with hip osteoarthritis: a Japanese case-control study. *J Rheumatol.* 2000;27:434-440.

15. Honkonen SE. Degenerative arthritis after tibial plateau fractures. *J Orthop Trauma*. 1995;9:273-277.
16. Volpin G, Dowd GS, Stein H, et al. Degenerative arthritis after intra-articular fractures of the knee. Long-term results. *J Bone Joint Surg Br*. 1990;72:634-638.
17. Stevens DG, Beharry R, McKee MD, et al. The long-term functional outcome of operatively treated tibial plateau fractures. *J Orthop Trauma*. 2001;15:312-320.
18. Beauchamp CG, Clay NR, Thexton PW. Displaced ankle fractures in patients over 50 years of age. *J Bone Joint Surg Br*. 1983;65:329-332.
19. Sommerlath K, Lysholm J, Gillquist J. The long-term course after treatment of acute anterior cruciate ligament ruptures. A 9 to 16 year followup. *Am J Sports Med*. 1991;19:156-162.
20. Echtermeyer F, Bertrand J, Dreier R, et al. Syndecan-4 regulates ADAMTS-5 activation and cartilage breakdown in osteoarthritis. *Nat Med*. 2009;15:1072-1076.
21. Kamekura S, Kawasaki Y, Hoshi K, et al. Contribution of runt-related transcription factor 2 to the pathogenesis of osteoarthritis in mice after induction of knee joint instability. *Arthritis Rheum*. 2006;54:2462-2470.
22. Glasson SS, Askew R, Sheppard B, et al. Deletion of active ADAMTS5 prevents cartilage degradation in a murine model of osteoarthritis. *Nature*. 2005;434:644-648.
23. Little CB, Barai A, Burkhardt D, et al. Matrix metalloproteinase 13-deficient mice are resistant to osteoarthritic cartilage erosion but not chondrocyte hypertrophy or osteophyte development. *Arthritis Rheum*. 2009;60:3723-3733.
24. Lin AC, Seeto BL, Bartoszko JM, et al. Modulating hedgehog signaling can attenuate the severity of osteoarthritis. *Nat Med*. 2009;15:1421-1425.
25. Hirata M, Kugimiya F, Fukai A, et al. C/EBPbeta Promotes transition from proliferation to hypertrophic differentiation of chondrocytes through transactivation of p57. *PLoS One*. 2009;4:e4543.
26. Little CB, Meeker CT, Golub SB, et al. Blocking aggrecanase cleavage in the aggrecan interglobular domain abrogates cartilage erosion and promotes cartilage repair. *J Clin Invest*. 2007;117:1627-1636.
27. Ewers BJ, Dvoracek-Driksna D, Orth MW, et al. The extent of matrix damage and chondrocyte death in mechanically traumatized articular cartilage explants depends on rate of loading. *J Orthop Res*. 2001;19:779-784.

28. Quinn TM, Allen RG, Schalet BJ, et al. Matrix and cell injury due to sub-impact loading of adult bovine articular cartilage explants: effects of strain rate and peak stress. *J Orthop Res.* 2001;19:242-249.
29. Milentijevic D, Helfet DL, Torzilli PA. Influence of stress magnitude on water loss and chondrocyte viability in impacted articular cartilage. *J Biomech Eng.* 2003;125:594-601.
30. Milentijevic D, Torzilli PA. Influence of stress rate on water loss, matrix deformation and chondrocyte viability in impacted articular cartilage. *J Biomech.* 2005;38:493-502.
31. Huser CA, Davies ME. Validation of an in vitro single-impact load model of the initiation of osteoarthritis-like changes in articular cartilage. *J Orthop Res.* 2006;24:725-732.
32. Natoli RM, Scott CC, Athanasiou KA. Temporal effects of impact on articular cartilage cell death, gene expression, matrix biochemistry, and biomechanics. *Ann Biomed Eng.* 2008;36:780-792.
33. Borrelli J, Jr., Tinsley K, Ricci WM, et al. Induction of chondrocyte apoptosis following impact load. *J Orthop Trauma.* 2003;17:635-641.
34. Patwari P, Gaschen V, James IE, et al. Ultrastructural quantification of cell death after injurious compression of bovine calf articular cartilage. *Osteoarthritis Cartilage.* 2004;12:245-252.
35. Loening AM, James IE, Levenston ME, et al. Injurious mechanical compression of bovine articular cartilage induces chondrocyte apoptosis. *Arch Biochem Biophys.* 2000;381:205-212.
36. Krueger JA, Thisse P, Ewers BJ, et al. The extent and distribution of cell death and matrix damage in impacted chondral explants varies with the presence of underlying bone. *J Biomech Eng.* 2003;125:114-119.
37. D'Lima DD, Hashimoto S, Chen PC, et al. Human chondrocyte apoptosis in response to mechanical injury. *Osteoarthritis Cartilage.* 2001;9:712-719.
38. D'Lima DD, Hashimoto S, Chen PC, et al. Impact of mechanical trauma on matrix and cells. *Clin Orthop Relat Res.* 2001;S90-99.
39. Chrisman OD, Ladenbauer-Bellis IM, Panjabi M, et al. 1981 Nicolas Andry Award. The relationship of mechanical trauma and the early biochemical reactions of osteoarthritic cartilage. *Clin Orthop Relat Res.* 1981;275-284.
40. Morel V, Berutto C, Quinn TM. Effects of damage in the articular surface on the cartilage response to injurious compression in vitro. *J Biomech.* 2006;39:924-930.

41. Morel V, Quinn TM. Short-term changes in cell and matrix damage following mechanical injury of articular cartilage explants and modelling of microphysical mediators. *Biorheology*. 2004;41:509-519.
42. Borrelli J, Jr., Zhu Y, Burns M, et al. Cartilage tolerates single impact loads of as much as half the joint fracture threshold. *Clin Orthop Relat Res*. 2004;266-273.
43. Jeffrey JE, Aspden RM. The biophysical effects of a single impact load on human and bovine articular cartilage. *Proc Inst Mech Eng [H]*. 2006;220:677-686.
44. Lewis JL, Deloria LB, Oyen-Tiesma M, et al. Cell death after cartilage impact occurs around matrix cracks. *J Orthop Res*. 2003;21:881-887.
45. Jeffrey JE, Gregory DW, Aspden RM. Matrix damage and chondrocyte viability following a single impact load on articular cartilage. *Arch Biochem Biophys*. 1995;322:87-96.
46. Thompson RC, Jr., Vener MJ, Griffiths HJ, et al. Scanning electron-microscopic and magnetic resonance-imaging studies of injuries to the patellofemoral joint after acute transarticular loading. *J Bone Joint Surg Am*. 1993;75:704-713.
47. Repo RU, Finlay JB. Survival of articular cartilage after controlled impact. *J Bone Joint Surg Am*. 1977;59:1068-1076.
48. Jeffrey JE, Thomson LA, Aspden RM. Matrix loss and synthesis following a single impact load on articular cartilage in vitro. *Biochim Biophys Acta*. 1997;1334:223-232.
49. Jeffrey JE, Aspden RM. Cyclooxygenase inhibition lowers prostaglandin E2 release from articular cartilage and reduces apoptosis but not proteoglycan degradation following an impact load in vitro. *Arthritis Res Ther*. 2007;9:R129.
50. DiMicco MA, Patwari P, Siparsky PN, et al. Mechanisms and kinetics of glycosaminoglycan release following in vitro cartilage injury. *Arthritis Rheum*. 2004;50:840-848.
51. Patwari P, Cook MN, DiMicco MA, et al. Proteoglycan degradation after injurious compression of bovine and human articular cartilage in vitro: interaction with exogenous cytokines. *Arthritis Rheum*. 2003;48:1292-1301.
52. Patwari P, Cheng DM, Cole AA, et al. Analysis of the relationship between peak stress and proteoglycan loss following injurious compression of human post-mortem knee and ankle cartilage. *Biomech Model Mechanobiol*. 2007;6:83-89.
53. Otsuki S, Brinson DC, Creighton L, et al. The effect of glycosaminoglycan loss on chondrocyte viability: a study on porcine cartilage explants. *Arthritis Rheum*. 2008;58:1076-1085.

54. Mow VC, Huiskes R. *Basic orthopaedic biomechanics & mechano-biology*. 3rd ed. Philadelphia, PA: Lippincott Williams & Wilkins; 2005.
55. Ericson MO, Bratt A, Nisell R, et al. Load moments about the hip and knee joints during ergometer cycling. *Scand J Rehabil Med*. 1986;18:165-172.
56. Ericson MO, Ekholm J, Svensson O, et al. The forces of ankle joint structures during ergometer cycling. *Foot Ankle*. 1985;6:135-142.

CHAPTER 2

LITERATURE REVIEW

The Joint is an Organ

Anatomy of Articular Cartilage

Articular cartilage is a hard, translucent tissue that covers the ends of articulating bones providing a surface for diarthrodial joints that reduces friction and dissipates force during movement. It is an inhomogenous material consisting of a single cell type (chondrocyte) embedded within a highly complex extracellular matrix of water (60-85% wet weight), type II collagen (15-22% wet weight), and aggrecan (4-7% wet weight) (Fig. 2-1). Other minor constituents include collagen type I, V, VI, IX, XI, hyaluronan, link protein, decorin, biglycan, fibromodulin, perlecan, thrombospondin, and cartilage oligomeric matrix protein.¹ The anisotropy of articular cartilage is indicated by three distinct zones within the tissue: superficial tangential, middle, and deep (Fig. 2-2).

Collagen is a rod-shaped protein with three polypeptide chains that form a characteristic tight right-handed triple helix. Type II collagen contains three identical $\alpha 1(\text{II})$ polypeptide chains. In contrast, type I collagen contains two $\alpha 1(\text{I})$ and one $\alpha 2(\text{I})$ polypeptide chains, type V contains two $\alpha 1(\text{V})$ and one $\alpha 2(\text{V})$ polypeptide chains, type VI contains one $\alpha 1(\text{VI})$, $\alpha 2(\text{VI})$, $\alpha 3(\text{VI})$ polypeptide chains, type IX contains one $\alpha 1(\text{IX})$, $\alpha 2(\text{IX})$, $\alpha 3(\text{IX})$ polypeptide chains, and type XI contains one $\alpha 1(\text{XI})$, $\alpha 2(\text{XI})$, $\alpha 3(\text{XI})$. Types I, II, V, XI belong to the class of fibril-forming collagens; Type VI belong to the beaded filament-forming collagens; Type IX also contain glycosaminoglycan chains attached to the α chains. Each α chain in collagen is composed of repeating $(\text{Gly-X-Y})_n$

triplets that form a left-handed helix, where X is usually proline, and Y is often hydroxyproline. This orientation allows for a tight triple helical structure that provides optimal tensile strength.

Aggrecan is a large proteoglycan that consists of a core protein surrounded by the glycosaminoglycan (GAG) chains: chondroitin sulfate and keratan sulfate. The core protein consists of ~10% of its molecular mass, thus most of the surface area of aggrecan is due to the surrounding GAG chains, resulting in its bottle-brush appearance. The negatively charged sulfate and carboxyl groups of GAGs enable the high negative charge to attract counterions which gives rise to Donnan osmotic pressure that favors hydration. GAGs also tend to repel each other, which is restrained by the collagen fibril network.

Chondrocytes are highly specialized, terminally differentiated cells that are surrounded by a ~2 μm thick pericellular matrix that is mostly comprised of type VI collagen. The term chondron refers to chondrocytes surrounded by its pericellular matrix. Even though chondrocytes occupy only a small proportion of the total volume (~10%) of articular cartilage, they are responsible for maintaining homeostasis in articular cartilage: organization, synthesis, degradation, and/or repair of the extracellular matrix. Chondrocytes in the superficial zone closest to the articular surface are flattened, oriented parallel to the surface, and maintain a matrix high in collagen and low in proteoglycans. In contrast, chondrocytes in the deep zone are lined up in columns perpendicular to the surface. Chondrocytes in the middle zone are rounded and are responsible for maintaining a higher concentration of proteoglycans and larger collagen fibrils. Cell density decreases from the superficial to deep zones as well as with age.²

Physiology of Articular Cartilage

Materials may behave like elastic solids (i.e. metal spring), viscous fluids (i.e. dashpot), or a combination of the two representing a viscoelastic material such as articular cartilage. The mechanical behavior of a purely elastic material may be characterized by a linear load-deformation, $F = kx$, where F (N) is force, k (N/m) is the slope of this curve representing structural stiffness, and x (m) is displacement of the material during loading. Likewise, a purely elastic material has a linear stress-strain relationship, $\sigma = E\varepsilon$, where σ (N/m² = Pa) is stress, E (Pa) is the Young's modulus of elasticity, and ε is strain (m/m) of the material during loading. In contrast to the Young's modulus of bone which has been reported in the literature as ranging from 0.1 to 15 GPa,¹ the modulus of articular cartilage is much lower ranging from 0.3 to 1.0 MPa.³⁻⁸

A dashpot is a piston moving through a closed cylinder within a viscous fluid. Thus, the measured force, F (N), is related to the piston's velocity (or rate of displacement, \dot{x} , m/s) by $F = c \dot{x}$, where c is the constant of proportionality c (N-sec/m), often referred to as the frictional damping coefficient of the dashpot. A linear, purely viscous material (defined as a Newtonian fluid) has a linear shear stress-shear rate relationship, $\tau = \eta \dot{\gamma}$, where τ (Pa) is shear stress, η (Pa-sec) is the viscosity coefficient, and $\dot{\gamma}$ (sec⁻¹) is the shear rate. For example, the viscosity coefficient of water at 20°C is 1 mPa-sec. In contrast to a purely elastic solid material, a viscous fluid does not recover to its original shape after the applied stress is removed. Thus, no energy is stored in the material during loading therefore all energy undergoes heat dissipation by internal friction.

A viscoelastic material such as articular cartilage may be modeled as combinations of a Kelvin-Voigt body (spring and dashpot connected in parallel) and a Maxwell body

(spring and dashpot connected in series). The equation governing the force-displacement curve for a Kelvin-Voigt body is

$$\mathbf{F} = \mathbf{k}\mathbf{x} + \mathbf{c}\dot{\mathbf{x}}, \quad \mathbf{x} = \mathbf{0} \text{ at } \mathbf{t} = \mathbf{0} \quad (2-1)$$

After load is applied, its initial response is governed by that of the dashpot (i.e. $x(0) = 0$). Thus, its creep response (deformation produced by a sudden application of a constant F at $t = 0$) is

$$\mathbf{x}(\mathbf{t}) = [\mathbf{F}/\mathbf{k}][1 - e^{-(\mathbf{k}/\mathbf{c})\mathbf{t}}], \quad \mathbf{t} > \mathbf{0} \quad (2-2)$$

The equation governing the force-displacement curve for a Maxwell body is

$$(\mathbf{F}/\mathbf{c}) + (\mathbf{F}/\mathbf{k}) = \mathbf{x}, \quad \mathbf{x} = \mathbf{F}/\mathbf{k} \text{ at } \mathbf{t} = \mathbf{0} \quad (2-3)$$

When load is applied to the Maxwell body its initial response is the sudden deformation of a spring (i.e. $x(0) = F/k$). Its creep response is governed by

$$\mathbf{x}(\mathbf{t}) = \mathbf{F}[(1/\mathbf{k}) + (\mathbf{t}/\mathbf{c})], \quad \mathbf{t} > \mathbf{0} \quad (2-4)$$

Comparisons of the theoretical load-deformation response (using appropriate combinations of the Kelvin-Voigt and Maxwell bodies) to experimental load-deformation response of the material of interest (i.e. articular cartilage) enables the calculation of the elastic and viscous material coefficients based on the assumed constitutive laws.

It is important to note that the viscoelastic behavior of articular cartilage is dependent upon its composition, molecular structure, water and electrolyte contents, especially during compressive loading where the frictional drag of interstitial fluid flow through the collagen-proteoglycan matrix subsequently causes viscous dissipation. Thus, the degree of hydration and permeability of articular cartilage are key parameters since they affect viscous dissipation which in turn affects the creep and stress-relaxation behaviors.

Interestingly, one of the earliest features of cartilage pathology are increases in hydration^{6,9-11} which subsequently affects the material properties of articular cartilage.^{3,12,13}

The anisotropy of uncalcified cartilage is indicated by three distinct zones within the tissue (Fig. 2-2): superficial tangential (STZ), middle (MZ), and deep (DZ). Water and collagen content decrease from STZ to DZ. Dense collagen fibrils are oriented parallel to the surface in the STZ, yet change orientation to perpendicular arrangements at the tidemark, or bottom of the DZ. Tensile strength has been shown to be highest at the STZ, indicating that perhaps the parallel arrangement of the collagen fibrils help resist shear forces generated during joint motion. Similarly, the collagen is primarily responsible for the dynamic compressive stiffness/modulus of cartilage. Proteoglycan (specifically glycosaminoglycan) content is highest in the middle zone. The negatively charged sulfate/carboxyl groups of GAGs enable the high negative charge to attract counterions which gives rise to Donnan osmotic pressure that favors hydration and contributes to cartilage compressive stiffness/elastic modulus. GAGs also tend to repel each other, which is restrained by the collagen fibril network.

The viscoelasticity of cartilage is dependent upon its composition, molecular structure, water/electrolyte contents, especially during compressive loading. Specifically, the frictional drag of interstitial fluid flow through the collagen-proteoglycan matrix subsequently causes viscous dissipation. Thus, the degree of hydration and permeability of cartilage are key parameters since they affect viscous dissipation, which affects creep and stress-relaxation behaviors during compressive testing.

The classical biphasic (fluid + solid) theory was developed by Mow et al. to describe the material behavior of cartilage under a variety of conditions.⁷ Essentially, it assumes four criteria:

- 1) Solid matrix may be linearly hyper/elastic and an/isotropic
- 2) Solid and fluid are intrinsically incompressible (requiring fluid exudation)
- 3) Viscous dissipation occurs mostly due to interstitial fluid flow
- 4) Frictional drag is directly proportional to relative velocity (may be strain-dependent and the proportionality factor, diffusive drag coefficient (K)

Recently, a triphasic theory (fluid + solid + ions) was developed by Ateshian et al. to describe all biphasic viscoelastic effects, Donnan equilibrium ion distributions, dimensional swelling effect, Donnan osmotic pressures, kinetics of swelling, and all diffusion and streaming potentials.^{14,15} The triphasic theory predicts that total equilibrium axial stress at the loading platen is the addition of the stress in the elastic solid matrix caused by applied uniaxial compression and the Donnan osmotic pressure, π . ($\sigma^T = \sigma^S + \pi$) It has been shown previously that the swelling pressure has a significant effect on tissue stiffness, other equilibrium material properties, and ultimately the stress-relaxation behavior of cartilage.^{14,16,17}

Compressive testing of cartilage can be performed under confined, unconfined, and indentation geometries as indicated in Fig. 2-3.¹⁸ Unconfined testing compresses the sample with a non-porous platen, exuding fluid in the lateral direction. Confined testing usually involves placing the sample in a confining chamber, compressing the sample with a porous platen, exuding fluid in the axial direction. Indentation testing compresses the

sample with a cylindrical indenter, exuding fluid in the lateral and axial directions.

Indentation testing may be used for *in vitro* and *in vivo* purposes.

Confined compressive testing is advantageous for biomechanical assessment of GAG. This is based upon the structure-function relationship between highly charged aggrecan molecules (i.e. GAG) and the mechanical integrity (i.e. elastic modulus) of the cartilage, yet it is disadvantageous because the limitation of fluid exudation in the axial direction is unlikely to occur naturally. Unconfined compressive testing is advantageous for biomechanical assessment of collagen II. Again, the structure-function relationship provides the framework for collagen and its capacity to restrain tissue “bulging” by its tensile strength (i.e. dynamic modulus). The disadvantage to unconfined testing is its restriction of fluid to the lateral direction. Perhaps, the ideal testing configuration is indentation compressive testing (i.e. 3.9mm-diameter indenter used to compress a 6mm-diameter sample) especially since it has been used to measure the stiffness of *in vivo* femoral condyle has been measured arthroscopically.¹⁹ However, the mathematics of modeling the indentation experiment of cartilage-on-bone configuration with both axial and lateral fluid exudation is very complex.^{20,21}

Failure of the Joint Organ: Osteoarthritis

OA affects all joint tissues (cartilage, subchondral bone, synovium, etc) as depicted in the Fig. 2-4.²² Post-traumatic OA due to joint injury may have various pathophysiological events involving mechanocoupling, coupling, signal transmission, and ECM coupling²³ depending on where and how much mechanical damage has accrued.²⁴ Yet, the commonality of PTOA injuries is that there is some type of disruption of the articular cartilage.²⁵ Clinical injury producing articular fracture fragments have proven a direct

effect on chondrocyte death.²⁶ Also, many *in vivo* and *in vitro* models have demonstrated chondrocyte death due to cartilage injury.²⁷⁻³⁷ In Chapter 4, both temporal and spatial mechanisms of chondrocyte death due to *in vitro* cartilage injury at early (day 0, superficial zone cell death) and later (day 12, superficial/middle/deep zones cell death) time points was reported.³⁸ There is a direction correlation between cell death and impact energy,³⁹ peak stress,³³ rate of loading,^{35,38} strain,^{38,40} and location of peak load.⁴¹⁻⁴³

Chondrocyte death after impact injury occurs via necrotic and apoptotic pathways with the latter predominantly occurring via the caspase-9/3 pathway as shown in Fig. 2-5.^{44,45} This is primarily due to calcium release from the endoplasmic reticulum via the ryanodine receptor, processed into the mitochondria by the uniport transporter, initiating mitochondrial depolarization, and activating caspase-9.^{30,46} With pre-treatment of a glucosamine derivative that reduced mitochondrial depolarization, Huser et al. were able to mitigate cell death in injured cartilage.⁴⁵

Recently, it was shown that chondrocyte apoptosis was mitigated by treating (within 2 hours after injury) injured osteochondral explants with rotenone (electron transport chain inhibitor).⁴⁷ Goodwin et al. concluded that chondrocyte apoptosis is highly dependent on the release of superoxide from damaged mitochondrial components during *in vitro* impact injury.

Another pathway that can affect chondrocyte death is the fibronectin ($\alpha 5\beta 1$ – integrin mechanoreceptor) pathway as shown in Fig. 2-6.⁴⁸ Cartilage injury has been shown to early activate p38 MAP kinase, JNK, and NF-kB within 1 hour followed by late activation of ERK1/2 and spread of p38 MAP kinase levels to non-impacted areas by 24

hours.⁴⁹ Thus, the blocking of p38 and ERK1/2 led to decreased injury-related chondrocyte death.⁵⁰

There are two main pathways that may drive effusion into synovitis once activated as shown in Fig. 2-7: 1) Toll-like receptors (TLRs) and 2) Complement cascade.⁵¹ Innate response (i.e. joint injury) may stimulate TLRs which are pattern recognition receptors involved in cellular inflammation that may act as “danger” signals by producing chemokines (i.e. IL-8, CCL5) and cytokines (i.e. IL-1, IL-6, TNF).⁵² Ligands that may activate TLRs such as fibronectin⁵³ have been shown to be released into the joint fluid after injury. Recently, plasma proteins in OA synovial fluid was shown to activate cytokines via TLR4.⁵⁴ Thus, the TLR4 monoclonal antibody is being explored as a therapy to limit the acute inflammatory response and associated synovitis.⁵⁵

The complement cascade is involved in the clearance of pathogens from the joint, but under excessive catabolic conditions can lead to tissue damage. Matrix components such as cartilage oligomeric matrix protein (COMP),⁵⁶ osteoadherin,⁵⁷ and fibromodulin⁵⁸ may activate the complement cascade. Conversely, other components such as the NC4 domain of Collagen IX⁵⁹ can inhibit this cascade. Thus, proposed mediators of synovitis are IL-1 β , TNF α , IL-17, IL-15, IL-7, CCL19, MCP-1, MIP-1 β , S100 proteins/alarmins as indicated in Table 2-1.²²

PTOA is initiated by traumatic, joint injuries that affect the articular surface.⁶⁰ Recently, MRI has been used to detect “mild” chondral defects and bone bruising immediately after injury.⁶¹ This suggests that there may already be an initial alteration to the osteochondral junction. If so, then it is plausible that there will be mechanical adaptations and molecular cross-talk among tissues as indicated in Fig. 2-8.⁶² If there is

demarcation loss between cartilage and bone, then there may be increased osteoclastic activity to permit the removal of “damaged” molecules within the non-calcified cartilage. If there is compromised joint health (i.e. due to excessive mechanical loading, synovial inflammation, etc), then fragmentation of the tidemark and additional cartilage fissuring can continue. As the calcified front advances up then perivascular ossification and thickening of the subchondral bone plate can occur. Thus, the bone can become sclerotic and stiff which can lead to secondary cartilage softening.⁶³ It still remains controversial whether non-steroidal anti-inflammatory drugs (NSAIDs) warrant contraindication during early phase bone healing.⁶⁴ Yet, it has been shown in numerous studies to delay bone healing. Moreover, treatment of COX-2 inhibitor reduced joint inflammation but increased osteopenia by suppressing bone formation in IL-1 α transgenic mice.⁶⁵ Therefore, there may be potential chondroprotective treatments (i.e. hyaluronan,⁶⁶ lubricin,⁶⁷ P188,⁶⁸ osteoprotegerin-1⁶⁸) for mitigating chondrocyte apoptosis, promoting bone health, and preventing PTOA.

The etiology of PTOA is multifactorial including various types of injuries from ligament/mensical tears (mild-severe) to articular fractures (severe). For example, ligament/meniscal tears have a 10-fold increased risk of OA as compared with patients without previous joint injury.⁶⁹ Further, intra-articular fractures of the hip, knee, and ankle increase the risk of OA to 25%,⁷⁰ 23-44%,⁷¹ and >50%,⁷² respectively.

The similarity among all PTOA cases is that there is mechanical insult(s) to the articular surface. These types of mechanical injuries may be broadly classified into 3 categories:⁷³

- I) Damage to chondral matrix/cells (no cartilage disruption)

II) Cartilage disruption

III) Cartilage-bone disruption

Typically, ligament/meniscal tears are due to low-moderate energy injuries (I-II), whereas articular fractures result from high-energy injuries (III).⁷⁴ Moreover, quantitative assessment of the energy absorbed during injury has been developed based on fracture displacement to evaluate injury severity.⁷⁵

Each joint injury elicits a different biologic response depending on the biological tissues damaged as well as severity of mechanical injury.⁷³ Mild injury of the articular surface (I) may illicit chondrocyte proliferation and/or matrix synthesis. If the affected tissues are able to adequately remodel then the cells can restore normal homeostasis. Yet, the addition of excessive mechanical loading and/or pathobiologic conditions may lead to fibrillation of the articular surface. This increases the shear stress in the collagen network at the articular surface making it susceptible to further degradation and upregulation in MMPs and interleukins.⁷⁶ Moderate injury (II) results in chondral fractures or ruptures. Similar as before, this injury may illicit chondrocyte proliferation, matrix synthesis, yet new tissue is unable to fill the cartilage defect. Severe injury (III) involves cell proliferation, formation of a fibrin clot, and production of new tissue. Depending on several factors (i.e. lesion size/location, joint alignment/stability), the repair tissue may remodel and maintain functionality or it may degenerate.

Clinical joint injuries may be classified into multiple categories (I-III). For example, the force delivered to rupture the ACL may also damage other ligaments, menisci, articular cartilage, subchondral bone.⁷⁷ This makes it very challenging to develop a clinically-relevant PTOA model. Again, the commonality among all PTOA injuries is

some type of cartilage injury. Fortunately, radiological advancements have been made so that even mild, chondral damage (I) during acute, isolated ACL tears can be detected at time of injury using MRI.⁶¹

Developing an optimal PTOA model involved delivering an impact injury (I-III) to cartilage (Ch. 4)^{78,79} as well as cartilage-bone explants (1-III) (Ch. 5-6).⁴¹ Similar to clinical responses, our results indicated that cell death and inflammation (PGE₂ release) was dependent on trauma severity. This discovery raised the question whether the mechanosensitivity of PGE₂ (or other potential biomarkers) could be measured immediately after injury to quantify trauma severity or used in conjunction with imaging modalities (i.e. nuclear medicine) to evaluate joint health during gait analysis.

It is likely that most joint injuries follow a timeline as proposed by Anderson et al. in Fig. 2-9.⁸⁰ This process will vary among individuals as it is dependent upon the pre-injury health of the joint (as well as injury severity, incongruity, instability, patient age, genetics, activity level, etc). Yet, it is apparent that three overlapping, catabolic, catabolic-anabolic, and anabolic phases occur in response to injury. One of the earliest events indicated is peak inflammation around day 2. In 1981, Chrisman et al. provided evidence that increased PGE₂ immediately after cartilage injury is due to cell membrane rupture that releases arachidonic acid, initiating the cyclooxygenase pathway.⁸¹ In our pursuit to mimic this response through *in vitro* models, we have discovered an increase in prostaglandin E₂ (PGE₂) released from injured cartilage-bone or cartilage tissue to the culture media up to day 3 for cartilage-bone (peak amount ~60,000pg)⁴¹ and up to day 9 for cartilage (peak amount ~600pg).^{38,82} Thus, PGE₂ release extends into the anabolic phase of the recovery process supporting the concept that PGE₂ may affect chondrocytes

in both catabolic and anabolic manners after injury.⁸³ Similarly, Joos et al. reported increased PGE₂ (as well as PGD₂ and IL-6) in human early OA cartilage 24 hours after impact injury.⁸⁴ Gosset et al. have described PGE₂ as a “mechanosensitive” biomarker and attribute this to the upstream enzyme microsomal prostaglandin E synthase type 1 (mPGES-1) which is highly sensitive to dynamic loading in cartilage explants.^{48,85}

The direct role PGE₂ has on chondrocytes after injury has not been fully elucidated. Thus, all of its reported roles (catabolic/anabolic) for cartilage or bone were evaluated to obtain a more comprehensive view as indicated in Table 2-2. The relationship between PGE₂ and normal, loaded, IL-1 treated, and OA chondrocytes appears to vary probably due to differences in cell/tissue sources, PGE₂ dose levels, loading regimens, etc. Within normal cartilage/chondrocytes, PGE₂ increases proline production, yet the effects are dose dependent with opposite actions depending on concentration.⁸⁶ Other potential anabolic roles PGE₂ has on cartilage include increased proteoglycan synthesis,⁸⁷ reversal of proteoglycan degradation,⁸⁸ and decreased collagen cleavage.⁸⁹ Moreover, PGE₂ plays a role in inducing MMP-3 and MMP-13 in an inflammatory (IL-1 induced) environment.⁹⁰ For example, it has been previously shown that there is increased PGE₂ production in osteoarthritic cartilage.⁹¹ Its catabolic roles involves mitigation of proteoglycan synthesis (high dose = 1000ng/ml)⁹² and increased stromelysin (MMP-3) production.⁹³ Yet, low dose (10pg/ml) PGE₂ seemed to be beneficially chondroprotective since it decreased COL2a1 cleavage.⁸⁹

Biomarkers Affected by Impact

Some of the pathologic responses typically reported for PTOA include chondrocyte cell death (viability),^{32,33,35,39,40,44,94,95} direct tissue disruption with cartilage GAG

(aggrecan),^{36,44,96,97} and collagen II loss,^{97,98} and increased release of prostaglandin E₂ (PGE₂)⁹⁹ and nitric oxide^{32,100} as well as other inflammatory and catabolic mediators.

Chondrocyte death has been associated with PTOA¹⁰¹ and degree of cell death is reportedly dependent on impact energy,³⁹ peak stress,³³ stress rate,³⁵ and compressive strain.⁴⁰ Chondrocyte death after impact injury occurs via necrotic and apoptotic pathways with the latter predominantly occurring via the caspase-9/3 pathway.^{30,45}

Jeffrey et al. provided evidence that chondrocyte viability reduces linearly with increasing impact energy from 0.2-0.98 J in calf articular cartilage explants.³⁹ Huser et al. suggest that chondrocyte death is primarily a result of calcium released from the endoplasmic reticulum via the ryanodine receptor⁴⁴ and is subsequently processed into the mitochondria by the uniport transporter, initiating mitochondrial depolarization and subsequent caspase-9-activation^{30,46} and may be reduced in explants by treatment of a glucosamine derivative, Glu5, prior to impact load.⁴⁵

Similarly, Loening et al. reported that chondrocyte apoptosis occurred at peak stresses as low as 4.5 MPa and increased with peak stress to >20 MPa with more than 50% cell death and maximal apoptosis occurring by 24 hours post-injury in calf articular cartilage explants.³² Duda et al. used a drop-tower to deliver an impact load energy of 0.06, 0.1, or 0.2 J to *ex vivo* porcine patellas that produced no gross structural damage, but significantly reduced cell viability in the tangential and middle zones with increasing impact energy.¹⁰² In a series of studies, D'Lima et al. evaluated the effect of mechanical injury on chondrocyte apoptosis in full-thickness human cartilage explants (5mm dia)²⁸ and bovine explants¹⁰³ as well as *in vivo* rabbit patella²⁹ loaded to 14 MPa for 500 ms, 23 MPa for 500 ms or 30% strain for 500 ms, respectively. The authors concluded that the

pan-caspase inhibitor, z-VAD.fmk [benzyloxycarbonyl-Val-Ala-Asp (OMe) fluoromethylketone], and IGF-1 (insulin growth factor-1) are effective in preventing chondrocyte apoptosis due to mechanical injury.

It has been shown in an *ex vivo* cartilage injury model that impact initiates immediate release of GAGs for up to 24 hours post-injury with the maximal amount occurring 4 hours post-injury.⁹⁶ Aggrecan contributes to the mechanical properties of cartilage such as compressive stiffness, thus it is expected that impact injury that releases GAG will likewise affect cartilage stiffness. Supportive of this concept, Natoli et al. reported a reduction in stiffness as early as 24 hours post-impact for the high energy insult (2.8 J) with a reduction by 4 weeks after low-energy impact (1.1 J).³⁶ While treatment with insulin-like growth factor 1 (IGF-1) reduced the amount of GAG released after low-energy impact, it had no effects in ameliorating the reduction in tissue stiffness¹⁰⁴ suggesting that quality as well as quantity (normal vs. pathologic state) of tissue GAG (aggrecan) is important to tissue mechanical properties.

Type II collagen (Col II) is instrumental for normal articular cartilage function by providing tensile stiffness/strength to the tissue as well as restraining the swelling pressure of negatively charged proteoglycans is susceptible to mechanical injury. For example, immunohistochemistry has revealed decreases in collagen II expression with increases in collagen I expression from articular cartilage in an *in vivo* canine impact model 6 months post-injury.⁹⁸ Moreover, minimal changes in type II procollagen mRNA were noted immediately post-impact compared to the sham-operated control in an *in vivo* rabbit model, whereas by 1 month post-impact there was a complete absence of type II procollagen mRNA in insulted cartilage.⁹⁷ The data suggest that reduction in Col II is a

consistent consequence of impact injury but may occur as a secondary effect involving intermediate factors based on the delayed nature of the changes.

One of the inflammatory mediators involved in OA is prostaglandin E₂ (PGE₂). PGE₂ is the most abundant and potent prostaglandin that affects bone remodeling and is required for healing.⁶⁴ As indicated by Fig. 2-10, it interacts with 4 main receptors (EP1R, EP3R, EP2R, EP4R), specifically EP2R and EP4R during bone metabolism (although it has been implicated to interact with other G-protein coupled receptors.¹⁰⁵ In 1970, exogenous PGE₂ was shown to stimulate cAMP production and resorption in bone organ cultures.¹⁰⁶ Also, PGE₂ is a strong stimulator of osteoclast differentiation in marrow cultures.¹⁰⁷ Exogenous PGE₂ can increase bone resorption and formation, however formation has resulted greater increases in bone mass of rats, dogs, and humans.¹⁰⁷ Further, the continuous dosing of PGE₂ has lead to bone resorption, whereas intermittent dosing yields bone formation.¹⁰⁸ There appears to be a concentration effect of PGE₂ on bone turnover such that *in vivo* studies have shown that high-dose, exogenous PGE₂ stimulates new bone formation (osteoblasts),^{109,110} whereas low-dose PGE₂ drives bone resorption (osteoclastic recruitment/activity).¹¹¹ Endogenous PGE₂ can stimulate resorption by increasing IL-1,-6,-11-17,TNF α , PTH, Vit.D, FGF-2, and BMP-2.¹⁰⁷ Perhaps, its most important role in resorption is upregulating RANKL and inhibiting OPG in osteoblasts. This widely accepted finding has been proven by Sanchez et al. when dynamic loading was applied to osteoblasts in 3D culture; they reported increased expression of COX-2 and production of IL-6 and PGE₂, but not mPGES-1.¹¹² It was concluded that PGE₂ and IL-6 were responsible for the decrease in the OPG/RANKL ratio. Yet, the exact mechanisms of PGE₂ during remodeling remain ambiguous. Bone

fractures stimulate high endogenous levels of PGE₂ especially during the first 14 days of callus formation¹¹³ which is critical for bone healing.¹¹⁴ However, PGE₂ can lead to excessive bone formation resulting in heterotrophic ossification after trauma or surgery.¹¹⁵ It has been postulated that PGE₂ may trigger the anabolic Wnt/ β catenin signaling pathway in osteocytes in response to loading.¹¹⁶ If loading results in severe cell damage, then it has been recently shown that the Wnt signaling pathway controls hematopoietic stem cells self renewal and bone marrow repopulation and its activation require PGE₂.¹¹⁷ Thus, PGE₂ may function as a crucial initiator of tissue repair.

Increased PGE₂ after cartilage injury is most likely due to cell membrane rupture during impact which has been shown to cause release of arachidonic acid effectively activating the cyclooxygenase-2 (COX-2) pathway.⁸¹ Jeffrey et al. provided evidence that cyclooxygenase inhibition lowers prostaglandin E₂ release from articular cartilage and reduces apoptosis but not proteoglycan degradation following an *in vitro* impact load.⁹⁹ Providing further support that PGE₂ production increases significantly during impact injury of cartilage due to generation of mechanical forces, Gosset et al. demonstrated that microsomal prostaglandin E synthase-1 (mPGES-1), a key enzyme required for PGE₂ formation, is a mechanosensitive gene.⁴⁸ Yet, the role of PGE₂ in osteoarthritis remains vague and is considered to have both anabolic and catabolic effects on joint tissues.⁸³

Another important inflammatory mediator involved in OA is nitric oxide (NO).^{100,118} The production of NO is dependent on nitric oxide synthase 2 (NOS2) and is associated with inflammation in arthritic disorders.¹¹⁹ There appear to be feedback-control mechanisms between PGE₂ and NO in cartilage physiology. For example, specific

inhibition of NOS2 (1400W) created an additional increase in PGE₂ production whereas the selective COX2 inhibitor (NS398) blocked both compression-induced NO and PGE₂ production during intermittent compressive loading at 0.5 Hz at 0.05, 0.1, 0.5, or 1.0 MPa.¹²⁰ The COX and NOS pathways are intricately linked,⁸³ thus more studies are needed to further establish their relationship especially if therapeutic strategies are targeted on these pathways.

Experimental Impact Devices

Various devices such as drop-tower,^{39,44,63,102,121-127} pendulum,^{81,128} servo-electrodynamic,^{33,40,129-131} and servo-hydraulic,^{29,132-134} and screw¹³⁵ devices have been developed to deliver a single impact (rapid, compressive load) to articular cartilage.

Drop-tower devices control the impact energy, E (Joules), delivered to the specimen by

$$E = mgh \quad (2-5)$$

where m is the mass of the impactor (kg), g is the gravitational acceleration constant (m/s²), and h is the height (m) from which the impactor falls. An accelerometer is used to measure the acceleration of the impactor while in contact with the specimen. The impact velocity of the impactor is determined through integration of the acceleration-time graph and cartilage displacement is determined through integration of the velocity-time graph. Strain is measured by dividing the displacement data by the original thickness of the specimen. A force transducer is used to measure the force during impact and stress is measured by dividing the force data by the original cross-sectional area of the specimen. Jeffrey et al. reported that impact energy of 0.12 J to cartilage explants results in the following: peak forces (294-580 N), maximum stresses (21.7-45.8 MPa), stress rates

(15,400-35,500 MPa/sec), maximum strain (0.55-0.80 mm/mm), and strain rates (303-523 s⁻¹).¹³⁶ Mrosek et al. fabricated a drop-tower apparatus to mimic a pathologic transarticular load by dropping a mass of 2.1 kg to the patellofemoral joint of an anaesthetized dog resulting in a peak force between 2010 and 2170 N with a time to peak force of ~1.5 ms.⁹⁸

Similar to drop-tower apparatuses, pendulum devices control impact energy, E, with the height of the pendulum arm related to its length L by

$$h = L - L \cos(\theta) \quad (2-6)$$

where θ is the angle between L and the vertical. Force is measured during impact with a piezoelectric load cell and super low pressure-sensitive film is used to measure contact surface area. Borrelli et al. used a mass of 2400 g attached to a pendulum arm to impact the posterior aspect of the medial femoral condyle of in vivo rabbits that resulted in a maximum force of 345.5 N (corresponding to a maximum stress of 54.8 MPa with a measured contact area of 6.38 mm²) and time to peak force of 0.021 sec.¹²⁸ To the author's knowledge, maximum strain during impact using pendulum devices has not been reported.

Milentijevic et al. developed a servo-controlled double-acting pneumatic cylinder³³ to impact cartilage explants by controlling peak stress (ranging from 10 to 60 MPa) and stress rate (ranging from 25 to 1000 MPa/s)³⁵ resulting in: peak forces (31.7-399 N), maximum strain (0.137-0.227 mm/mm), and time to peak force (10-1600 ms). In a follow-up study, Milentijevic et al. used the same device to apply a known stress magnitude (15-50 MPa) at a stress rate of 420 MPa/sec to the articular surface of the lateral femoral condyle of cadaveric and live anesthetized rabbits.³⁵ Cell death and

matrix damage was observed in explants at stress magnitudes >20 and 30 MPa, respectively. The articular cartilage in the live rabbit knees was analyzed at 0 and 3 weeks post-injury with visible surface damage observed immediately post-injury, but no gross changes present by 3 weeks post-injury. The system used was able to generate signs of late-stage osteoarthritis (e.g. matrix damage, chondrocyte death, and proteoglycan loss) by delivering an impact load to 35 MPa.

Frank et al. developed a custom-made servo electro-dynamic device with an axial motor capable of applying compressive ramps at rates up to 1 mm/sec (corresponding to a strain rate of 1 s⁻¹) with a maximum force of 400 N.¹²⁹ Kurz et al. used the device developed by Frank et al.¹²⁹ to impact calf cartilage explants to 50% strain of 1 mm thick cartilage for strain rates of 0.01 , 0.1 , and 1 s⁻¹ resulted in peak stresses of 12 , 18 , and 24 MPa, respectively.⁹⁵ Quinn et al. developed a similar electro-dynamic device to impact cartilage explants to maximum stresses of 3.5 , 7.0 , or 14 MPa at strain rates of 3×10^{-5} , 0.3 , 0.5 , or 0.7 s⁻¹ that resulted in more tissue damage present with higher strain rates.¹³⁰ The maximum strain incurred by the tissue was not reported. Furman et al.¹³¹ and Ward et al.¹³⁷ used a materials testing system (BOSE, ElectroForce 3200) to apply an impact force of 55 N at a rate of 20 N/sec to produce intra-articular tibial plateau fractures in anesthetized mice.

D'Lima et al.²⁹ used a servo-hydraulic test machine (Instron 8511) to impact cartilage explants to either a maximum stress of 14 MPa or 30% strain at a rate of 3 s⁻¹ lasting for 500 ms. Ewers et al. used a smaller servo-hydraulic test machine (Instron 1331) to impact cartilage explants to a maximum force of 1247 N, resulting in ~ 40 MPa at a rate of ~ 900 MPa/sec with a time to peak force of 45 ms and 1 sec, respectively.¹³² Ashwell

et al. used a servo-hydraulic test machine (MTS 858 Mini Bionix II) to impact *ex vivo* porcine patella to 2000 N at a rate of 25 mm/sec.¹³³

One of the primary challenges of creating an effective PTOA model is that of mimicking clinically-relevant cartilage injury in a reproducible manner, thus devices have been used to control various impact parameter magnitudes and rate or duration (Table 2-3) which have been shown to affect cartilage physiology, i.e. with findings that supra- and sub-physiologic loading conditions can be detrimental. For example, Ewers et al.^{132,138,139} reported that the rate of loading affects the degree of acute and chronic injury, matrix damage, chondrocyte death, changes in retropatellar cartilage and underlying bone such that a low rate of loading generated more cell death while a high rate of loading created more matrix damage and subchondral bone thickening. Quinn et al.¹³⁰ studied the effects of two strain rates and peak stress on adult bovine cartilage matrix and cell injury, and reported that a similar amount of cell death occurred for both strain rates, but the low rate created a greater distribution of cell death compared to the high rate of loading cell death being predominantly near fissures. Matrix damage as well as GAG release (up to 24 hours post-impact) was observed for the high rate of strain. Jeffrey et al.¹⁴⁰ compared the effects of a single energy drop tower fast impact loading to a slower constant 40 mm/s crosshead speed loading up to the average strain observed during drop tower tests on articular cartilage. The slower rate of loading (30 times longer to reach peak stress and peak stress a factor of 20 lower than drop test) caused more rapid apoptosis although similar levels were reached after 3 days. Milentijevic et al.³³ investigated the influence of impact load stress magnitude and stress rate³⁵ on water loss, matrix deformation, and chondrocyte viability and reported that

greater compressive strains were incurred in the superficial zone (as compared to the deep zone) and that cell death increased with increasing stress magnitude and decreasing stress rate.

Previous investigations have controlled and/or reported (Table 2-3): energy of impact, maximum stress, and maximum strain delivered along with corresponding rate of stress, rate of strain, velocity and/or duration of impact and constraint or not on lateral expansion. Cartilage is a viscoelastic type material, and thus its resistance to load (stiffness) is velocity (strain rate) and time relaxation dependent, as well as being dependent upon its biomechanical material properties, thickness, cross section area of the impacted region and constraints placed on its lateral expansion during the traumatic event. Thickness of a cartilage explant with all physiologic layers of interest in a particular study is measurable, but it is not easy to obtain multiple samples of like thickness. Thus ideally the magnitude of the controlled impact parameter (energy, maximum stress, or maximum strain) should be normalized relative to cartilage thickness and set to this value before delivery. This is impossible to do with energy and maximum stress since these parameters are also dependent upon unknown cartilage material properties and time history of delivery. Jeffrey et al.¹⁴⁰ reported that, “the peak stresses reached in the fast, drop tower impact loading were more than 20 times that of the slow velocity controlled, severe load suggesting that stress alone is not a good indicator of damage.” Control of maximum strain and strain rate on the other hand are strictly thickness dependent, and thus are theoretically achievable to define a repeatable thickness normalized “severity of trauma.” However, to achieve the same selected strain rate would require for the software available in the COL lab that the impact velocity be

normalized and thus changed for each specimen of different thickness, which would require altering the control program's desired velocity and reloading the program after thickness measurement was made. We thus selected to use impact velocity and maximum strain as the two parameters to define repeatable “severity of trauma” categories. Previous investigations using controlled impact velocity to different levels of maximum strain were at relatively slow rates (< 1 mm/sec),¹²⁹ compared to estimated average *in vivo* joint trauma rates of 12.5 and 25 mm/sec (assuming 50% strain of 0.5 mm thick cartilage) corresponding to maximum force to the cartilage reported time for falling injury to occur within 20 ms¹⁴¹ and for vehicular knee-dashboard injuries within 10 ms,¹⁴² respectively.

It was decided to investigate using the Comparative Orthopaedic Laboratory's (COL's) *Instron 8821s*, servo-hydraulic testing machine as shown in Fig. 2-11 to achieve the objective(s) primarily due to: 1) minimal cost (since the machine was previously purchased and has been used for several other projects and the cost estimate of purchasing an servo-controlled electrodynamic machine (TestResources, 200LM25) with a force capability up to 740 N at a rate of 4600 mm/sec was approximately \$50,000), and 2) the minimal effect the 4 mm diameter cartilage explant resistive force to impact would have on the controlled motion of the test machine's massive ram.

Therefore, the objective of this work was to develop a clinically-relevant *ex vivo* PTOA model with repeatable severity of mechanical injury by delivering a single impact load with controlled combinations of velocity and maximum strain (i.e. severity of trauma categories) to a laterally-constrained articular cartilage explant to study their effect on articular cartilage's biomarkers: cell viability, extracellular matrix, and material

properties. This is part of our broader goal of finding post trauma biomarkers that could clinically be measured to predict the likelihood of the onset of PTOA and its progression for purposes of selecting or determining optimum treatments.

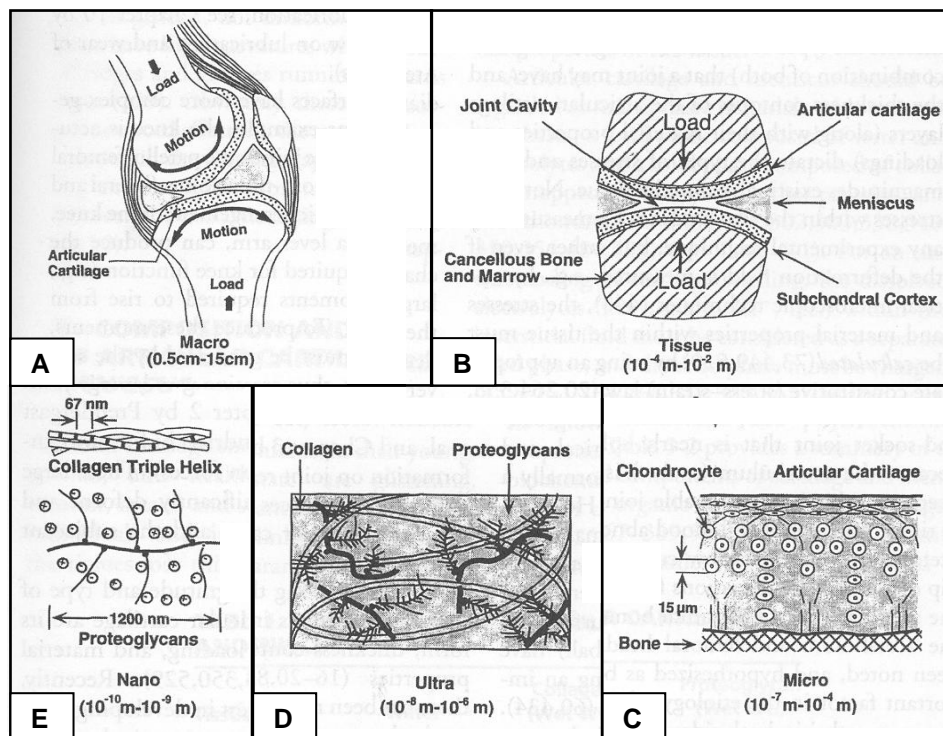


Figure 2-1. Views of a diarthroidal joint. Some of the important structural features of a typical diarthroidal joint at different hierarchical scale: A) macro (0.5 to 15 cm), B) tissue (10^{-4} to 10^{-2} m), C) micro (10^{-7} to 10^{-4} m), D) ultra (10^{-8} to 10^{-6} m), and E) nano (10^{-10} to 10^{-9} m).¹⁴³

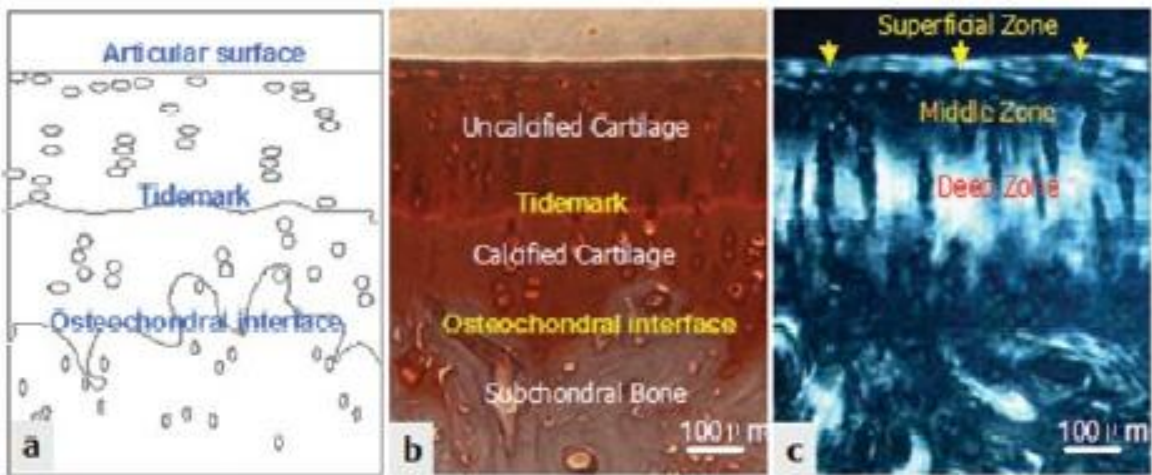


Figure 2-2. Ultrastructure of articular cartilage. Three distinct zones by depth of articular cartilage. (a) Schematic photomicrograph. (b) Tissue section stained by safranin O. (c) Photomicrograph of the serial section under polarized light.¹⁴⁴

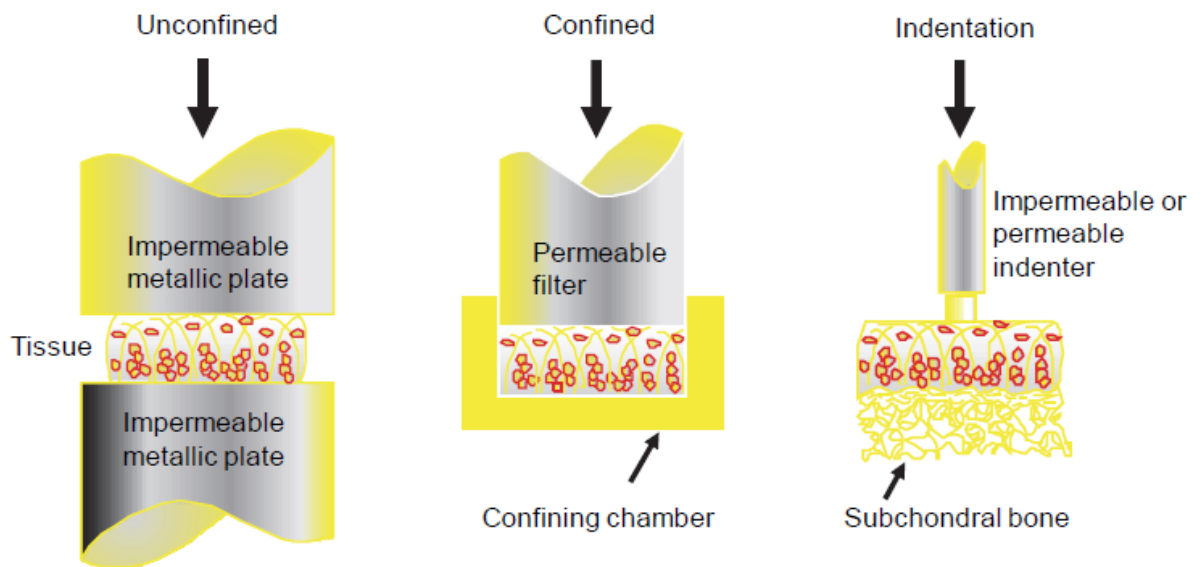


Figure 2-3. Unconfined, confined, and indentation test set-up.
 (Korhonen R, Saarakkala S. Biomechanics and modeling of skeletal soft tissues: InTech; 2011.)

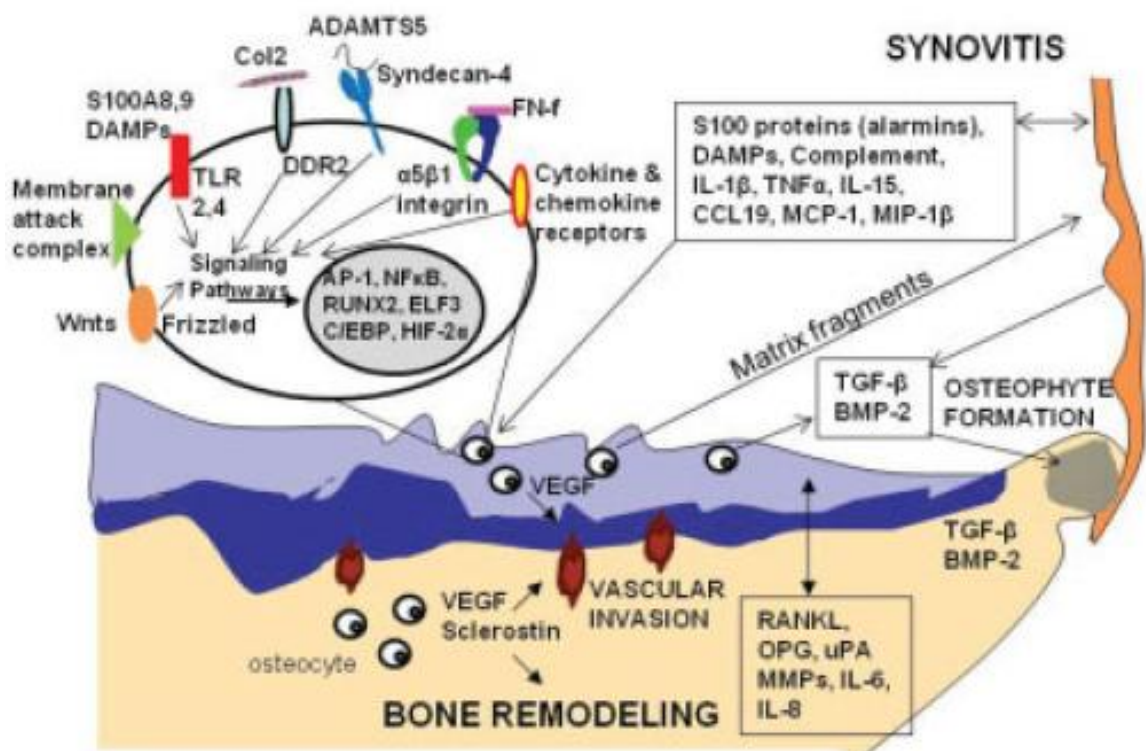


Figure 2-4. Molecular factors involved in osteoarthritis.²²

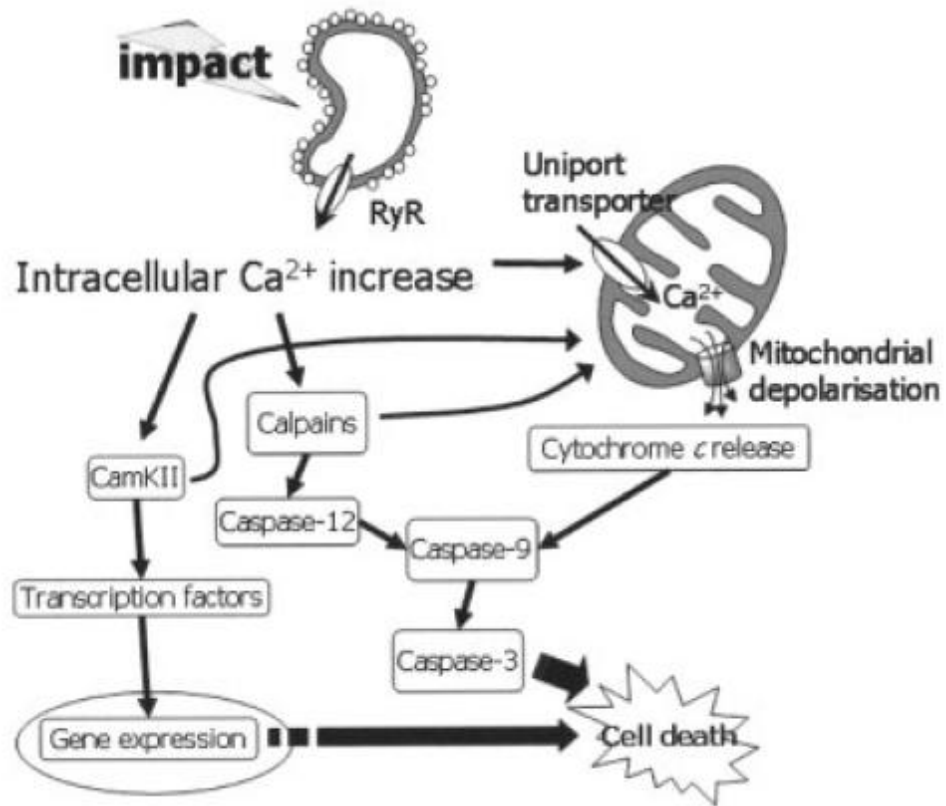


Figure 2-5. Signaling cascades activated following a single impact load, leading to apoptosis-like cell death. RyR = ryanodine receptor, CaMKII = calcium/calmodulin-regulated kinase II.⁴⁶

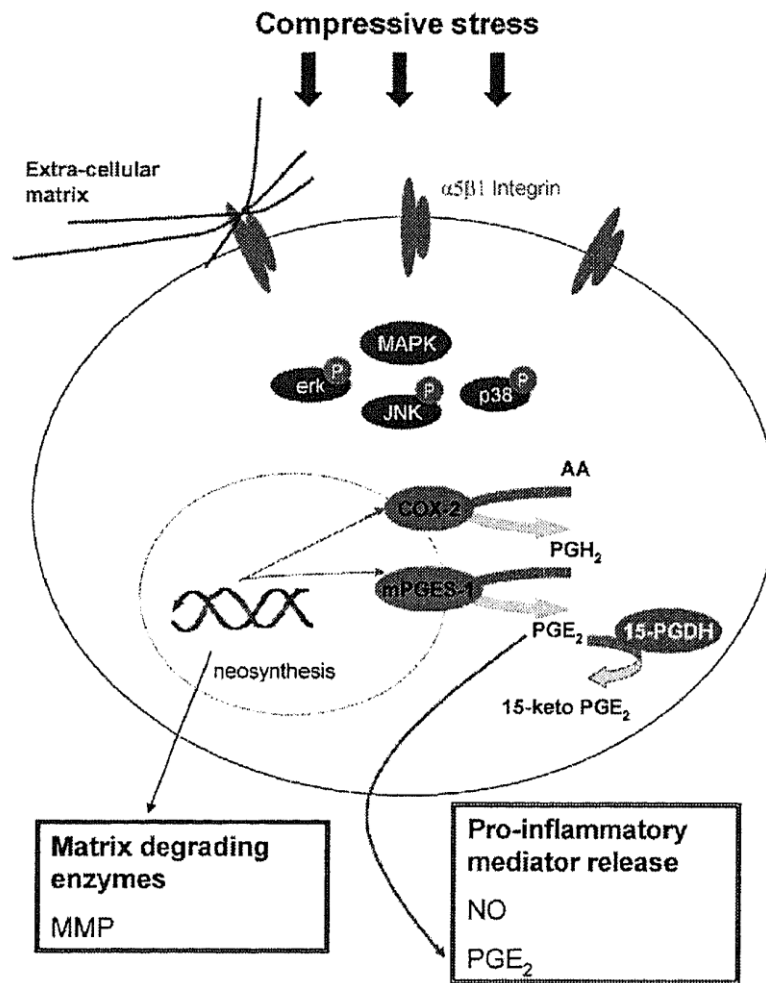


Figure 2-6. Proposed signal transduction pathway that leads to the induction of COX-2, mPGES-1 and 15-PGDH by compressive stress in cartilage. Compressive stress stimulates $\alpha 5 \beta 1$ integrin and phosphorylation of p38, ERK-1/2, and JNK MAPKs. The resulting expression of COX-2, mPGES-1 and 15-PGDH genes lead to the release of the pro-inflammatory mediator PGE₂. Moreover, an increase of NO release and of the matrix degrading enzymes MMP expressions is observed.⁴⁸

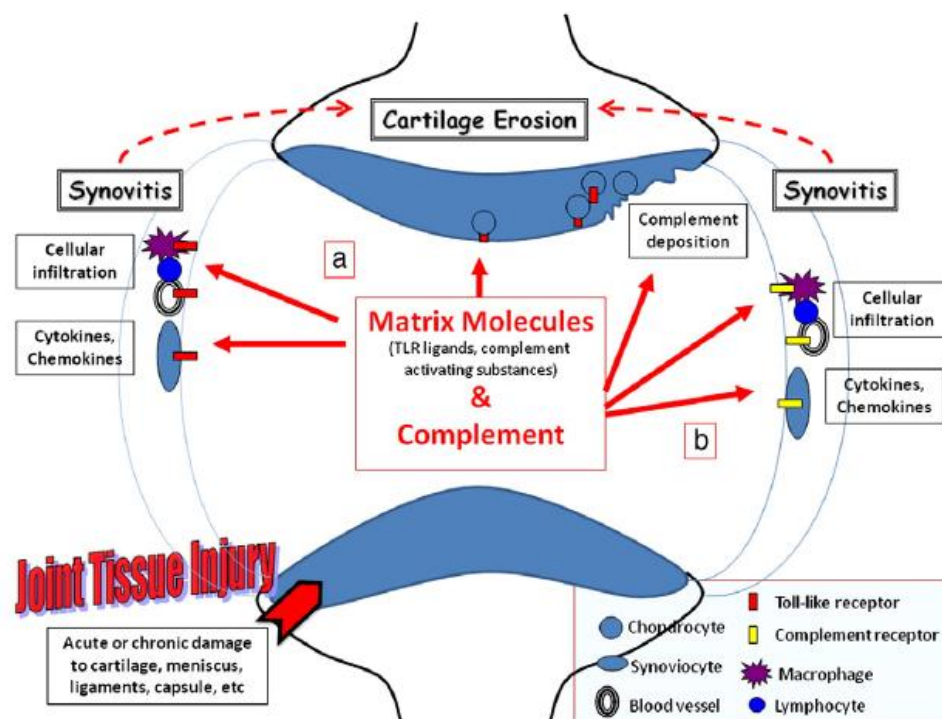


Figure 2-7. A model of Toll-like Receptor (a) and complement activation (b) in the joint leading to synovitis and potentiation of cartilage erosion in OA.⁵¹

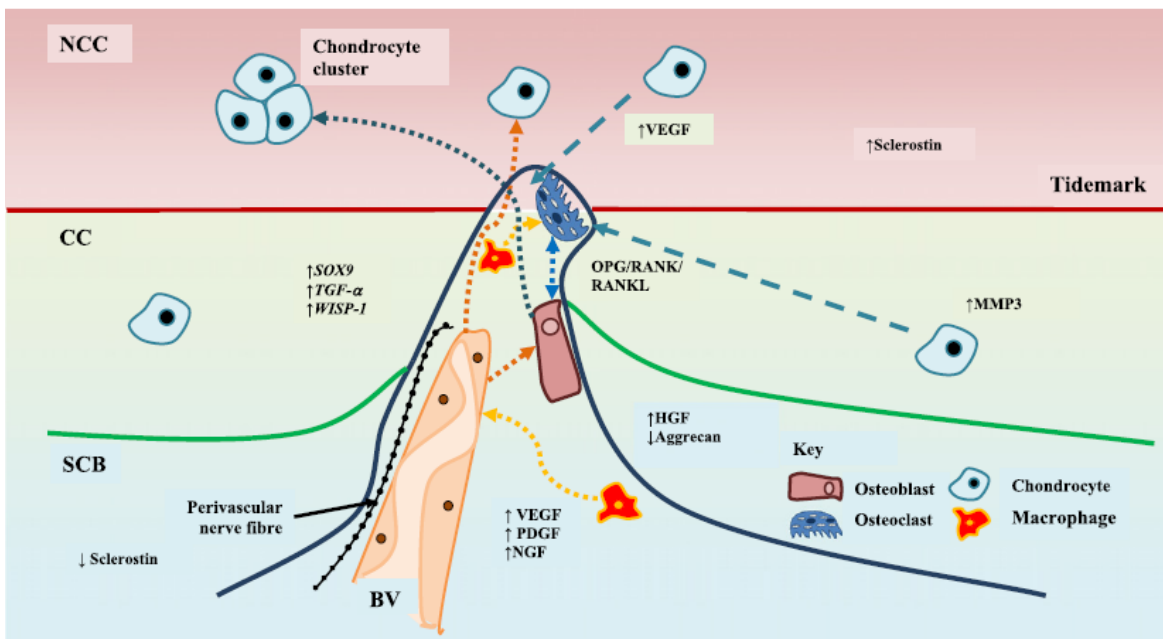


Figure 2-8. Molecular cross-talk at the osteochondral junction. A vascular channel is shown breaching from the subchondral bone (SCB), through the calcified cartilage (CC) into the non-calcified cartilage (NCC).⁶²

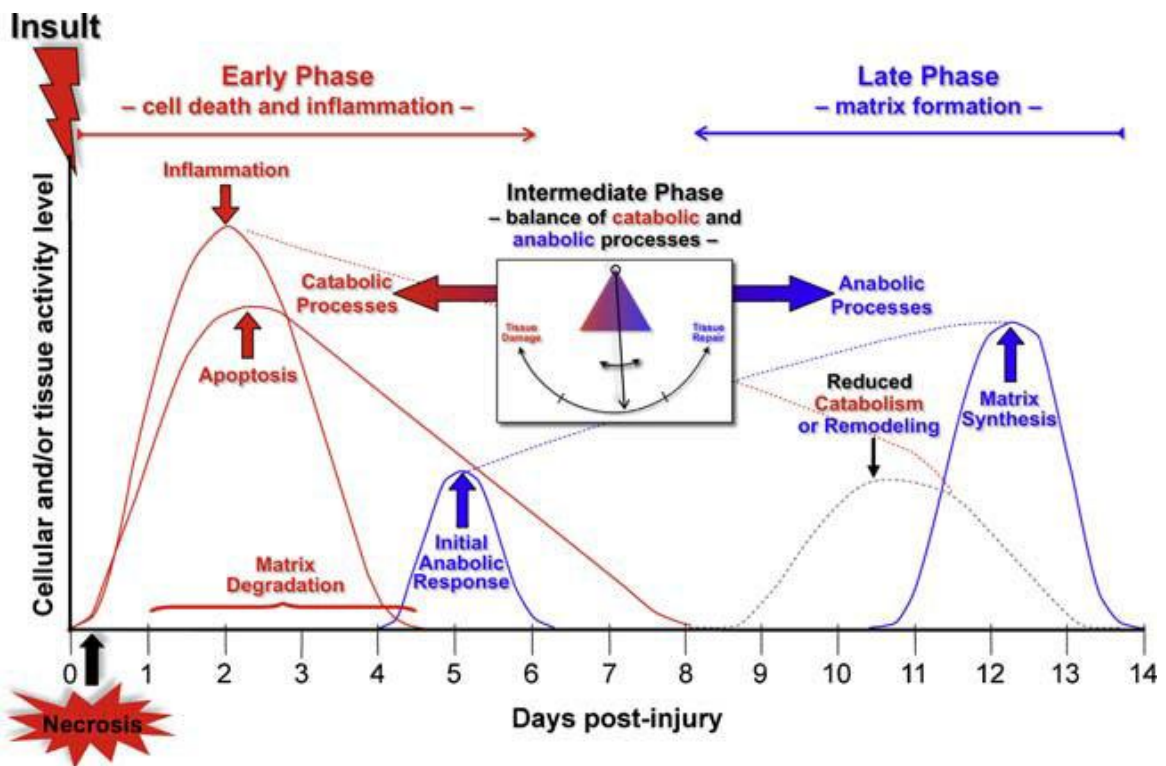


Figure 2-9. Immediate cellular responses within 14 days after acute joint trauma. Catabolic and anabolic processes are involved in the response to the injury and overlap with one another.⁸⁰

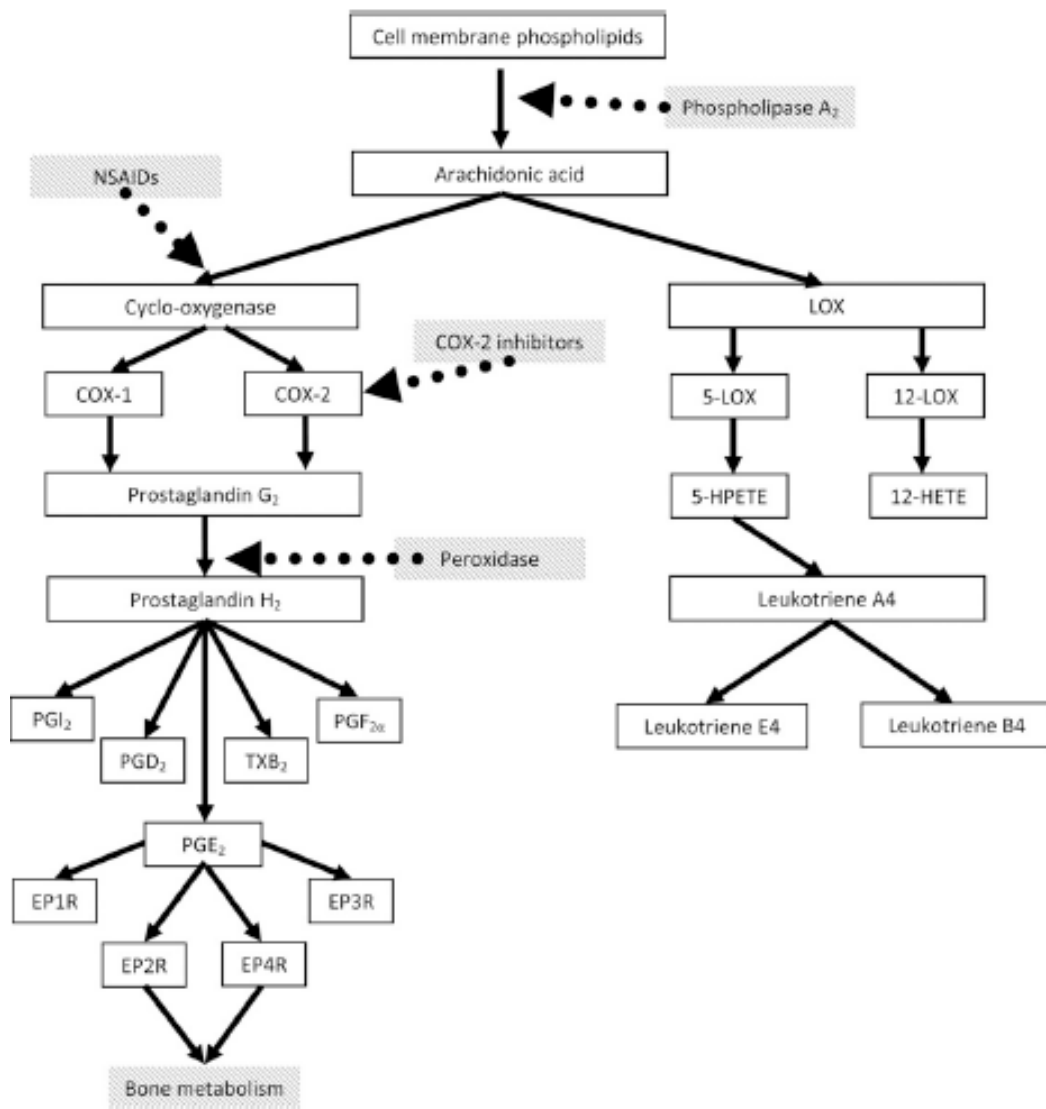


Figure 2-10. Cell membrane phospholipids pathway involving PGE₂.



Figure 2-11. Instron 8821s servo-hydraulic testing machine in the biomechanics lab of the Comparative Orthopaedic Laboratory (COL). For this project, the machine was equipped with a 1000 N load cell attached to the ram which has a maximum ram travel of 260 mm. A stainless steel impactor (tip diameter of 3.9 mm) attached to the end of the ram (below the load cell) and a stainless steel base (containing a stainless steel anvil with specimen-restraining well located in the center) was attached to the test table (See Appendix B for detailed fixture drawings).

Table 2-1. Biologic processes and mediators responsible for joint tissue destruction in osteoarthritis and potential therapeutic interventions.²²

Biologic process	Proposed mediators	Potential therapeutics
Matrix degradation	MMPs 1, 3, 9, and 13, ADAMTS 4 and 5, cathepsin K, serine proteases (HTRA-1) driven by cytokines (ILs 1, 6, 7, 8, 17, and 18, OSM), chemokines (IL-8, GRO α , GRO γ , RANTES, MCP-1) and others (S100 proteins, TGF α , matrix fragments, leukotrienes, and prostaglandins)	Protease inhibitors, TIMPs, anticytokine therapy, TLR inhibition, MAP kinase inhibition, NF- κ B inhibition, lipoxygenase and cyclooxygenase inhibitors
Reduced matrix repair	↓ activity of IGF-1, TGF β , BMP-7 (OP-1), FGF-18	Growth factors (IA or by gene therapy)
Cell death	↓ HMGB-2, ↓ autophagy, reactive oxygen and nitrogen species	Caspase inhibitors, antioxidants, iNOS inhibitors
Chondrocyte hypertrophy	RUNX-2, HIF-2 α , Wnt/ β -catenin, IL-8	PTH, calcitonin
Calcification and crystals	Transglutaminase, inorganic pyrophosphate, TLRs, NLRP3	Phosphocitrates, TLR and NLRP3 inhibition
Subchondral bone sclerosis	Wnt/ β -catenin, ↓ sclerostin, BMPs, IGF-1	Wnt or BMP antagonists, slowing bone remodeling with bisphosphonates or anti-RANKL
Osteophyte formation	TGF β , BMP-2	Since these may stabilize the joint, should probably not be targeted directly
Focal bone remodeling (bone marrow lesions)	RANKL, VEGF	Bisphosphonates, anti-RANKL
Synovitis	IL-1 β , TNF α , IL-17, IL-15, IL-7, CCL19, MCP-1, MIP-1 β , S100 proteins/alarmins	Anticytokine therapy, TLR antagonism, complement inhibition

* MMPs = matrix metalloproteinases; ILs = interleukins; OSM = oncostatin M; GRO α = growth-related oncogene α ; MCP-1 = monocyte chemotactic protein 1; TGF α = transforming growth factor α ; TIMPs = tissue inhibitor of metalloproteinases; TLR = Toll-like receptor; IGF-1 = insulin-like growth factor 1; BMP-7 = bone morphogenic protein 7; OP-1 = osteogenic protein 1; FGF-18 = fibroblast growth factor 18; IA = intraarticular; HMGB-2 = high mobility group box protein 2; iNOS = inducible nitric oxide synthetase; RUNX-2 = runt-related transcription factor 2; HIF-2 α = hypoxia-inducible factor 2 α ; PTH = parathyroid hormone; VEGF = vascular endothelial growth factor; TNF α = tumor necrosis factor α ; MIP-1 β = macrophage inflammatory protein 1 β .

Table 2-2. Reported roles of prostaglandin E2 (PGE2) on cartilage and bone.

Type of Tissue	Normal	Loaded	IL-1	OA
Non-calcified cartilage (NCC)	<p>↑proline⁸⁶</p> <p>↑PG⁸⁷</p> <p>↓DNA synthesis¹⁴⁵</p>		<p>↓PG deg.-↑PG syn.⁸⁸</p> <p>↑MMP-3,-13⁹⁰</p>	<p>↑MMP-3⁹³</p> <p>↓PG syn.⁹²</p> <p>(high dose = 1000ng/ml)</p> <p>↓collagen cleavage</p> <p>(low dose = 10pg/ml⁸⁹)</p>
Calcified cartilage (CC)	<p>↑PG syn.¹⁴⁶</p> <p>↓collagen syn.¹⁴⁶</p>			
Subchondral bone (SCB)	<p>↑collagen II¹⁴⁷</p> <p>↓α1(I) procollagen¹⁴⁸</p> <p>↑IL-1,-6,-11,-17, TNFα, PTH, Vit.D, FG F-2, BMP-2¹⁰⁷</p> <p>↑RANKL/OPG¹⁰⁷</p>	<p>↓OPG/RANKL¹¹²</p>		

Table 2-3. Work by others studying the effect of impact load conditions on cartilage.

Author	Device	Type of Impact		Magnitude	Rate/Duration	Results
Ewers, 2001 ¹³²	Servo-hydraulic	<i>in vitro</i>	unconfined	40 MPa	<i>Low</i> (40 MPa/s)	↑↑ cell death (more distribution) ↑ matrix damage
					<i>High</i> (900 MPa/s)	↑ cell death (near fissures) ↑↑ matrix damage
Ewers, 2002 ¹³⁹	Servo-hydraulic	<i>in vivo</i>	confined		<i>Low</i> (50 ms)	↑ cartilage softening ↑ bone thickening
	Drop-tower	<i>in vivo</i>	confined		<i>High</i> (5 ms)	↑ cartilage softening ↑↑ bone thickening
Quinn, 2001 ¹³⁰	Electro-dynamic	<i>in vitro</i>	unconfined	3.5,7,14 MPa	<i>Low</i> (3×10^{-5} strain/sec)	↑ cell death (more distribution)
					<i>Medium-High</i> (0.3,0.5, 0.7 strain/sec)	↑ cell death (near fissures) ↑ matrix damage ↑ GAG release (up to 24 hrs)
Jeffrey, 2006 ¹⁴⁰	Screw	<i>in vitro</i>	unconfined	Same max strain (%) = average from drop-tower	<i>Low</i> (40 mm/s) cross-head speed	↑ cell death (immediate) ↑↑ matrix damage ↑ peak stress (0.8 MPa) ↑↑ time duration (42 ms) ↑ dynamic modulus (4.5 MPa)
	Drop-tower	<i>in vitro</i>	unconfined	0.12 J Average max strain (%) determined but values not reported	<i>High</i>	↑ cell death (delayed ~72 hrs) ↑ matrix damage ↑↑ peak stress (21.7 MPa) ↑ time duration (1.5 ms) ↑↑ dynamic modulus (87.8 MPa)
Milentijevic, 2003 ³³	Servo-controlled pneumatic	<i>in vitro</i>	confined	10-60 MPa	<i>Medium</i> (350 MPa/s)	↑ compressive strains in the superficial compared to deep zones
Milentijevic, 2005 ³⁵	Servo-controlled pneumatic	<i>in vitro</i>	confined	10,20,30,40 MPa	<i>Low-High</i> (25,50,130,1000 MPa/s)	↑ cell death with higher stress and lower stress rate

↑ or ↑↑ indicates increased minor or major differences compared to control

References

1. Mow VC, Huijskes R. *Basic orthopaedic biomechanics & mechano-biology*. 3rd ed. Philadelphia, PA: Lippincott Williams & Wilkins; 2005.
2. Mitrovic D, Quintero M, Stankovic A, et al. Cell density of adult human femoral condylar articular cartilage. Joints with normal and fibrillated surfaces. *Lab Invest*. 1983;49:309-316.
3. Armstrong CG, Mow VC. Variations in the intrinsic mechanical properties of human articular cartilage with age, degeneration, and water content. *J Bone Joint Surg Am*. 1982;64:88-94.
4. Athanasiou KA, Rosenwasser MP, Buckwalter JA, et al. Interspecies comparisons of in situ intrinsic mechanical properties of distal femoral cartilage. *J Orthop Res*. 1991;9:330-340.
5. Athanasiou KA, Agarwal A, Muffoletto A, et al. Biomechanical properties of hip cartilage in experimental animal models. *Clin Orthop Relat Res*. 1995;254-266.
6. Froimson MI, Ratcliffe A, Gardner TR, et al. Differences in patellofemoral joint cartilage material properties and their significance to the etiology of cartilage surface fibrillation. *Osteoarthritis Cartilage*. 1997;5:377-386.
7. Mow VC, Kuei SC, Lai WM, et al. Biphasic creep and stress relaxation of articular cartilage in compression? Theory and experiments. *J Biomech Eng*. 1980;102:73-84.
8. Mow VC, Holmes MH, Lai WM. Fluid transport and mechanical properties of articular cartilage: a review. *J Biomech*. 1984;17:377-394.
9. Bollet AJ, Nance JL. Biochemical Findings in Normal and Osteoarthritic Articular Cartilage. II. Chondroitin Sulfate Concentration and Chain Length, Water, and Ash Content. *J Clin Invest*. 1966;45:1170-1177.
10. Mankin HJ, Thrasher AZ. Water content and binding in normal and osteoarthritic human cartilage. *J Bone Joint Surg Am*. 1975;57:76-80.
11. Maroudas A, Venn M. Chemical composition and swelling of normal and osteoarthrotic femoral head cartilage. II. Swelling. *Ann Rheum Dis*. 1977;36:399-406.
12. Setton LA, Mow VC, Muller FJ, et al. Altered structure-function relationships for articular cartilage in human osteoarthritis and an experimental canine model. *Agents Actions Suppl*. 1993;39:27-48.

13. Setton LA, Mow VC, Muller FJ, et al. Mechanical properties of canine articular cartilage are significantly altered following transection of the anterior cruciate ligament. *J Orthop Res.* 1994;12:451-463.
14. Lai WM, Hou JS, Mow VC. A triphasic theory for the swelling and deformation behaviors of articular cartilage. *J Biomech Eng.* 1991;113:245-258.
15. Lai WM, Mow VC, Sun DD, et al. On the electric potentials inside a charged soft hydrated biological tissue: streaming potential versus diffusion potential. *J Biomech Eng.* 2000;122:336-346.
16. Lu XL, Sun DD, Guo XE, et al. Indentation determined mechano-electrochemical properties and fixed charge density of articular cartilage. *Ann Biomed Eng.* 2004;32:370-379.
17. Wan LQ, Miller C, Guo XE, et al. Fixed electrical charges and mobile ions affect the measurable mechano-electrochemical properties of charged-hydrated biological tissues: the articular cartilage paradigm. *Mech Chem Biosyst.* 2004;1:81-99.
18. Korhonen R, Saarakkala S. *Biomechanics and modeling of skeletal soft tissues*: InTech; 2011.
19. Vasara AI, Jurvelin JS, Peterson L, et al. Arthroscopic cartilage indentation and cartilage lesions of anterior cruciate ligament-deficient knees. *Am J Sports Med.* 2005;33:408-414.
20. Mak AF, Lai WM, Mow VC. Biphasic indentation of articular cartilage--I. Theoretical analysis. *J Biomech.* 1987;20:703-714.
21. Mow VC, Gibbs MC, Lai WM, et al. Biphasic indentation of articular cartilage--II. A numerical algorithm and an experimental study. *J Biomech.* 1989;22:853-861.
22. Loeser RF, Goldring SR, Scanzello CR, et al. Osteoarthritis: a disease of the joint as an organ. *Arthritis Rheum.* 2012;64:1697-1707.
23. Duncan RL, Turner CH. Mechanotransduction and the functional response of bone to mechanical strain. *Calcif Tissue Int.* 1995;57:344-358.
24. Buckwalter JA, Brown TD. Joint injury, repair, and remodeling: roles in post-traumatic osteoarthritis. *Clin Orthop Relat Res.* 2004;423:7-16.
25. Buckwalter JA. Articular cartilage injuries. *Clin Orthop Relat Res.* 2002;21-37.
26. Kim HT, Lo MY, Pillarisetty R. Chondrocyte apoptosis following intraarticular fracture in humans. *Osteoarthritis Cartilage.* 2002;10:747-749.

27. Borrelli J, Jr., Tinsley K, Ricci WM, et al. Induction of chondrocyte apoptosis following impact load. *J Orthop Trauma*. 2003;17:635-641.
28. D'Lima DD, Hashimoto S, Chen PC, et al. Human chondrocyte apoptosis in response to mechanical injury. *Osteoarthritis Cartilage*. 2001;9:712-719.
29. D'Lima DD, Hashimoto S, Chen PC, et al. Impact of mechanical trauma on matrix and cells. *Clin Orthop Relat Res*. 2001;S90-99.
30. Huser CA, Peacock M, Davies ME. Inhibition of caspase-9 reduces chondrocyte apoptosis and proteoglycan loss following mechanical trauma. *Osteoarthritis Cartilage*. 2006;14:1002-1010.
31. Krueger JA, Thisse P, Ewers BJ, et al. The extent and distribution of cell death and matrix damage in impacted chondral explants varies with the presence of underlying bone. *J Biomech Eng*. 2003;125:114-119.
32. Loening AM, James IE, Levenston ME, et al. Injurious mechanical compression of bovine articular cartilage induces chondrocyte apoptosis. *Arch Biochem Biophys*. 2000;381:205-212.
33. Milentijevic D, Helfet DL, Torzilli PA. Influence of stress magnitude on water loss and chondrocyte viability in impacted articular cartilage. *J Biomech Eng*. 2003;125:594-601.
34. Milentijevic D, Rubel IF, Liew AS, et al. An in vivo rabbit model for cartilage trauma: a preliminary study of the influence of impact stress magnitude on chondrocyte death and matrix damage. *J Orthop Trauma*. 2005;19:466-473.
35. Milentijevic D, Torzilli PA. Influence of stress rate on water loss, matrix deformation and chondrocyte viability in impacted articular cartilage. *J Biomech*. 2005;38:493-502.
36. Natoli RM, Scott CC, Athanasiou KA. Temporal effects of impact on articular cartilage cell death, gene expression, matrix biochemistry, and biomechanics. *Ann Biomed Eng*. 2008;36:780-792.
37. Patwari P, Gaschen V, James IE, et al. Ultrastructural quantification of cell death after injurious compression of bovine calf articular cartilage. *Osteoarthritis Cartilage*. 2004;12:245-252.
38. Waters NP, Stoker AM, Carson WL, et al. Effects of impact velocity and maximum strain on articular cartilage matrix composition, cell viability, and culture media. *55th Annual Meeting of the Orthopaedic Research Society*. Las Vegas, NV. 2009;Paper 1088.

39. Jeffrey JE, Gregory DW, Aspden RM. Matrix damage and chondrocyte viability following a single impact load on articular cartilage. *Arch Biochem Biophys*. 1995;322:87-96.
40. Torzilli PA, Deng XH, Ramcharan M. Effect of compressive strain on cell viability in statically loaded articular cartilage. *Biomech Model Mechanobiol*. 2006;5:123-132.
41. Waters NP, Stoker AM, Pfeiffer FM, et al. Biological effects of impact maximum compression on osteochondral explants. *58th Annual Meeting of the Orthopaedic Research Society*. San Francisco, CA. 2012;Paper 829.
42. Backus JD, Furman BD, Swimmer T, et al. Cartilage viability and catabolism in the intact porcine knee following transarticular impact loading with and without articular fracture. *J Orthop Res*. 2011;29:501-510.
43. Hembree WC, Ward BD, Furman BD, et al. Viability and apoptosis of human chondrocytes in osteochondral fragments following joint trauma. *J Bone Joint Surg Br*. 2007;89:1388-1395.
44. Huser CA, Davies ME. Validation of an in vitro single-impact load model of the initiation of osteoarthritis-like changes in articular cartilage. *J Orthop Res*. 2006;24:725-732.
45. Huser CA, Davies ME. Effect of a glucosamine derivative on impact-induced chondrocyte apoptosis in vitro. A preliminary report. *Osteoarthritis Cartilage*. 2008;16:125-128.
46. Huser CA, Davies ME. Calcium signaling leads to mitochondrial depolarization in impact-induced chondrocyte death in equine articular cartilage explants. *Arthritis Rheum*. 2007;56:2322-2334.
47. Goodwin W, McCabe D, Sauter E, et al. Rotenone prevents impact-induced chondrocyte death. *J Orthop Res*. 2010;28:1057-1063.
48. Gosset M, Berenbaum F, Levy A, et al. Mechanical stress and prostaglandin E2 synthesis in cartilage. *Biorheology*. 2008;45:301-320.
49. Ding L, Stroud NJ, McCabe DJ, et al. A single blunt impact to cartilage activates MAP kinases and NF- κ B radially from impact zone within 24 hours. *55th Annual Meeting of the Orthopaedic Research Society*. Vol Paper No. 1085. Las Vegas, NV2009.
50. Ding L, Heying E, Nicholson N, et al. Mechanical impact induces cartilage degradation via mitogen activated protein kinases. *Osteoarthritis Cartilage*. 2010;18:1509-1517.

51. Scanzello CR, Goldring SR. The role of synovitis in osteoarthritis pathogenesis. *Bone*. 2012;51:249-257.
52. Akira S, Takeda K. Toll-like receptor signalling. *Nat Rev Immunol*. 2004;4:499-511.
53. Pickvance EA, Oegema TR, Jr., Thompson RC, Jr. Immunolocalization of selected cytokines and proteases in canine articular cartilage after transarticular loading. *J Orthop Res*. 1993;11:313-323.
54. Sohn DH, Sokolove J, Sharpe O, et al. Plasma proteins present in osteoarthritic synovial fluid can stimulate cytokine production via Toll-like receptor 4. *Arthritis Research and Therapy*. 2012;14:
55. Seeherman H, Georgiadis K, Flannary C. Chondroprotection Following Acute Joint Injury: Prevention of Osteoarthritis. *HSS Journal*. 2012;8:75-77.
56. Happonen KE, Saxne T, Aspberg A, et al. Regulation of complement by cartilage oligomeric matrix protein allows for a novel molecular diagnostic principle in rheumatoid arthritis. *Arthritis Rheum*. 2010;62:3574-3583.
57. Sjöberg AP, Manderson GA, Mörgelin M, et al. Short leucine-rich glycoproteins of the extracellular matrix display diverse patterns of complement interaction and activation. *Molecular Immunology*. 2009;46:830-839.
58. Sjöberg A, Önnarfjord P, Mörgelin M, et al. The extracellular matrix and inflammation: Fibromodulin activates the classical pathway of complement by directly binding C1q. *Journal of Biological Chemistry*. 2005;280:32301-32308.
59. Kalchishkova N, Fürst CM, Heinega D, et al. NC4 domain of cartilage-specific collagen IX inhibits complement directly due to attenuation of membrane attack formation and indirectly through binding and enhancing activity of complement inhibitors C4B-binding protein and factor H. *Journal of Biological Chemistry*. 2011;286:27915-27926.
60. Brown TD, Johnston RC, Saltzman CL, et al. Posttraumatic osteoarthritis: a first estimate of incidence, prevalence, and burden of disease. *J Orthop Trauma*. 2006;20:739-744.
61. Potter HG, Jain SK, Ma Y, et al. Cartilage injury after acute, isolated anterior cruciate ligament tear: immediate and longitudinal effect with clinical/MRI follow-up. *Am J Sports Med*. 2012;40:276-285.
62. Suri S, Walsh DA. Osteochondral alterations in osteoarthritis. *Bone*. 2012;51:204-211.

63. Haut RC, Ide TM, De Camp CE. Mechanical responses of the rabbit patello-femoral joint to blunt impact. *J Biomech Eng.* 1995;117:402-408.
64. Kurmis AP, Kurmis TP, O'Brien JX, et al. The effect of nonsteroidal anti-inflammatory drug administration on acute phase fracture-healing: a review. *J Bone Joint Surg Am.* 2012;94:815-823.
65. Niki Y, Takaishi H, Takito J, et al. Administration of cyclooxygenase-2 inhibitor reduces joint inflammation but exacerbates osteopenia in IL-1 alpha transgenic mice due to GM-CSF overproduction. *J Immunol.* 2007;179:639-646.
66. Teeple E, Elsaid KA, Jay GD, et al. Effects of supplemental intra-articular lubricin and hyaluronic acid on the progression of posttraumatic arthritis in the anterior cruciate ligament-deficient rat knee. *Am J Sports Med.* 2011;39:164-172.
67. Jay GD, Elsaid KA, Kelly KA, et al. Prevention of cartilage degeneration and gait asymmetry by lubricin tribosupplementation in the rat following anterior cruciate ligament transection. *Arthritis Rheum.* 2012;64:1162-1171.
68. Olewinski R, Wimmer MA, Hakimiyan AA, et al. Therapeutic interventions to inhibit cartilage degeneration, promote cartilage repair, and prevent the development of post-traumatic OA. *58th Annual Meeting of the Orthopaedic Research Society.* Vol Paper No. 1786. San Francisco, CA2012.
69. Gillquist J, Messner K. Anterior cruciate ligament reconstruction and the long-term incidence of gonarthrosis. *Sports Med.* 1999;27:143-156.
70. Laird A, Keating JF. Acetabular fractures: a 16-year prospective epidemiological study. *J Bone Joint Surg Br.* 2005;87:969-973.
71. Weigel DP, Marsh JL. High-energy fractures of the tibial plateau. Knee function after longer follow-up. *J Bone Joint Surg Am.* 2002;84-A:1541-1551.
72. Marsh JL, Weigel DP, Dirschl DR. Tibial plafond fractures. How do these ankles function over time? *J Bone Joint Surg Am.* 2003;85-A:287-295.
73. Buckwalter JA, Brown TD. Joint injury, repair, and remodeling: roles in post-traumatic osteoarthritis. *Clin Orthop Relat Res.* 2004;7-16.
74. Buckwalter JA, Saltzman C, Brown T. The impact of osteoarthritis: implications for research. *Clin Orthop Relat Res.* 2004;S6-15.
75. Thomas TP, Anderson DD, Mosqueda TV, et al. Objective CT-based metrics of articular fracture severity to assess risk for posttraumatic osteoarthritis. *J Orthop Trauma.* 2010;24:764-769.

76. Chaudhari AM, Briant PL, Bevill SL, et al. Knee kinematics, cartilage morphology, and osteoarthritis after ACL injury. *Med Sci Sports Exerc.* 2008;40:215-222.
77. Lohmander LS, Englund PM, Dahl LL, et al. The long-term consequence of anterior cruciate ligament and meniscus injuries: osteoarthritis. *Am J Sports Med.* 2007;35:1756-1769.
78. Waters NP, Stoker AM, Carson WL, et al. Effects of impact velocity and maximum strain on articular cartilage matrix composition, cell viability, and culture media. *55th Annual Meeting of the Orthopaedic Research Society.* Las Vegas, NV. 2009;Paper 1088.
79. Waters NP, Stoker AM, Carson WL, et al. Effects of impact velocity and maximum strain on articular cartilage material properties, extracellular matrix, and tissue inflammation. *56th Annual Meeting of the Orthopaedic Research Society.* New Orleans, LA. 2010;Paper 942.
80. Anderson DD, Chubinskaya S, Guilak F, et al. Post-traumatic osteoarthritis: improved understanding and opportunities for early intervention. *J Orthop Res.* 2011;29:802-809.
81. Chrisman OD, Ladenbauer-Bellis IM, Panjabi M, et al. 1981 Nicolas Andry Award. The relationship of mechanical trauma and the early biochemical reactions of osteoarthritic cartilage. *Clin Orthop Relat Res.* 1981;275-284.
82. Waters NP, Stoker AM, Pfeiffer FM, et al. Effects of impact velocity and maximum strain on articular cartilage material properties, extracellular matrix, and tissue inflammation. *56th Annual Meeting of the Orthopaedic Research Society.* New Orleans, LA. 2010;Paper 942.
83. Guilak F, Fermor B, Keefe FJ, et al. The role of biomechanics and inflammation in cartilage injury and repair. *Clin Orthop Relat Res.* 2004;17-26.
84. Joos H, Hogrefe C, Rieger L, et al. Single impact trauma in human early-stage osteoarthritic cartilage: implication of prostaglandin D2 but no additive effect of IL-1beta on cell survival. *Int J Mol Med.* 2011;28:271-277.
85. Gosset M, Berenbaum F, Levy A, et al. Prostaglandin E2 synthesis in cartilage explants under compression: mPGES-1 is a mechanosensitive gene. *Arthritis Res Ther.* 2006;8:R135.
86. Di Battista JA, Dore S, Martel-Pelletier J, et al. Prostaglandin E2 stimulates incorporation of proline into collagenase digestible proteins in human articular chondrocytes: Identification of an effector autocrine loop involving insulin-like growth factor I. *Mol Cell Endocrinol.* 1996;123:27-35.

87. Lowe GN, Fu YH, McDougall S, et al. Effects of prostaglandins on deoxyribonucleic acid and aggrecan synthesis in the RCJ 3.1C5.18 chondrocyte cell line: role of second messengers. *Endocrinology*. 1996;137:2208-2216.
88. Dingle T. Prostaglandins in human cartilage metabolism. *J Lipid Mediat*. 1993;6:303-312.
89. Tchetina EV, Di Battista JA, Zukor DJ, et al. Prostaglandin PGE₂ at very low concentrations suppresses collagen cleavage in cultured human osteoarthritic articular cartilage: This involves a decrease in expression of proinflammatory genes, collagenases and COL10A1, a gene linked to chondrocyte hypertrophy. *Arthritis Research and Therapy*. 2007;9:
90. Gosset M, Pigenet A, Salvat C, et al. Inhibition of matrix metalloproteinase-3 and -13 synthesis induced by IL-1 β in chondrocytes from mice lacking microsomal prostaglandin E synthase-1. *J Immunol*. 2010;185:6244-6252.
91. Abramson SB. The role of COX-2 produced by cartilage in arthritis. *Osteoarthritis Cartilage*. 1999;7:380-381.
92. Torzilli PA, Tehrany AM, Grigiene R, et al. Effects of misoprostol and prostaglandin E₂ on proteoglycan biosynthesis and loss in unloaded and loaded articular cartilage explants. *Prostaglandins*. 1996;52:157-173.
93. Amin AR, Baraji V, Attur M, et al. Inflammatory mediators (nitric oxide, PGE₂) spontaneously produced by osteoarthritis-affected cartilage regulate stromelysin (MMP-3) production. *Arthritis Rheum*. 1997;40(Suppl):(Abstr).
94. Torzilli PA, Grigiene R, Borrelli J, Jr., et al. Effect of impact load on articular cartilage: cell metabolism and viability, and matrix water content. *J Biomech Eng*. 1999;121:433-441.
95. Kurz B, Jin M, Patwari P, et al. Biosynthetic response and mechanical properties of articular cartilage after injurious compression. *J Orthop Res*. 2001;19:1140-1146.
96. DiMicco MA, Patwari P, Siparsky PN, et al. Mechanisms and kinetics of glycosaminoglycan release following in vitro cartilage injury. *Arthritis Rheum*. 2004;50:840-848.
97. Borrelli J, Jr., Silva MJ, Zaegel MA, et al. Single high-energy impact load causes posttraumatic OA in young rabbits via a decrease in cellular metabolism. *J Orthop Res*. 2009;27:347-352.
98. Mrosek EH, Lahm A, Erggelet C, et al. Subchondral bone trauma causes cartilage matrix degeneration: an immunohistochemical analysis in a canine model. *Osteoarthritis Cartilage*. 2006;14:171-178.

99. Jeffrey JE, Aspden RM. Cyclooxygenase inhibition lowers prostaglandin E2 release from articular cartilage and reduces apoptosis but not proteoglycan degradation following an impact load in vitro. *Arthritis Res Ther.* 2007;9:R129.
100. Green DM, Noble PC, Bocell JR, Jr., et al. Effect of early full weight-bearing after joint injury on inflammation and cartilage degradation. *J Bone Joint Surg Am.* 2006;88:2201-2209.
101. Borrelli J, Jr. Chondrocyte apoptosis and posttraumatic arthrosis. *J Orthop Trauma.* 2006;20:726-731.
102. Duda GN, Eilers M, Loh L, et al. Chondrocyte death precedes structural damage in blunt impact trauma. *Clin Orthop Relat Res.* 2001;302-309.
103. D'Lima DD, Hashimoto S, Chen PC, et al. Prevention of chondrocyte apoptosis. *J Bone Joint Surg Am.* 2001;83-A Suppl 2:25-26.
104. Natoli RM, Athanasiou KA. P188 reduces cell death and IGF-I reduces GAG release following single-impact loading of articular cartilage. *J Biomech Eng.* 2008;130:art. no. 041012.
105. Blackwell KA, Raisz LG, Pilbeam CC. Prostaglandins in bone: bad cop, good cop? *Trends Endocrinol Metab.* 2010;21:294-301.
106. Klein DC, Raisz LG. Prostaglandins: stimulation of bone resorption in tissue culture. *Endocrinology.* 1970;86:1436-1440.
107. Pilbeam CC, Choudhary S, Blackwell K, et al. Prostaglandins and bone metabolism. *Principles of Bone Biology.* 2008;1235-1271.
108. Tian XY, Zhang Q, Zhao R, et al. Continuous PGE2 leads to net bone loss while intermittent PGE2 leads to net bone gain in lumbar vertebral bodies of adult female rats. *Bone.* 2008;42:914-920.
109. High WB. Effects of orally administered prostaglandin E-2 on cortical bone turnover in adult dogs: a histomorphometric study. *Bone.* 1987;8:363-373.
110. Weinreb M, Rutledge SJ, Rodan GA. Systemic administration of an anabolic dose of prostaglandin E2 induces early-response genes in rat bones. *Bone.* 1997;20:347-353.
111. Endo K, Sairyo K, Komatsubara S, et al. Cyclooxygenase-2 inhibitor delays fracture healing in rats. *Acta Orthop.* 2005;76:470-474.
112. Sanchez C, Gabay O, Salvat C, et al. Mechanical loading highly increases IL-6 production and decreases OPG expression by osteoblasts. *Osteoarthritis and Cartilage.* 2009;17:473-481.

113. Simon AM, O'Connor JP. Dose and time-dependent effects of cyclooxygenase-2 inhibition on fracture-healing. *J Bone Joint Surg Am.* 2007;89:500-511.
114. Xie C, Ming X, Wang Q, et al. COX-2 from the injury milieu is critical for the initiation of periosteal progenitor cell mediated bone healing. *Bone.* 2008;43:1075-1083.
115. Rapuano BE, Boursiquot R, Tomin E, et al. The effects of COX-1 and COX-2 inhibitors on prostaglandin synthesis and the formation of heterotopic bone in a rat model. *Arch Orthop Trauma Surg.* 2008;128:333-344.
116. Bonewald LF, Johnson ML. Osteocytes, mechanosensing and Wnt signaling. *Bone.* 2008;42:606-615.
117. Goessling W, North TE, Loewer S, et al. Genetic interaction of PGE2 and Wnt signaling regulates developmental specification of stem cells and regeneration. *Cell.* 2009;136:1136-1147.
118. Abramson SB. Osteoarthritis and nitric oxide. *Osteoarthritis Cartilage.* 2008;16 Suppl 2:S15-20.
119. Grabowski PS, Wright PK, Van 't Hof RJ, et al. Immunolocalization of inducible nitric oxide synthase in synovium and cartilage in rheumatoid arthritis and osteoarthritis. *Br J Rheumatol.* 1997;36:651-655.
120. Fermor B, Weinberg JB, Pisetsky DS, et al. Induction of cyclooxygenase-2 by mechanical stress through a nitric oxide-regulated pathway. *Osteoarthritis Cartilage.* 2002;10:792-798.
121. Radin EL, Paul IL, Lowy M. A comparison of the dynamic force transmitting properties of subchondral bone and articular cartilage. *J Bone Joint Surg Am.* 1970;52:444-456.
122. Repo RU, Finlay JB. Survival of articular cartilage after controlled impact. *J Bone Joint Surg Am.* 1977;59:1068-1076.
123. Burgin LV, Aspden RM. A drop tower for controlled impact testing of biological tissues. *Med Eng Phys.* 2007;29:525-530.
124. Scott CC, Athanasiou KA. Design, validation, and utilization of an articular cartilage impact instrument. *Proc Inst Mech Eng [H].* 2006;220:845-855.
125. Thompson RC, Jr., Oegema TR, Jr., Lewis JL, et al. Osteoarthrotic changes after acute transarticular load. An animal model. *J Bone Joint Surg Am.* 1991;73:990-1001.

126. Vrahas MS, Smith GA, Rosler DM, et al. Method to impact in vivo rabbit femoral cartilage with blows of quantifiable stress. *J Orthop Res.* 1997;15:314-317.
127. Lahm A, Uhl M, Erggelet C, et al. Articular cartilage degeneration after acute subchondral bone damage: an experimental study in dogs with histopathological grading. *Acta Orthop Scand.* 2004;75:762-767.
128. Borrelli J, Jr., Burns ME, Ricci WM, et al. A method for delivering variable impact stresses to the articular cartilage of rabbit knees. *J Orthop Trauma.* 2002;16:182-188.
129. Frank EH, Jin M, Loening AM, et al. A versatile shear and compression apparatus for mechanical stimulation of tissue culture explants. *J Biomech.* 2000;33:1523-1527.
130. Quinn TM, Allen RG, Schalet BJ, et al. Matrix and cell injury due to sub-impact loading of adult bovine articular cartilage explants: effects of strain rate and peak stress. *J Orthop Res.* 2001;19:242-249.
131. Furman BD, Strand J, Hembree WC, et al. Joint degeneration following closed intraarticular fracture in the mouse knee: a model of posttraumatic arthritis. *J Orthop Res.* 2007;25:578-592.
132. Ewers BJ, Dvoracek-Driksna D, Orth MW, et al. The extent of matrix damage and chondrocyte death in mechanically traumatized articular cartilage explants depends on rate of loading. *J Orthop Res.* 2001;19:779-784.
133. Ashwell MS, O'Nan AT, Gonda MG, et al. Gene expression profiling of chondrocytes from a porcine impact injury model. *Osteoarthritis Cartilage.* 2008;16:936-946.
134. Borrelli J, Jr., Torzilli PA, Grigiene R, et al. Effect of impact load on articular cartilage: development of an intra-articular fracture model. *J Orthop Trauma.* 1997;11:319-326.
135. Jeffrey JE, Thomson LA, Aspden RM. Matrix loss and synthesis following a single impact load on articular cartilage in vitro. *Biochim Biophys Acta.* 1997;1334:223-232.
136. Jeffrey JE, Aspden RM. The biophysical effects of a single impact load on human and bovine articular cartilage. *Proc Inst Mech Eng [H].* 2006;220:677-686.
137. Ward BD, Furman BD, Huebner JL, et al. Absence of posttraumatic arthritis following intraarticular fracture in the MRL/MpJ mouse. *Arthritis Rheum.* 2008;58:744-753.

138. Ewers BJ, Jayaraman VM, Banglmaier RF, et al. The effect of loading rate on the degree of acute injury and chronic conditions in the knee after blunt impact. *Stapp Car Crash J.* 2000;44:299-313.
139. Ewers BJ, Jayaraman VM, Banglmaier RF, et al. Rate of blunt impact loading affects changes in retropatellar cartilage and underlying bone in the rabbit patella. *J Biomech.* 2002;35:747-755.
140. Jeffrey JE, Brodie JP, Aspden RM. The effects of a single fast impact load compared with slow severe loading on articular cartilage in vitro. *Osteoarthritis Cartilage.* 2006;14:S81-S82.
141. Robinovitch SN, Chiu J. Surface stiffness affects impact force during a fall on the outstretched hand. *J Orthop Res.* 1998;16:309-313.
142. King AI. Fundamentals of impact biomechanics: Part 2--Biomechanics of the abdomen, pelvis, and lower extremities. *Annu Rev Biomed Eng.* 2001;3:27-55.
143. Mow VC, Ratcliffe A, Poole AR. Cartilage and diarthrodial joints as paradigms for hierarchical materials and structures. *Biomaterials.* 1992;13:67-97.
144. Li C, Pruitt LA, King KB. Nanoindentation differentiates tissue-scale functional properties of native articular cartilage. *J Biomed Mater Res A.* 2006;78:729-738.
145. Lowe GN, Fu YH, McDougall S, et al. Prostaglandin effects on proliferation and second messenger generation in the rat RCJ 3.1CS.18 chondrocyte line. *J Bone Miner Res.* 1992;7(Suppl1):675.
146. O'Keefe RJ, Crabb ID, Puzas JE, et al. Influence of prostaglandins on DNA and matrix synthesis in growth plate chondrocytes. *J Bone Miner Res.* 1992;7:397-404.
147. Raisz LG, Fall PM, Gabbitas BY, et al. Effects of prostaglandin E2 on bone formation in cultured fetal rat calvariae: role of insulin-like growth factor-I. *Endocrinology.* 1993;133:1504-1510.
148. Raisz LG, Fall PM, Petersen DN, et al. Prostaglandin E2 inhibits alpha 1(I)procollagen gene transcription and promoter activity in the immortalized rat osteoblastic clonal cell line Py1a. *Mol Endocrinol.* 1993;7:17-22.

CHAPTER 3

OPTIMIZATION OF AN IN VITRO MECHANICAL INJURY DEVICE

Introduction

The initial investigation of using a servo-hydraulic testing machine (Instron 8821s, Canton, MA) to approach constant velocity impact to desired maximum strain of canine cartilage for development of an *in vitro* post-traumatic osteoarthritis model is described fully in a final report for the graduate course, Biological Engineering (BE 7001):

Problems in Biological Engineering completed by Nicole Poythress Waters on December 31, 2008. A hard copy is stored on file in the Department of Biological Engineering office at the University of Missouri-Columbia. The purpose of this chapter is to summarize and provide a working reference for future studies to the impact protocol developed and used to measure the thickness of and impact the specimens for the studies in this dissertation.

The objectives of the work in the aforementioned final report were to:

- 1) Determine whether the Instron 8821s servo-hydraulic testing machine was capable of impacting canine cartilage at a constant velocity to a specified maximum strain (compression divided by initial specimen thickness)
- 2) Determine the maximum impact velocity capability of the Instron by tuning its proportional-integral-derivative (PID) values
- 3) Develop a method to measure specimen thickness and then use this thickness to impact the specimen to a desired maximum strain

- 4) Determine if a cartilage specimen's impact resistance force (which is unknown and thus uncontrollable) would have a significant effect on the ram's impact position response (i.e. desired impact velocity and maximum strain).

Methods

The custom designed fixtures used to measure thickness and deliver impact load to a 4.0 mm diameter cartilage explant specimen is shown in Fig. 3-1. Appendix B contains shop drawings for each component. Optimal PID values were found to be 40, 0, 0. A relative ram displacement impact control program was used to run impact tests with no cartilage specimen in the well (hereafter referred to as “no load”) tests at programmed constant impact velocities v_1 of 125, 100, 50, 25, and 1 mm/sec to evaluate the ram's actual velocity, v_1 , and its overshoot, T_o . The maximum ram velocity that the Instron could produce was found to be 100 mm/sec. Overshoot T_o was found to be dependent upon the selected input velocity, but repeatable for a selected velocity. The protocol and equations for measuring thickness of a specimen and thereafter determining the absolute initial ram position to use to impact the specimen at the selected velocity to the desired maximum level of compressive strain were derived. The resistance force of a rubber simulated specimen was found to have negligible effect on ram impact velocity and overshoot, and thus should have negligible effect when impacting cartilage specimens as further discussed. An attempt was made to use the force indicated by the 1000 N (Lebow model 3173 strain gauge, Eaton Corporation, Troy, MI) load cell attached between the ram and the punch (Fig. 3-1) to determine impact stress delivered to (resisted by) the specimen, the specimen's material moduli (stiffness parameters), and the energy absorbed by the specimen during impact. The load cell was not an inertia force compensated

model. Attempts to compensate the indicated force to obtain reliable measurement of the resistance force during impact of the specimen failed, and thus corresponding stress, moduli and energy results are not available for the specimens tested for the studies presented in Chapter 4.

Results

Impact Protocol with Controlled Impact Velocity and Maximum Strain

The following position-control impact program with set maximum ram velocity, v_1 , was generated using Instron's RS BasLab Scheduler Editor computer software to control the Instron 8821s ram position. An actual response for the numerical value of parameters given in the program listing, and definition of parameters is illustrated in Fig. 3-2:

Constant Velocity Impact Program

Step 1 (Hold)

Time duration (sec)	2
---------------------	---

Step 2 (Trapezoid waveform)

End Point 1, EP ₁ (mm)	-2.25
Rate 1, v_1 (mm/sec)	100
Dwell 1, D ₁ (sec)	1.0
End Point 2, EP ₂ (mm)	0
Rate 2, v_2 (mm/sec)	1.0
Dwell 2, D ₂ (sec)	1.0
Reset after (cycles)	1.0

Step 3 (Hold)

Time duration (sec)	2
---------------------	---

End point relative ram travel, EP₁, was selected to be -2.25 mm (for all tests) to assure that the ram has reached constant velocity prior to making contact with the specimen at

displacement, P_i , that corresponds to the superior surface of a specimen with initial thickness, T_i , placed in the bottom of the well in the anvil. The final compressed thickness of the specimen is, T_f . The maximum compressed thickness of the specimen is T_m , which results from ram overshoot T_o beyond EP_1 . The trapezoid waveform was used due to its intrinsic dwell time characteristics, thus minimizing additional hold steps. A nominal rate of $v_2 = 1.00$ mm/sec was arbitrarily selected to remove the ram from the specimen.

Controlling Maximum Specimen Compression for Various Impact Velocities

Overshoot, T_o , is a function of the selected desired “set” impact velocity v_1 as shown in the representative ram displacement versus time impact traces for the set velocities (100, 50, 25, 10, 1 mm/sec) in Fig. 3-3 – 3-7, respectively, and as summarized in Table 3-1. The resolution of the numerical values for T_m , T_f and thus T_o are limited to that produced by the Instron’s 16 bit data acquisition software in conjunction with the ram’s 254 mm total possible range of travel, i.e. resolution = $254 / 2^{16} = 0.00388$ mm. The effect of this resolution limitation can be observed in Fig. 3-3 – 3-7 as 0.00388 mm step changes in indicated ram displacement. Suggestions to improve ram displacement resolution are further summarized.

Discussion

The following are important observations relative to the characteristics of the Instron's ram displacement-time examples in Fig. 3-3 – 3-7.

1. The velocity (slope of the ram displacement trace) during impact (red data points in the figures) is essentially constant (to within 0.05 mm of maximum travel for

set velocity $v_1 = 100$ mm/sec with range of constant impact velocity improving with decreasing set velocity).

2. Final compressed thickness T_f was repeatable to within the resolution of the Instron for repeated test runs, and was not effected by the set velocity v_1 .
3. Overshoot T_o was repeatable to within the resolution of the Instron for repeated runs with the same set velocity, but was a function of set velocity.

Setting Initial Absolute Ram Position to Achieve Desired Maximum Strain

The Instron's control panel displays absolute ram position, AP, and likewise the data acquisition software records absolute ram position. The relationship between absolute initial ram position, AP_i , and the impact displacement parameters illustrated in Fig. 3-8 is

$$AP_i = AP_b + T_m + T_o + |EP_1| \quad (3-1)$$

AP_b is the absolute ram position with punch tip touching the bottom of the empty well (in anvil), which is a measurement made and recorded in the first step in measuring an explants thickness. T_m is the maximum compressed cartilage thickness. T_o is the compression overshoot. EP_1 is the set ram displacement at end point 1.

Maximum strain, ϵ , is defined as the change in explant thickness ($T_i - T_m$) divided by initial thickness, T_i . Solving this relationship for T_m and substituting it into Eq. 3-1 yields

$$AP_i = AP_b + (1-\epsilon)T_i + T_o + |EP_1| \quad (3-2)$$

Overshoot, T_o , is dependent on impact velocity as was shown in Table 3-1.

Appendix A contains the step-by-step protocol to measure thickness T_i of an explant, use Eq. 3-2 to determine initial ram position, AP_i , and then impact cartilage to the desired strain.

Effect of Specimen Impact Resistance Force

The impact program was used to impact a 4.0 mm diameter, $T_i = 0.73$ mm thick rubber cylinder simulated explant at a set velocity of 100 mm/sec and desired maximum 50% strain to investigate what effect an explant's resistive force would have on the ram's impact motion. Of particular importance was to determine if the existence of an explant would affect the magnitude of ram overshoot T_o , and thus the ability to use no load determined values of overshoot T_o in Table 3-1 to calculate and set the ram's initial absolute position AP_i to achieve the desired maximum strain.

Fig. 3-9A contains a trace of the indicated force (from the 1000N Lebow strain gauge load cell shown in Fig. 3-1) with no explant (i.e. no resistive force applied to tip of the punch) during impact motion created with same set parameters used when impacting the rubber specimen. Fig. 3-9B contains a trace of the indicated force during impact of the rubber specimen, with corresponding ram position trace shown in Fig. 3-10.

If the load cell was an inertial force compensated model, theoretically the indicated force trace with no specimen would be zero during the entire impact motion, regardless of whether the ram-punch was accelerating or decelerating. The indicated force with no specimen present was zero during the zero acceleration initial and final hold periods, and nearly so during the nearly constant velocity v_1 (zero acceleration) portion of ram travel. This is an indication that the load cell had been properly zeroed. However, during the acceleration-deceleration from the initial hold to the constant velocity impact the indicated force ranged from a maximum compression (-120.94 N) to maximum tension force (+ 64.09 N), and during the deceleration to dwell 2 a maximum tension force (109.86 N), which is an indication that the 1000 N load cell with attached mass of punch

is not inertial force compensated, and would need to be for accurate measurement of the dynamic resistance of an explant.

With the rubber explant in place, the load cell correctly indicated zero force during the initial ram position hold, which is proof that it was and remained correctly zeroed. Thus assuming it was correctly calibrated (which is required by the Instron controller upon start up) the constant indicated compressive force (-28.57 N) during the end of dwell 2 should be an accurate indication of the force on the specimen when compressed to its final compressed thickness T_f . The corresponding final compressive stress would be $\sigma_f = (-28.57) / \pi(0.00195)^2 = 2.392$ MPa. One can obtain an indication of the maximum compressive force applied to the rubber explant if one assumes that it occurred at maximum compression T_m and that the indicated maximum force (-1.53 N and +109.86 N) during impact with and without the specimen present, respectively, occurred at the same maximum ram position. Subtracting the without specimen maximum indicated force from the with specimen gives a predicted maximum compressive force of -111.39 N resisted by the rubber specimen, with corresponding stress of 9.32 MPa.

By comparing the ram displacement trace results in Fig. 3-10 (with specimen) to Fig. 3-3 (without specimen), overshoot (0.13 mm) was the same to within the resolution of the Instron ram position measurement capabilities. The maximum strain observed with the rubber specimen was 46.6 % compared to the desired 50%. The lower observed strain is likely the result of an accumulation of resolution errors in measuring thickness T_i , determination of T_o values in Table 3-1, measurement of AP_b to calculate the initial ram position AP_i and then the ability to set the ram to the exact AP_i position.

Thus, it was concluded that the rubber specimen impact resistance force had a negligible effect on the impact motion of the massive ram of the Instron 8821s. Cartilage specimens with maximum resistive stress of the order of 10 MPa or less should likewise have negligible effect. In the literature (see Table 2-3), the maximum resistive stress while impacting cartilage was reported to range from 3 to 60 MPa. If these higher maximum resistive stress values (>10) are experienced while using the Instron 8821s, overshoot T_o actually achieved during these tests may be less than the “no load” values in Table 3-1, and thus the actual maximum strain (compression T_m) achieved may be less than the desired controlled value. Overshoot T_o can be checked for actual cartilage runs (particularly those that produce high stress values) to determine if higher explant resistive force is having a notable effect on T_o .

For future impact work with the Instron 8821s, a miniature piezoelectric load cell should be placed under the anvil, which will eliminate the effect of acceleration since the load cell itself would be stationary and the anvil in which the explant is placed would be nearly stationary during the impact test.

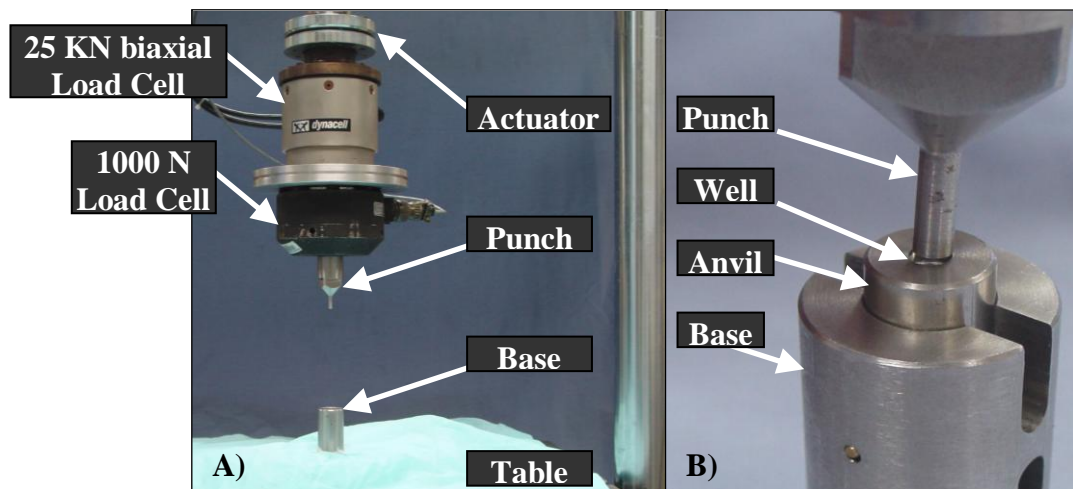


Figure 3-1. Custom designed stainless steel fixtures used to measure thickness and deliver impact load to ex vivo cartilage explants: A) Flat-tip punch (3.9-mm diameter) attached to load cell on test machine (Instron 8821S) actuator and fixture base attached to test machine table, and B) Removable anvil with 4.0 dia. by 2.54 mm deep well to laterally-constrain explant.

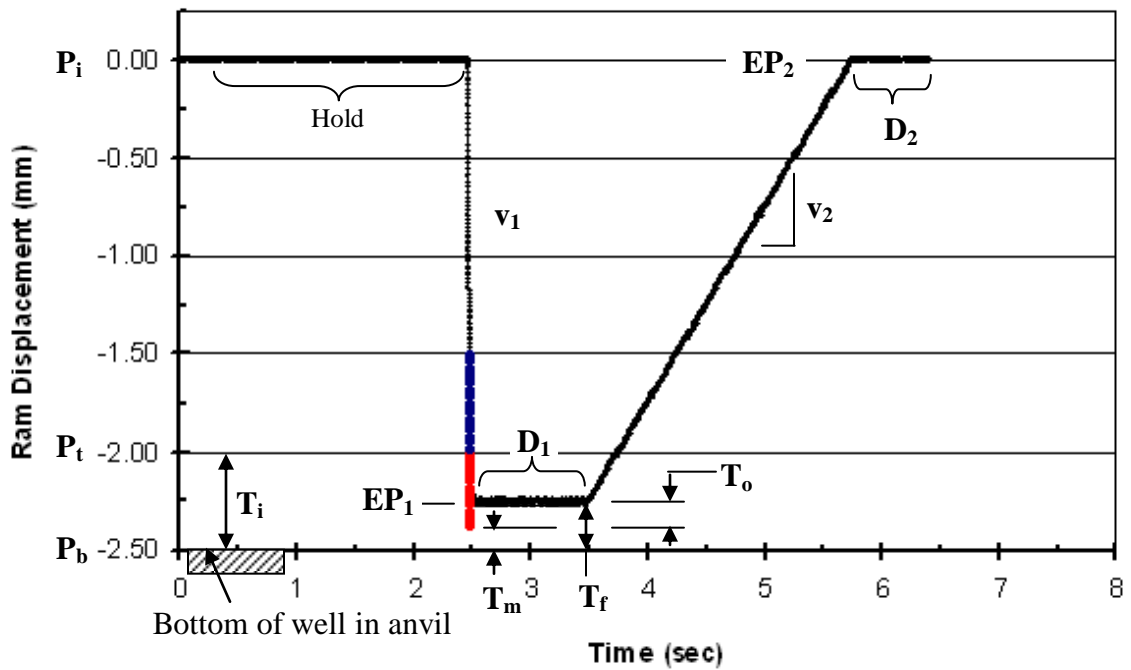


Figure 3-2. Impact parameter terminology and actual response generated using given parameter values for Instron computer software program and PID values 40, 0, 0. A specimen with assumed initial thickness $T_i = 0.5$ mm is used for illustrative purposes.

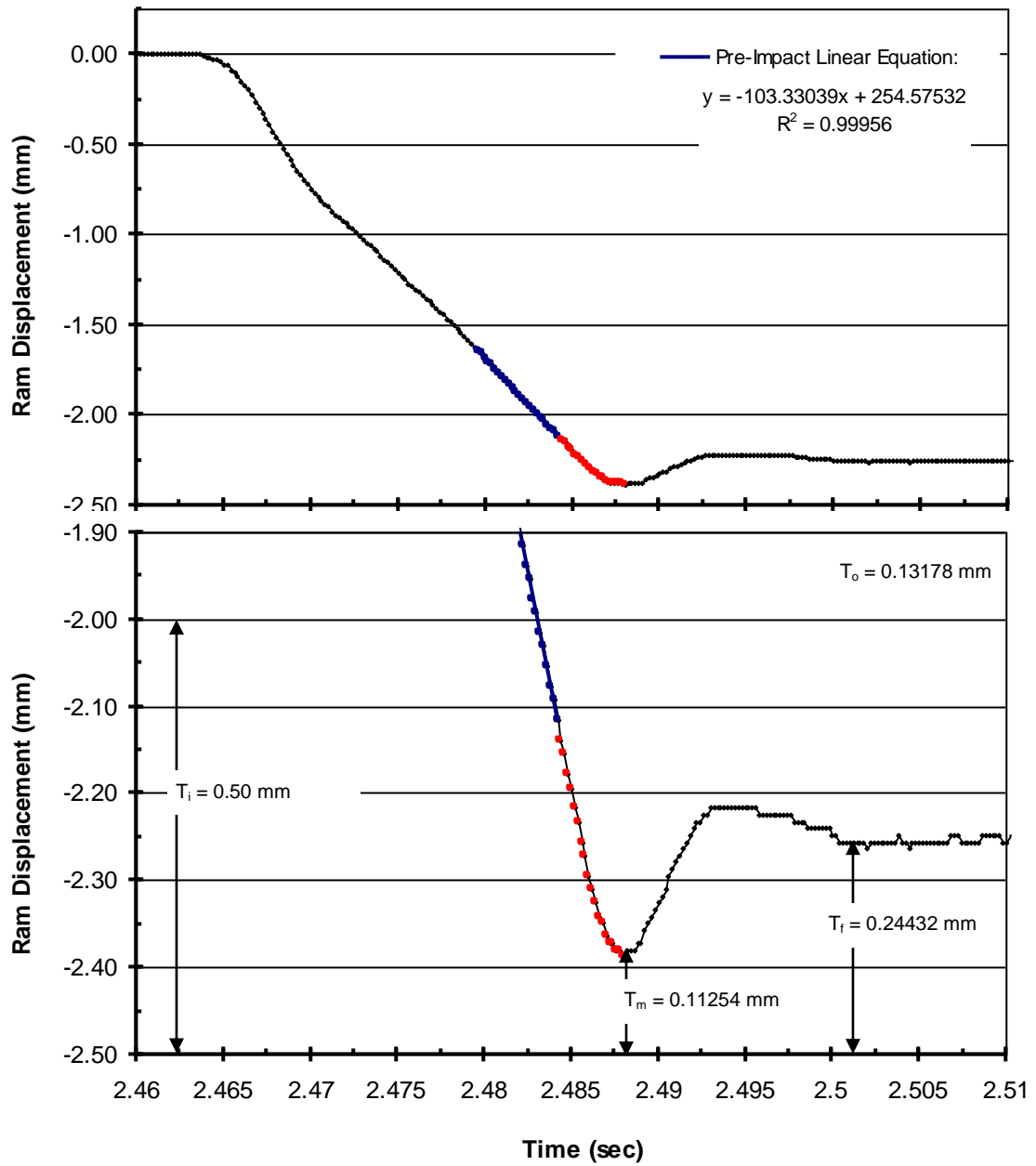


Figure 3-3. 100 mm/sec set velocity v1 no load impact ram displacement (PID = 40, 0, 0; EP1 = -2.25 mm). Red indicates data in impact region assuming cartilage initial thickness, $T_i = 0.5$ mm.

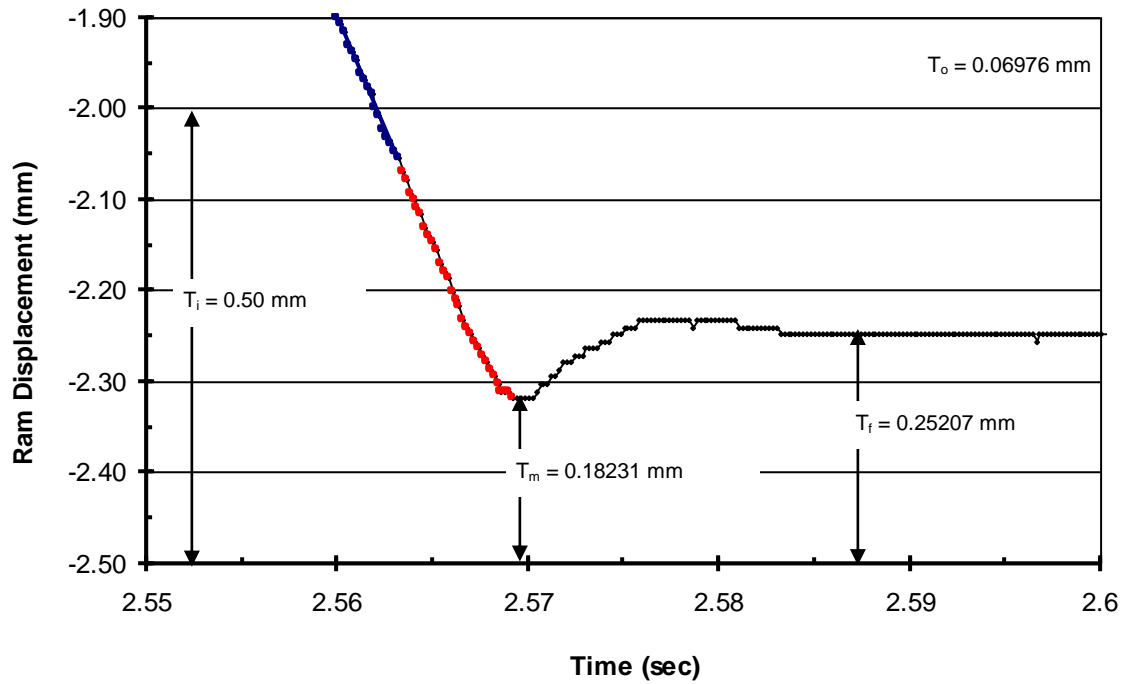
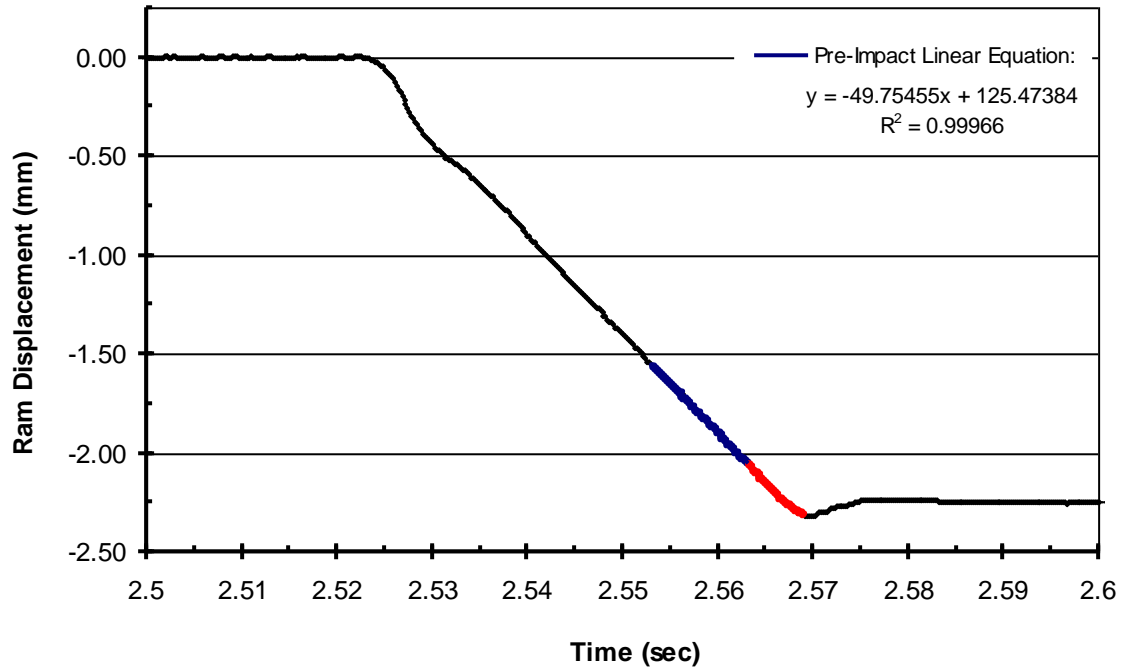


Figure 3-4. 50 mm/sec set velocity v1 no load impact ram displacement (PID = 40, 0, 0; EP1 = -2.25 mm). Red indicates data in impact region assuming cartilage initial thickness, $T_i = 0.5$ mm.

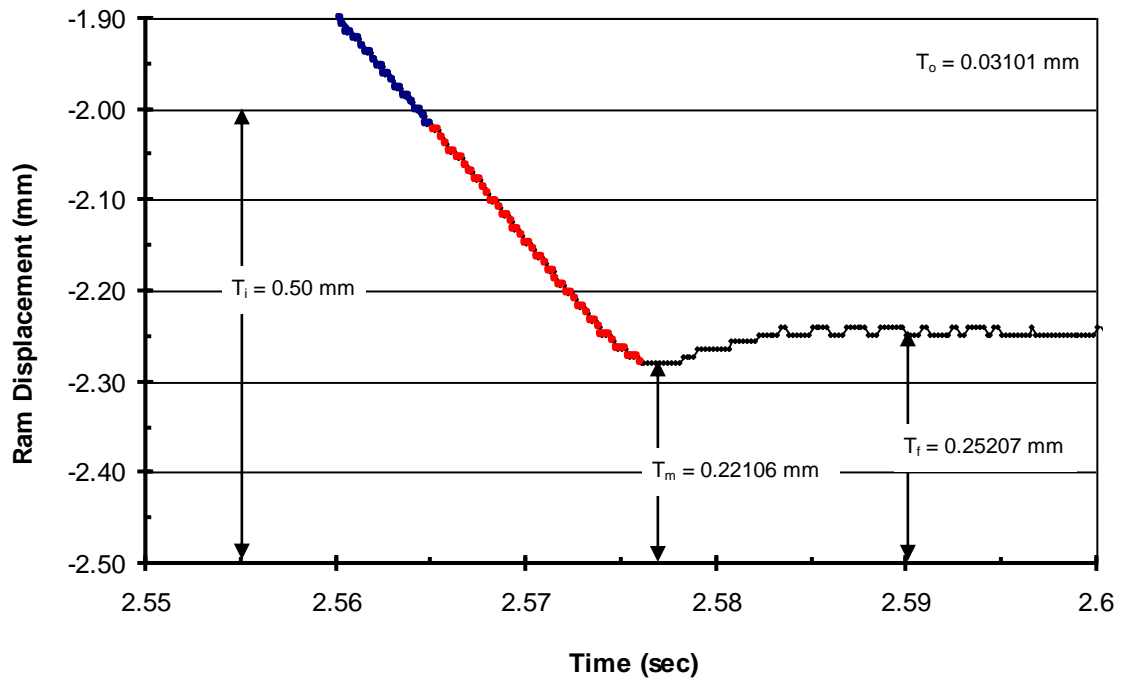
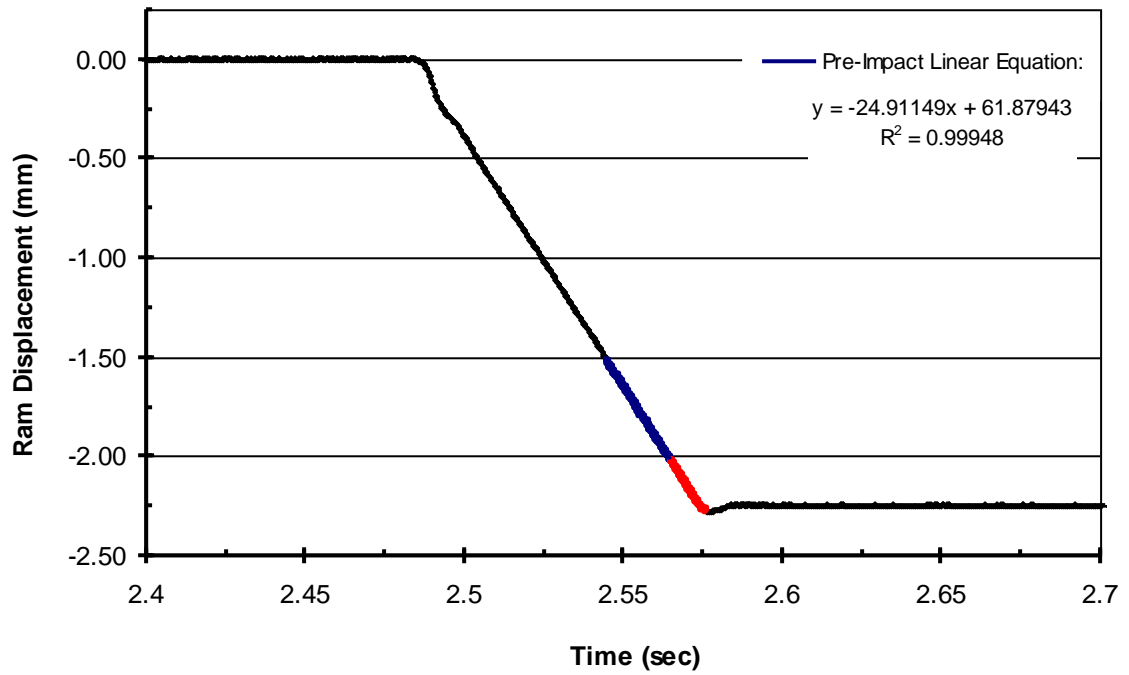


Figure 3-5. 25 mm/sec set velocity v1 no load impact ram displacement (PID = 40, 0, 0; EP1 = -2.25 mm). Red indicates data in impact region assuming cartilage initial thickness, $T_i = 0.5 \text{ mm}$.

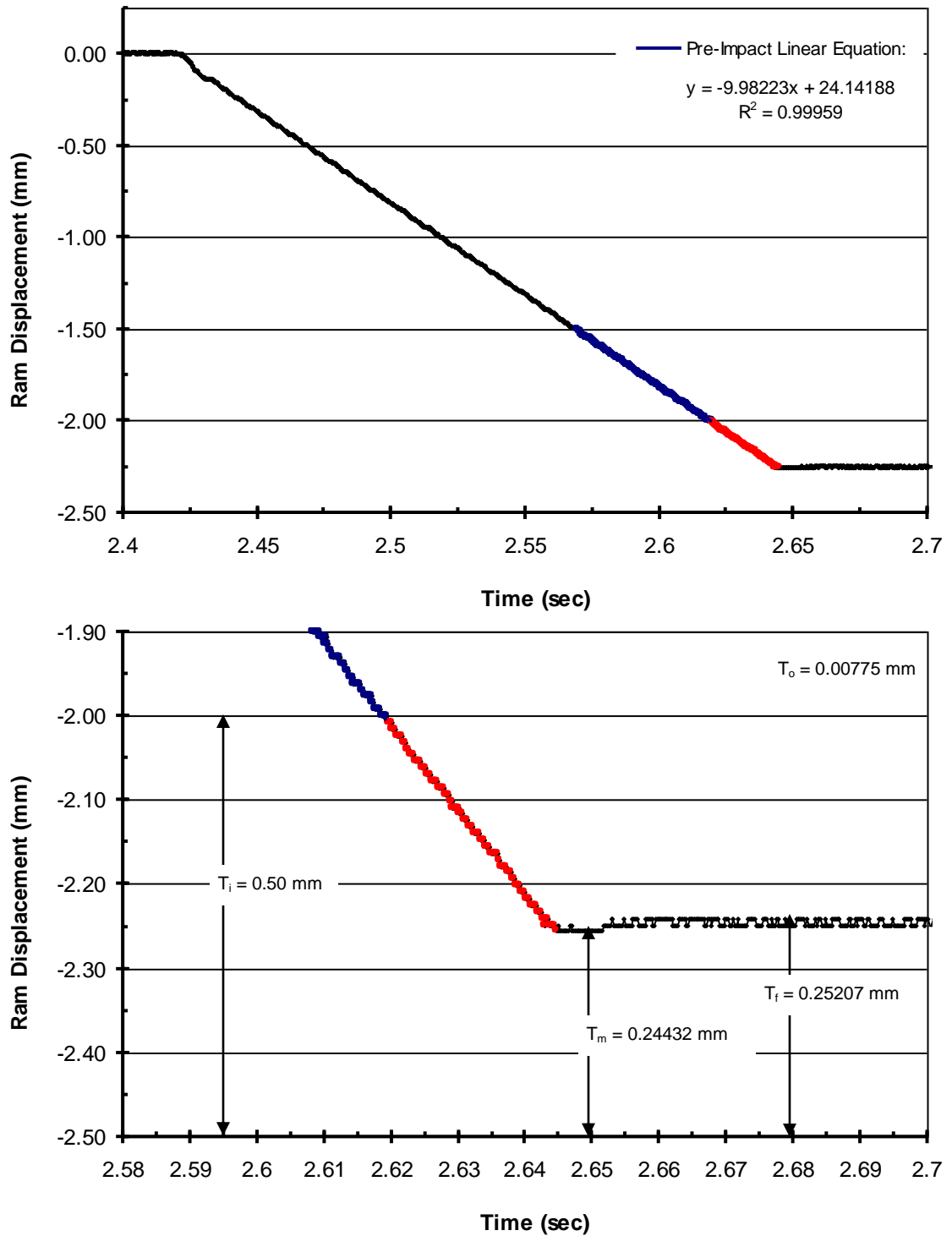


Figure 3-6. 10 mm/sec set velocity v1 no load impact ram displacement (PID = 40, 0, 0; EP1 = -2.25 mm). Red indicates data in impact region assuming cartilage initial thickness, $T_i = 0.5$ mm.

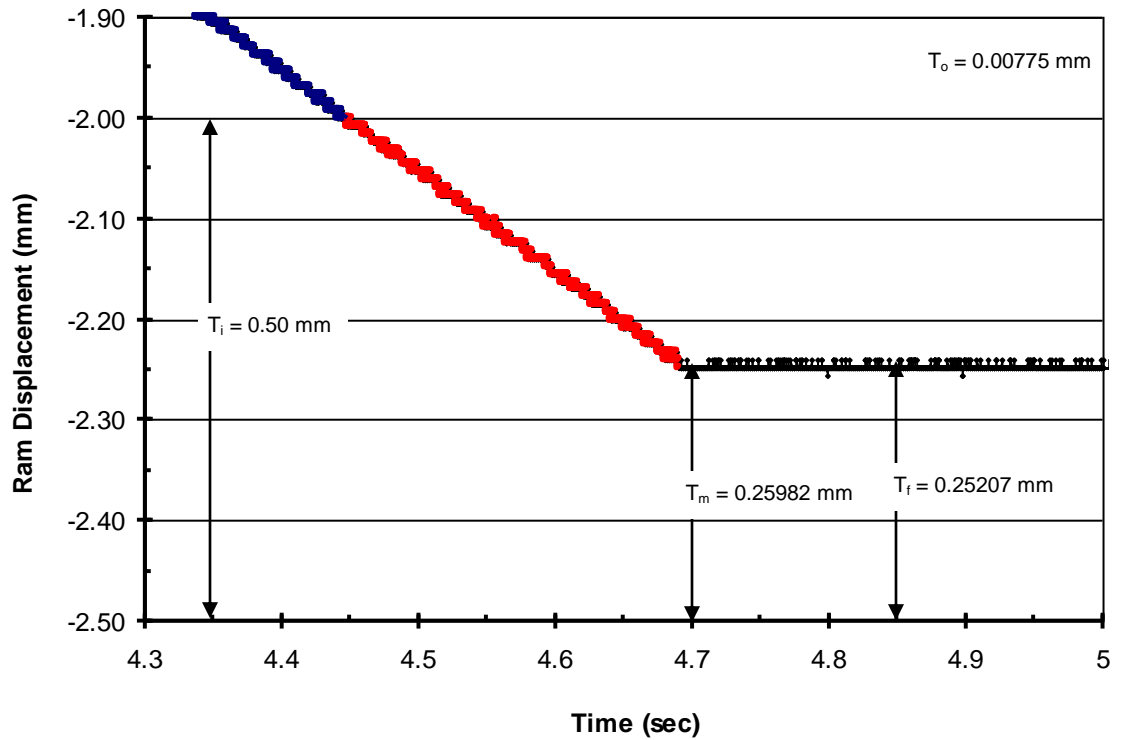
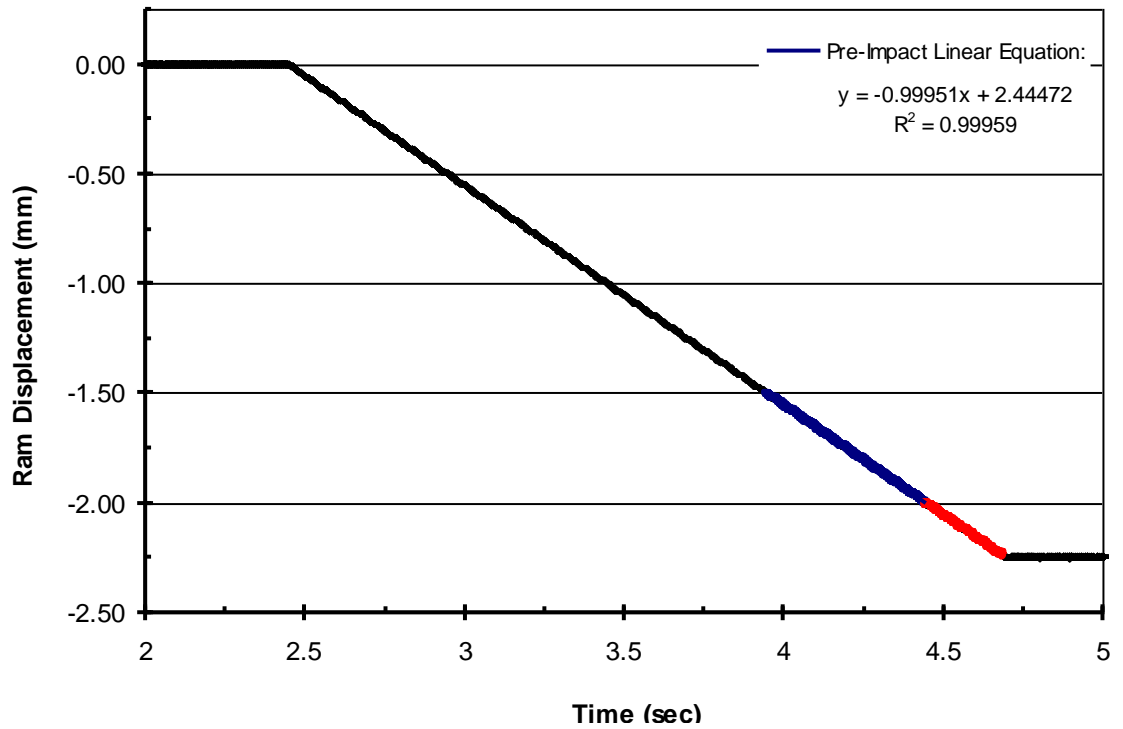


Figure 3-7. 1 mm/sec set velocity v1 no load impact ram displacement (PID = 40, 0, 0; EP1 = -2.25 mm). Red indicates data in impact region assuming cartilage initial thickness, $T_i = 0.5$ mm.

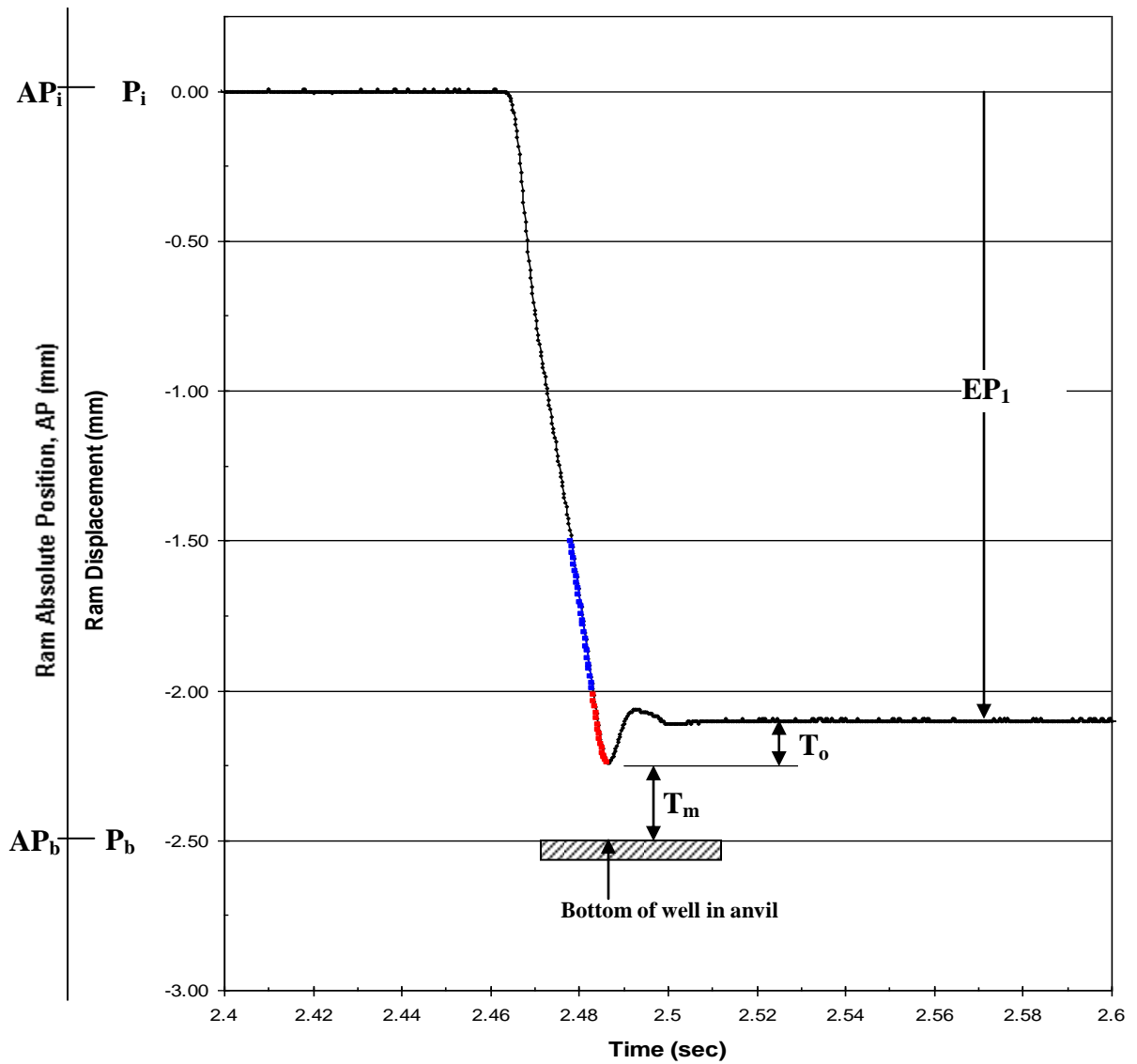


Figure 3-8. Visual representation of relationship between absolute ram position AP and ram displacement P, and parameters used in equation 2-2 to calculate the ram's absolute initial ram position AP_i that is set on the Instron to achieve desired maximum compression T_m (thus maximum strain ϵ) of cartilage that has a measured thickness T_i when using impact program with set endpoint $EP_1 = -2.25$ mm.

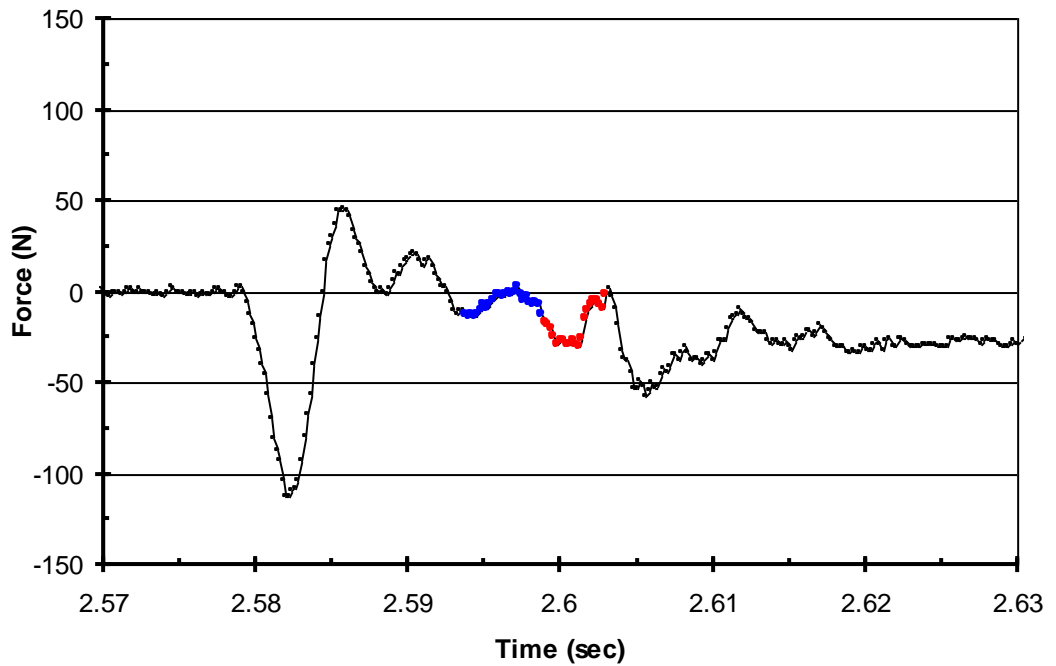
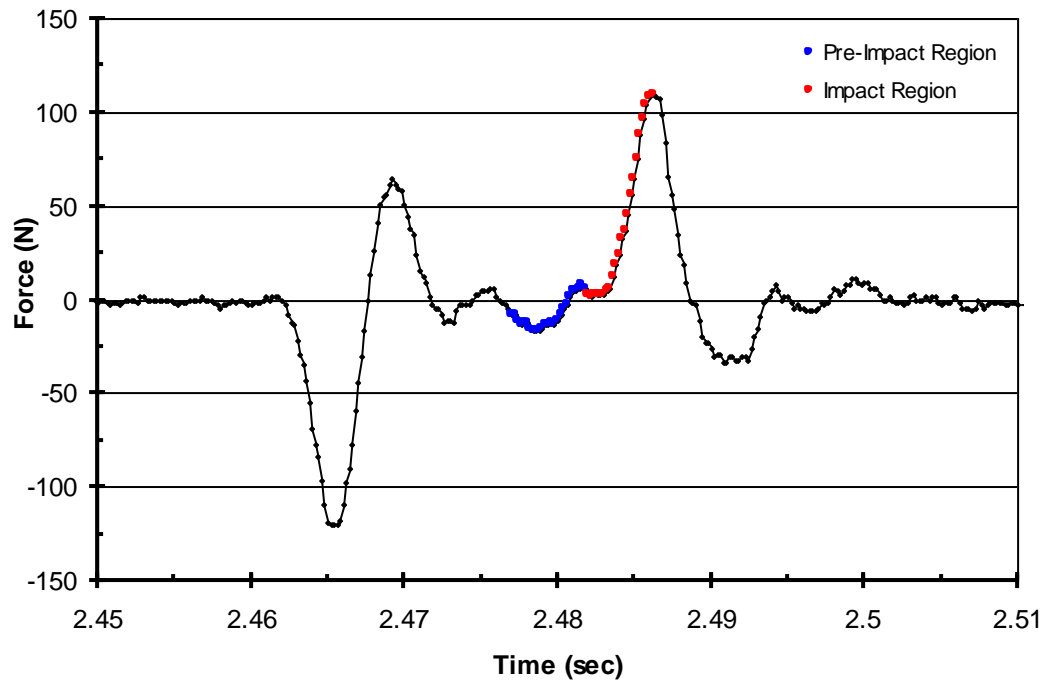


Figure 3-9. Indicated force, F , from impacting to $50\% \epsilon$ (PID = 40, 0, 0; EP1 = -2.10 mm; $v_1 = 100$ mm/sec) for A) no specimen and B) rubber. Red indicates data in impact region of rubber initial thickness, $T_i = 0.73$ mm.

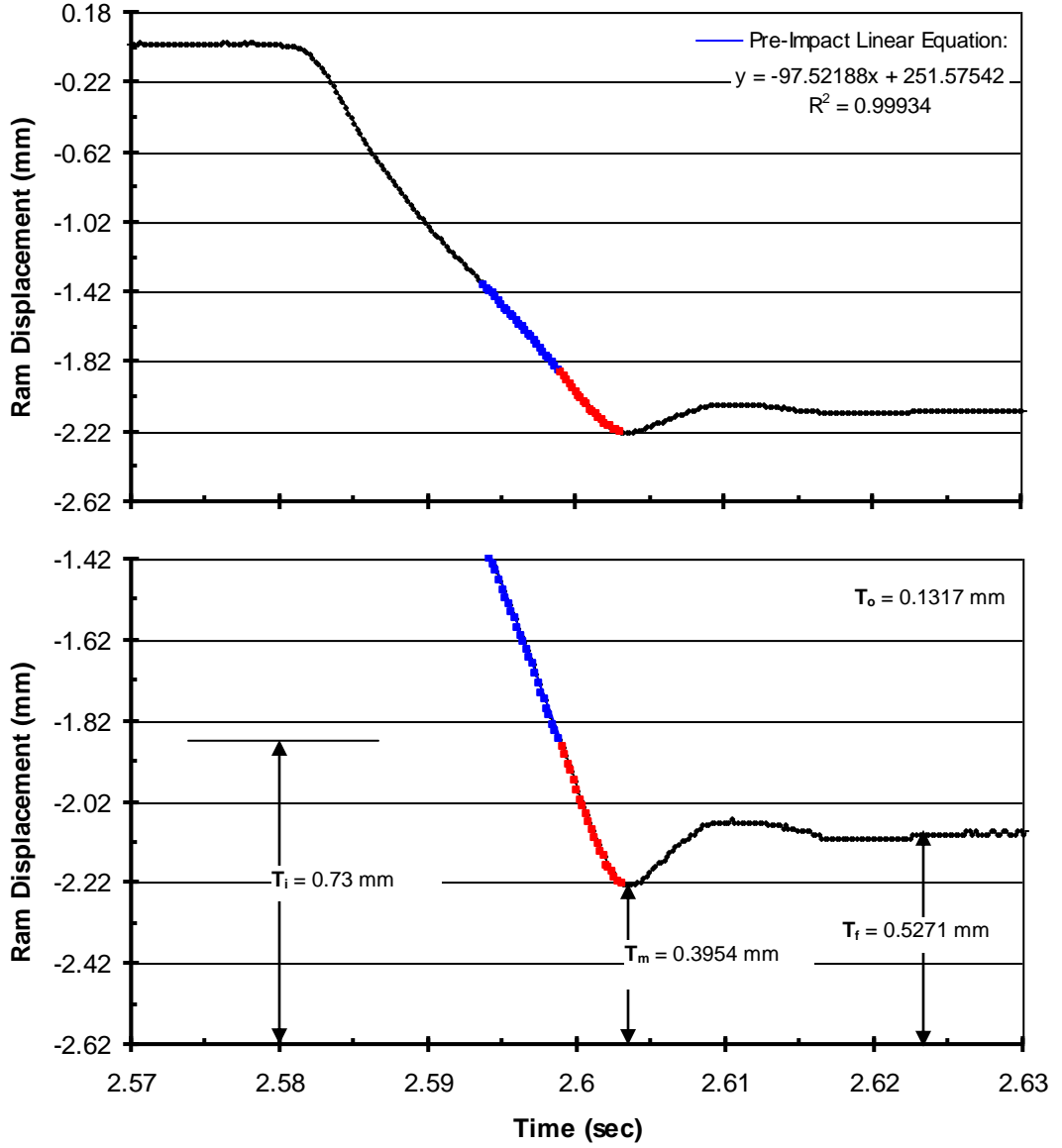


Figure 3-10. Ram displacement from impacting rubber to 50%ε (PID = 40, 0, 0; EP1 = -2.10 mm; v1 = 100 mm/sec). Red indicates data in impact region of rubber initial thickness, $T_i = 0.73$ mm.

Table 3-1. Effect of set impact velocity v_1 on observed impact velocity v_1 and overshoot T_o . (n = 1 tested with no cartilage, thus no resistance force).

Figure	Set					Observed		Used in Ch. 4 tests
Number	P (dB)	I (I/sec)	D (msec)	EP₁ (mm)	v₁ (mm/sec)	v₁ (mm/sec)	T_o (mm)	T_o (mm)
3-3	40	0	0	-2.25	100	103.33039	0.13178	0.13
3-4					50	49.75455	0.06976	
3-5					25	24.91149	0.03101	
3-6					10	9.98223	0.00775	
3-7					1	0.99951	0.00775	0.01

CHAPTER 4

BIOMARKERS AFFECTED BY IMPACT VELOCITY AND MAXIMUM STRAIN DURING CARTILAGE INJURY

Introduction

Osteoarthritis (OA) is a painful and debilitating whole joint disease involving cartilage degradation, sclerosis of subchondral bone, and inflamed synovial tissue that is anticipated to affect 59 million Americans by 2020.¹ Out of the 46 million Americans currently diagnosed with OA, approximately 12% of cases are associated with traumatic injuries resulting in annual costs over 3 billion dollars.² Although the exact etiology and pathogenesis of OA is often unknown, acute joint trauma to articular cartilage during sports injuries, vehicular accidents, or falls may initiate a common series of events culminating in post-traumatic osteoarthritis (PTOA).³ Some of the pathologic responses typically reported for mechanically-injured cartilage include cell (chondrocyte) death,⁴⁻¹¹ direct tissue disruption with loss of cartilage proteoglycan^{8,12-14} and collagen II,^{14,15} and increased release of prostaglandin E₂^{16,17} and nitric oxide.^{9,18} The degree of chondrocyte death associated with PTOA¹⁹ is reportedly dependent on impact energy,⁴ peak stress,⁵ stress rate,⁶ and compressive strain.⁷ However, the severity of injury to cartilage, and the rate and magnitude of impact load (trauma severity) to produce the injury needed to initiate this process as well as the subsequent pathologic changes in functional material properties of cartilage and the corresponding relationship with its biochemical changes are not fully understood.

Recently, our lab discovered potential diagnostic biomarker candidates (monocyte chemoattractant protein 1 [MCP-1], interleukin 8 [IL8], keratinocyte-derived chemoattractant [KC], matrix metalloprotease [MMP2 and MMP3]) that exhibited significant differences between canine groups with surgically induced and naturally occurring OA compared to canines without OA.²⁰ As part of our broader goal of identifying prognostic biomarkers for clinical PTOA, we sought to create a repeatable and controlled severity of cartilage injury model in order to translate early *in vitro* responses to future *in vivo* PTOA studies. A variety of models have been used to investigate the effect of rate, magnitude, and/or duration of the impact load delivered as summarized in Table 4-1.^{4-8,21-31} The severity of injury to cartilage by traumatic loading will depend upon its pre-injury health, biological characteristics, material biomechanical properties, and thickness; constraints imposed by the surrounding tissue and subchondral bone, and the magnitude (energy of impacting object, maximum stress, maximum strain) and rate of the impact loading itself. Ideally all of these parameters would be independently controlled to create a quantifiable and repeatable severity of injury model to a cartilage explant. This is impossible when using energy of the impacting object or maximum stress as the controlled impact parameter magnitude, since they are dependent upon unknown cartilage material properties and time history of the compression. Compression of isolated cartilage to desired maximum strain ϵ_{\max} at a desired constant strain rate $d\epsilon/dt$ is feasible once pre-impact thickness T_i of the cartilage itself is measured since impact punch velocity $V = d\epsilon/dt * T_i$ can be independently controlled. With explants radially constrained within a well, chondrocyte death has been observed to increase with increased maximum impact stress without the occurrence of articular

surface fissures.^{5,6} When radially unconstrained, an increase in chondrocyte death with maximum stress was likewise reported, but with the added variability of articular surface (AS) fissures occurring (greater probability with increasing strain rate and/or maximum stress).^{23,25,26} Since articular surface fissuring is not a prerequisite to chondrocyte death^{30,32} or *in vivo* development of PTOA,³³ we chose to control fissuring by radially constraining explants within a well. Previous investigations studying the effect of different controlled strain rates were to selected maximum stress levels,^{23,25} and were at relatively slow strain rates (≤ 0.7 (mm/mm)/sec), compared to estimated average *in vivo* joint trauma strain rates of 25 and 50 (i.e. $V = 50$ and 100 mm/sec to compress 2mm thick cartilage of human knees³⁴ to $\epsilon_{\max} = 0.5$ corresponding to the time duration of maximum force generated for falling injuries within 20 milliseconds³⁵ and for vehicular knee-dashboard injuries within 10 milliseconds,³⁶ respectively). Likewise, investigations into the effect of different stress rates were to selected maximum stress levels, and were at relatively low equivalent strain rates ≤ 1.2 ^{5,6,26} and ≤ 8.38 .²¹ Previous investigations (see Table 4-1) primarily concentrated on studying the effect of impact loading on cartilage, with biomarker release to media limited to GAG^{8,21,23,25,26} and NO.²¹ Other possible media biomarkers involved in cartilage injury have been observed. Gosset et al. demonstrated that microsomal prostaglandin E synthase-1 (mPGES-1), a key enzyme required for PGE2 formation, and PGE2 increase during dynamic compressive loading (1MPa, 0.5Hz) up to 24 hours in murine cartilage explants.^{37,38} Joos et al. reported increased PGD2 and later PGE2 release from human osteoarthritic cartilage 24 hours after impact injury of 0.59 or 1.18J.¹⁷

The objective in this investigation was to develop a cartilage injury model by delivering a single impact load with clinically relevant controlled combinations of impact velocity (strain rate) and maximum strain that is independent of tissue load resistance properties, and to study their effects on articular cartilage cell viability and potential biomarkers for onset of PTOA. Our hypothesis was that an impact load model with controlled strain rate and maximum strain to radially constrained explants will produce a quantifiable and repeatable severity of injury to cartilage that will be able to identify pathologic responses related to onset of PTOA.

Methods

Table 4-2 summarizes the test groups and protocols used in Study 1 and Study 2. Study 1 was conducted to determine if the 25 kN, 25cm stroke materials test machine (model 8821s, Instron, Canton, Massachusetts) that was available in our lab could be used to measure explant thickness under repeatable pressure conditions, and to deliver a constant velocity V (up to 100mm/sec) impact to a controlled desired strain ϵ (up to 50%) independent of an explant's load resistance. Study 1 tests were limited to groups at low and high end of the velocity:strain conditions to see if any difference in cell viability and biomarkers could be detected prior to launching Study 2 involving a more comprehensive group of conditions.

Using a scalpel blade, normal full thickness articular cartilage was aseptically harvested from the humeral heads of adult dogs within four hours after euthanasia for reasons unrelated to this study. Cartilage explants were created using a 4 mm diameter biopsy punch. Explants were assigned to test groups so each would have one explant from each of the dogs. Explants were cultured using 24-well plates in 1 ml Dulbecco's

modified Eagle's medium high glucose supplemented with 1X ITS, penicillin, streptomycin, amphotericin B, L-glutamine, sodium pyruvate, L-ascorbic acid, and non-essential amino acids at 37°C, 95% humidity, and 6% CO₂ for 48 hours prior to injury.

The test machine in conjunction with custom designed fixtures was used to measure thickness and to deliver the impact load to each explant (Fig. 4-1A). To measure cartilage thickness, the punch was lowered in position-control at 0.01 mm/sec into the empty well and stopped by a load limit detect when punch touched well bottom with 10 N compression. With punch raised an explant was inserted into the empty well, and then punch was lowered as before. Explant pre-injury initial thickness, T_i , was calculated as the difference in ram position with and without explant. Day 6 and 12 thickness (T_6 , T_{12}) was similarly measured in Study 2.

Immediately after measuring T_i , the desired impact's maximum compressed thickness of each explant $T_m = T_i(1-\varepsilon/100)$ was calculated from T_i and the desired maximum % strain ε . Fig. 4-1B contains a representative punch tip motion profile during impact and illustration of T_i , T_m , and ram overshoot T_o . The ram was raised to $T_o+2.25\text{mm}$ above T_m , then a relative (-2.25mm) displacement ramp function was used to deliver the impact. Each explant was then removed from well and cultured as previously described for 12 days, with media changed on the days shown in Table 4-2 and stored at -20°C for analysis.

Cell viability was determined by stereomicroscopy using a mixture of fluorescent live (CellTracker Green CMFDA) and dead (ethidium homodimer-1) cell stains (Invitrogen, Carlsbad, California) following manufacturer's guidelines. A slice (~1mm thick across full diameter) of each explant was taken to expose a cross section perpendicular to the

articulating surface, which was stained in 200 μ l for 30 minutes at room temperature then rinsed and stored in phosphate buffer saline. Fluorescence images (Leica MZFLIII stereo microscope) were quantitatively assessed for cell viability with an in-house developed computer algorithm that does a steepest decent optimization search of the gray scale pixelated domain to identify and count white spots that exceeded a white intensity threshold. The algorithm was validated against multiple observer manual counting, and had superior repeatability. The remaining tissue was stored at -20°C for biochemical analysis of tissue proteoglycan and collagen content. For biochemical analysis, tissues were lyophilized, weighed to determine dry weight, and digested with papain. The glycosaminoglycan (GAG) and collagen content of the tissue was determined using the 1,9-dimethylmethylene blue (DMMB) assay³⁹ and hydroxyproline (HP) assay,⁴⁰ respectively, then normalized to tissue dry weight ($\mu\text{g}/\text{mg}$).

Media GAG content was assessed using the DMMB assay.⁴¹ Type II collagen (Col II) was determined using the CPII enzyme-linked immunosorbent assay (IBEX, Mont Royal, Quebec, CAN). Nitric oxide (NO) concentration was determined using the Griess assay (Promega, Madison, Wisconsin). Prostaglandin E₂ (PGE₂) concentration was measured using an enzyme immunoassay (Cayman Chemical, Ann Arbor, Michigan). Aggrecan synthesis was analyzed using CS-846 assay (IBEX, Mont Royal, Quebec, CAN). All were done according to manufacturer's protocol. Results for each explant were normalized to its initial volume ($T_1 \cdot \text{well area}$).

The effect of time or treatment on all groups were analyzed by one-way repeated measures analysis of variance or one-way analysis of variance, respectively, followed by an all pairwise multiple comparison procedure using the Holm-Sidak method or Kruskal-

Wallis One Way Analysis of Variance on Ranks as indicated by SigmaPlot (Systat Software, Inc., Chicago, Illinois). Statistical significance was taken as $p \leq 0.05$.

Results

The test machine's thickness measurement and control of desired impact velocity and maximum strain is illustrated in Table 4-3.

As illustrated in Fig. 4-2A, a localized superficial zone of cartilage cell death was visible at days 0 and 12 for both high strain (50 ϵ) groups, with a greater spatial distribution of cell death propagating to the deep zone in the 100V:50 ϵ group at day 12. This correlates with total % live cell count results in Fig. 4-2B. On day 0 the impacted groups had lower % cell viability than the control. By day 12, the 100V:50 ϵ group had lower cell viability than control and 100V:10 ϵ ; and likewise 1V:50 ϵ than 100V:10 ϵ .

These results are from Study 1 since stain malfunction occurred in Study 2.

Table 4-4 summarizes total collagen (HP) and GAG content of the tissue at day 12. There were no significant differences in HP of the tissue between any of the groups, and likewise for GAG (with one exception).

Release of GAG and PGE₂ to the media was primarily strain dependent (Fig. 4-3). Day 1 release of PGE₂ of all impacted groups was significantly higher than all subsequent days, and likewise for GAG release by the 30 ϵ and 50 ϵ strain groups. On day 1 both 50 ϵ groups released significantly more GAG to the media than control-sham, both 10 ϵ and both 30 ϵ groups. Both 50 ϵ groups continued releasing higher GAG than control-sham, 10 ϵ and 30 ϵ groups on day 2 (with two exceptions that approached significance ≤ 0.088). On day 1, both 30 ϵ and 50 ϵ groups released significantly more

PGE₂ to the media than the control-sham, both 50ε more than either 10ε, and 100V:50ε more than either 30ε. On day 2, both 50ε groups continued greater release than the control-sham group. The only apparent velocity-dependent observation is that the 100V:50ε group continued to release more PGE₂: through day 9 than the control-sham and 1V:10ε, through day 6 than 1V:30ε and 100V:10ε, and through day 3 than 100V:30ε. The release of nitric oxide was below the quantitation limit of the assay for all groups. There were no significant differences observed during Study 1 for CPII (for day 3, 6, 9, 12) and likewise CS-846 (with two exceptions at day 3), and thus media was not analyzed for these in Study 2.

There were no significant differences in pre-injury (day 0) thickness of all groups, Fig. 4-4. On day 6, the 1V groups exhibited a trend of being thinner with increasing strain (reaching significance between 50ε compared to 10ε), and likewise for the 100V groups.

Discussion

With the 25kN servo-hydraulic testing machine, we were able to deliver to radially constrained explants a single impact with clinically relevant combinations of controlled velocity and maximum strain. Release of GAG and PGE₂ to the media, and cell death in a primarily maximum strain dependent manner were observed, which is supporting evidence to our hypothesis that this cartilage severity of injury model will be able to identify pathologic responses related to onset of PTOA.

To conduct tests at exactly the same strain rate for explants of different thickness T_i , impact velocity V would need to be changed. Doing so would require alteration-reloading of the test machine's position control program for each explant. Since

thickness of the canine explants was fairly uniform (average 0.55mm), we chose to keep impact velocity $V = 1\text{mm/sec}$ for all specimens within groups tested at this velocity and likewise at 100mm/sec . The corresponding nominal strain rates were 1.82 and 182 1/sec. Thus our lowest strain rate was comparable to the ≤ 1.4 strain rate of strain rate controlled^{23,25} and stress rate controlled^{5,6,26} impact to different levels of maximum stress, and the estimated rate of creep tests⁷ (Table 4-1). Our 1V group measured stress rates (23.2 to 25.8 MPa/s, Table 4-3) were on the low end of the range (25 to 1000, Table 1) previously reported for stress rate controlled,^{5,6,21,29} while our 100V group stress rates (1633 to 2992) were above. These studies observed chondrocyte death that started at the articular surface (AS) that increased in depth with greater maximum applied stress (thus strain) for each loading rate. Chondrocyte death remained within the superficial zone for: a) strain rates^{23,25} $\geq 7 \times 10^{-3}$ after 4 days in culture, b) all stress rates tested after 1 hour in culture^{5,6} and 2 days (with one exception of extending into the intermediate zone by the highest 23 MPa loading group),²⁶ and c) for mature cartilage all levels of maximum strain (0.1 to 0.7) after 15 to 30 minutes in culture⁷ (immature cartilage having greater cell death that also extended into the intermediate zone for strains ≥ 0.6). Milentijevic et al.^{5,6} observed that for the same stress rate, cell depth increased with increasing peak stress and also strain, and that higher stress rates tended to produce less depth. For slow strain rates $\leq 3 \times 10^{-5}$, Quinn et al.²³ and Morel et al.²⁵ observed that cell death extended through the full depth of the cartilage for the higher 7 and 14 MPa peak stress values, and no significant loss of cell viability in any zone regardless of peak stress for strain rate = 7×10^{-4} which is approximately the gel diffusion rate.²⁵ Cell death was observed to increase with impact energy^{4,8,27,30} (and presumably peak axial strain

although not reported but implied by the greater visible damage^{4,8}), and to be within the superficial zone at lower energies that extended to middle-deep zone at higher impact energies.^{27,30} As we observed in our study, results of the aforementioned studies indicate that the superficial zone is most sensitive to chondrocyte death, and that chondrocyte death is primarily peak strain/stress dependent for strain rates greater than the gel diffusion rate²⁵ with implication being irrespective of species, cartilage site-thickness, and radial constraint of the explant.

The increased release of GAG to the media in 50 ϵ strain groups provides supporting evidence that single impact injury causes release of GAG from the tissue.^{7,9,12} The majority of GAG released was detected at the earliest time point (1 day) post-injury, and occurred primarily in a strain-dependent manner. This is consistent with the findings of DiMicco et al. who reported that initial GAG release of cartilage explants (1mm thick) compressed to 50% thickness at a strain rate 1mm/sec (1V:50 ϵ) cannot be mitigated with inhibitors of biosynthesis nor MMP activity,¹² suggesting that initial release of GAG is due to mechanical damage. Since the extracellular matrix of articular cartilage consists of collagen II tightly interwoven with GAG, it may be that the collagen fibrils were damaged following impact injury allowing the release of GAG from the cartilage. Increased GAG release to media for up to 4 days has been reported for higher magnitude impact irrespective of the controlled impact parameter (strain rate,^{23, 25} stress rate,^{21,26} or energy⁸). We similarly observed that GAG release was primarily impact magnitude dependent (Fig. 4-3A).

The strain dependent increase in PGE₂ that we observed is most likely due to cell membrane rupture during impact, which has been shown to cause release of arachidonic

acid effectively activating the cyclooxygenase-2 (COX2) pathway.⁴² Inhibition of the COX2 pathway via celecoxib or indomethacin has been shown by Jeffrey et al. to lower PGE₂ release from human articular cartilage and reduce cell death but not proteoglycan degradation following an *in vitro* impact load of 0.13J resulting in a peak stress of approximately 25MPa for 3ms.¹⁶ Also, Gosset et al. demonstrated that microsomal prostaglandin E synthase-1 (mPGES-1), a key enzyme required for PGE₂ formation, and PGE₂ increase during dynamic compressive loading (1MPa, 0.5Hz) up to 24 hours in murine cartilage explants.^{37,38} Joos et al. reported increased PGD₂ and later PGE₂ release from human osteoarthritic cartilage 24 hours after impact injury of 0.59 or 1.18J.¹⁷ These findings support our results that PGE₂ is a mechanosensitive biomarker. Furthermore, we were able to demonstrate that release of PGE₂ becomes statistically significant at lower strain levels than does GAG and thus may be a more sensitive biomarker. Since PGE₂ is formed through the COX2 pathway, then COX inhibitors (i.e. non-steroidal anti-inflammatory drugs) may decrease its levels. Yet, the role that PGE₂ plays in anabolic or catabolic cartilage remodeling remains vague and warrants further investigation. Thus, it is plausible that sustained or increased levels of PGE₂ several months after injury may indicate an associated risk of developing PTOA especially since elevation of plasma PGE₂ has been associated with disease severity in symptomatic knee OA patients.⁴³

The initial condition of the cartilage may also have a significant influence on its responsive biomarkers, since we interestingly observed that samples from a fifth dog released substantially more PGE₂ at day 1 than the average of samples from the other four dogs (3.8, 4.6, 2.4, and 1.6 times more PGE₂ in the sham, control, 1V:10ε, and

100V:10ε groups respectively), but with similar release for both 50ε groups. Gross evaluation verified that this tissue was osteoarthritic, and was thus not included in our n=4 group average results. The stage of osteoarthritis within cartilage and induced degeneration has been correlated to biomechanical load resistance characteristics of cartilage measured with hand held indentation probes⁴⁴⁻⁴⁶ that can potentially be used to arthroscopically assess the post-trauma biomechanical load resistance condition of cartilage. Clinical follow up studies have correlated the presence/severity of PTOA to articular fracture severity score (involving disruption and fracture energy),⁴⁷ and elevated stress time exposure.⁴⁸ Stress and energy absorption that occurs during impact should be measured to obtain an assessment of the pre-impact condition of the cartilage, since the mechanical resistance to load and energy absorption properties of tissue have been shown to correlate to the macroscopic^{49,50} and histologic⁴⁴ scores of human OA cartilage tissue. To correlate our biomarker results to these and future results requires accurate measurement of the force resistance and energy absorption characteristics of the cartilage during impact. A limitation of our study was that we were unable to report accurate force measurements near peak strain since a reliable means to compensate for the loads cell's inertial effects could not be found.

In conclusion, cell viability, tissue thickness, and GAG and PGE₂ release after impact were primarily maximum strain-dependent, with the prolonged significant release of PGE₂ also being velocity-dependent. The controlled velocity to maximum strain impact model appears to be useful for investigating the relationship between impact severity of injury to cartilage and the onset of PTOA, specifically for discovery of biomarkers to

evaluate the risk of developing clinical PTOA and compare effective treatments for arthritis prevention.

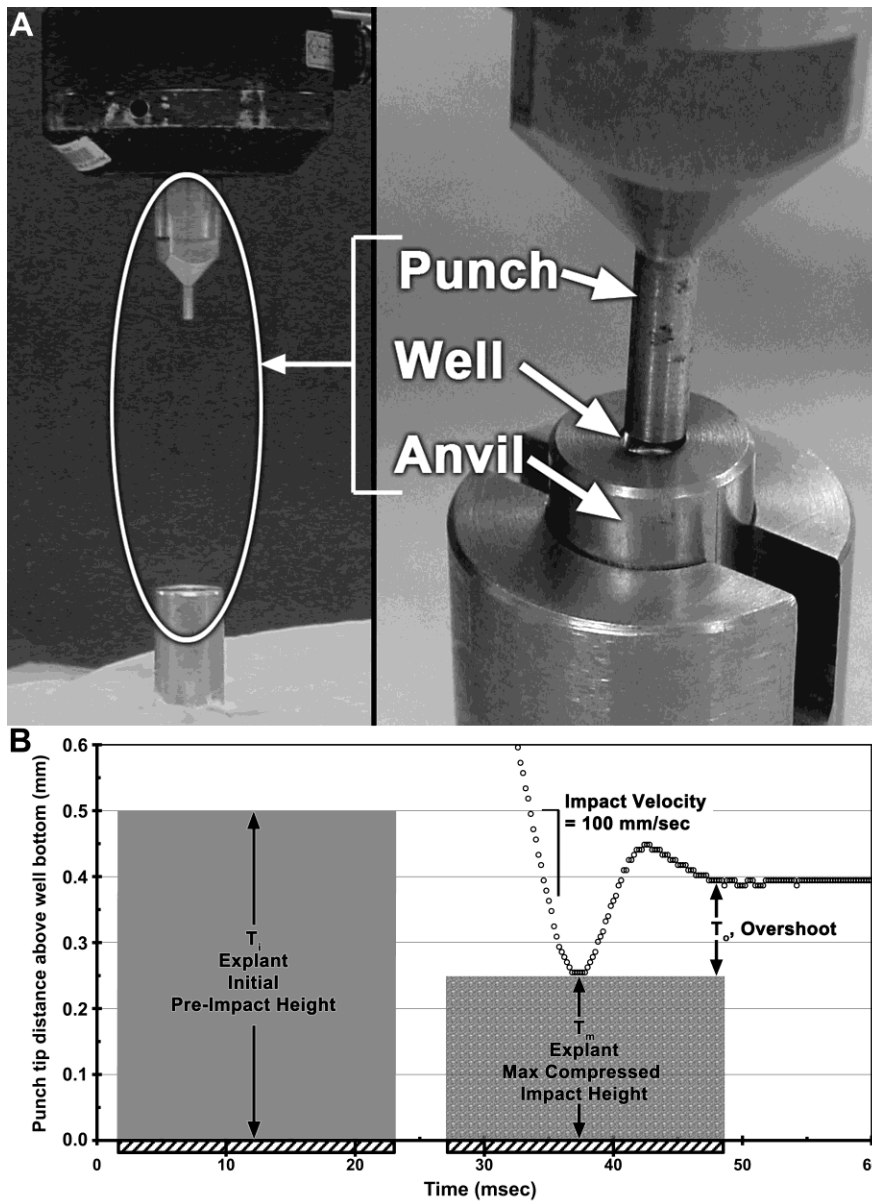


Figure 4-1. Test cell configuration and non-porous stainless steel fixtures: flat surface impact punch (3.9mm dia.) attached to a 1000N load cell (Lebow model 3173, Eaton Corporation, Troy, Michigan) on end of test cell ram, a removable anvil with cylindrical well (4.0mm dia. x 2.54mm deep) to radially constrain the explant. The anvil rested upon a cylindrical base attached by a punch-overload protecting shear pin to a support on the test machine's table (A). Representative motion profile of punch tip distance above bottom of well for nominal impact velocity $V = 100$ mm/sec to desired maximum strain $\epsilon = 50\%$ of explant having initial thickness $T_i = 0.5$ mm. Illustration of desired maximum compressed thickness T_m , and ram overshoot T_o . Ram overshoot was a repeatable value ($T_o = 0.01$ mm for $V = 1$ mm/sec, and 0.13 mm for $V = 100$) irrespective of explant thickness and stiffness due to the relative size of the 25 kN actuator (B).

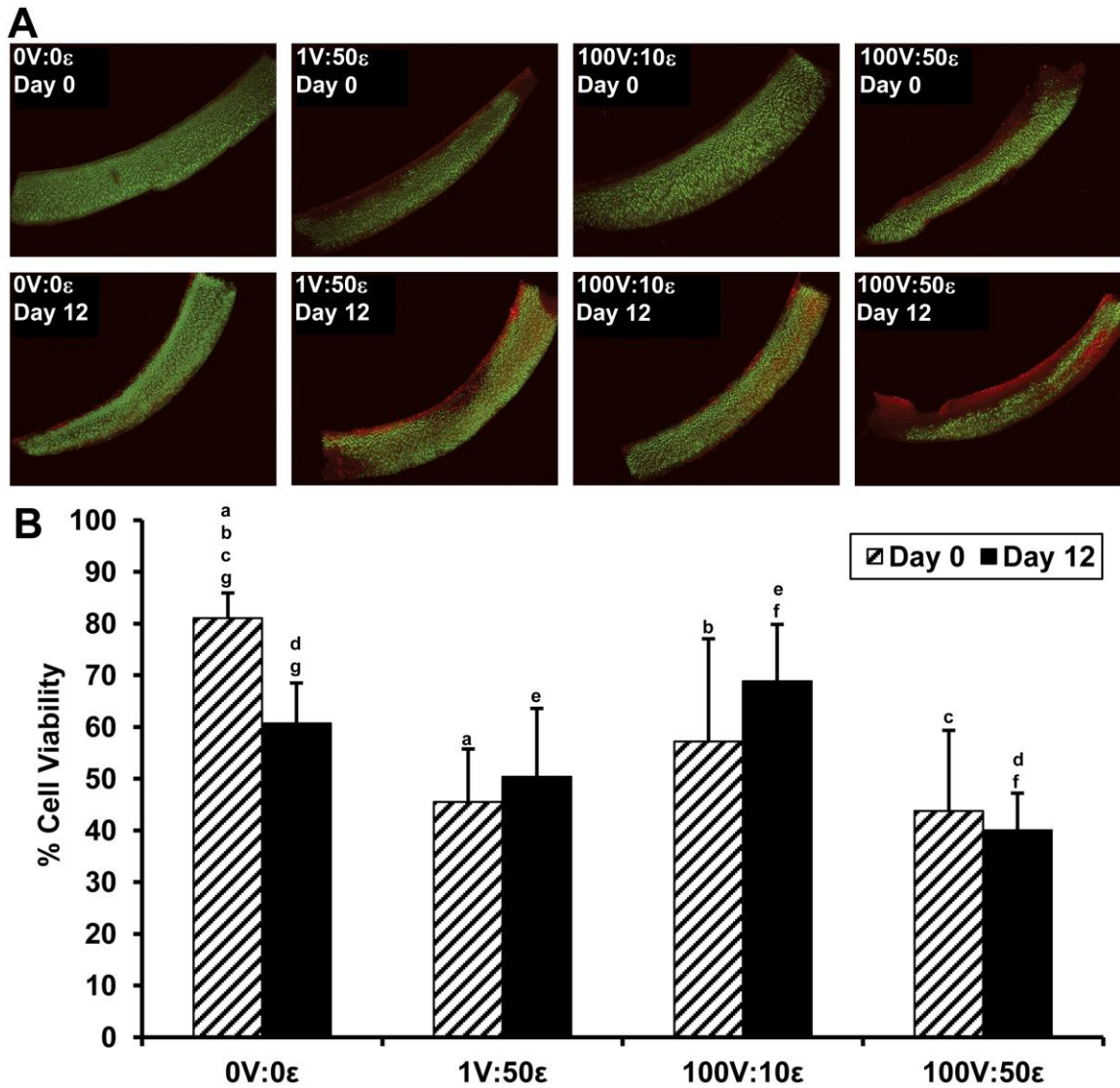


Figure 4-2. Effect of impact velocity and maximum strain on cell viability at day 0 and 12: red = dead cells, green = live cells (A). Percentage of cell viability at day 0 and 12: Common symbol above a pair of bars indicates they are significantly different ($p \leq 0.05$) (B).

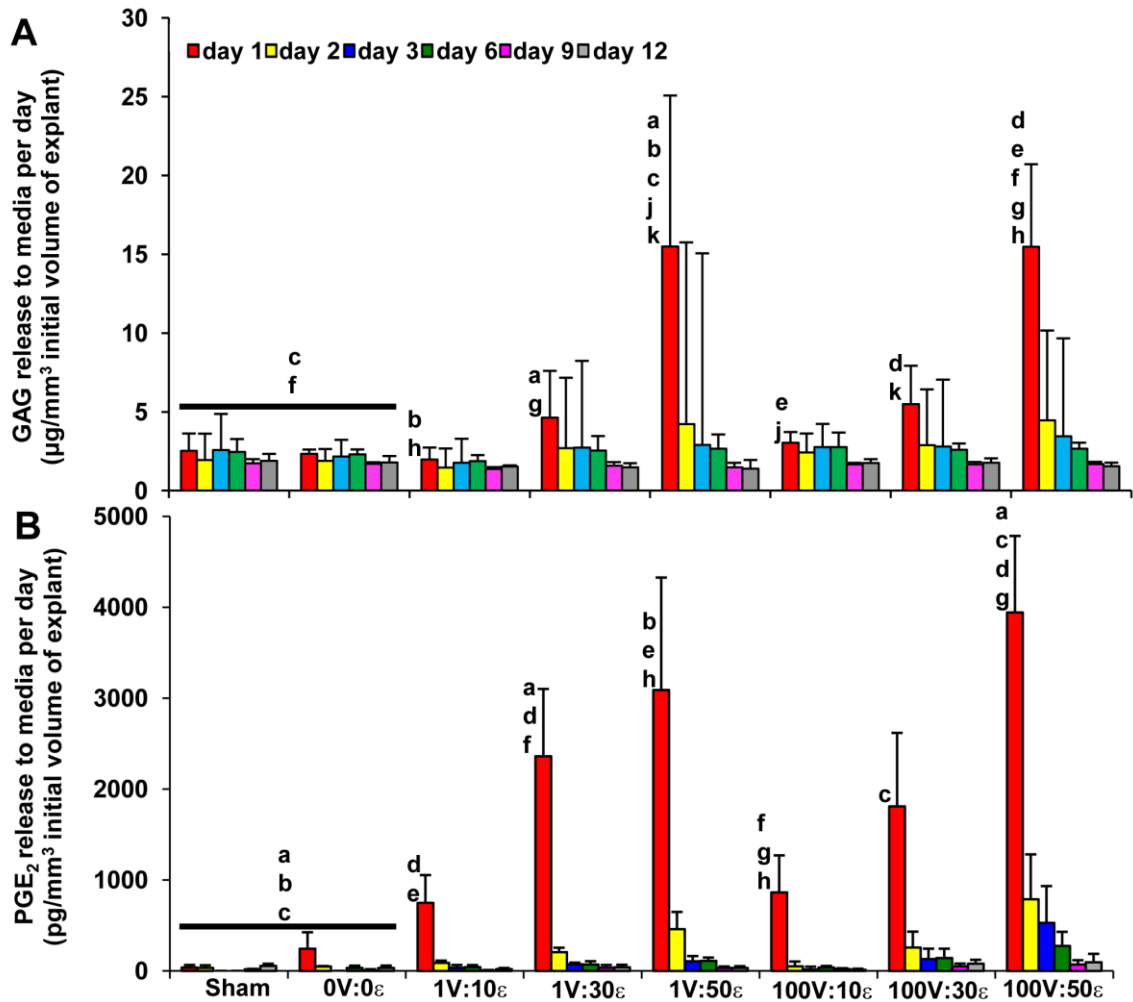


Figure 4-3. Effect of impact velocity and maximum strain on glycosaminoglycan (A) and Prostaglandin E2 (B) released from the articular cartilage explant post-injury into the culture media. Common symbol above a pair of bars indicates they are significantly different ($p \leq 0.05$), shown only for day 1. Significance for subsequent days generalized in Results section.

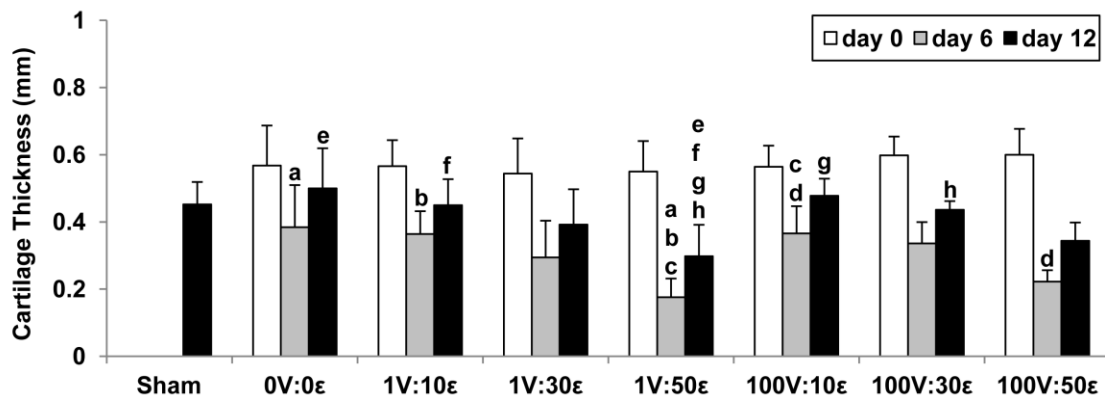


Figure 4-4. Thickness of cartilage explants at day 0 (pre-injury), and the effect of impact velocity and maximum strain on cartilage thickness at days 6 and 12 (post-injury). Common symbol above a pair of bars indicates they are significantly different within each time frame ($p \leq 0.05$). In addition, within each group thickness was statistically different for each time frame.

Table 4-1. Summary of investigations into effect of impact magnitude and/or rate on tissue parameters and constituents released to culture media.

Author	Impact/Loading Device ^a	Explant			Reported Impact			Impact equivalent ^e		Investigated effect on																		
		Species ^b	Constraint ^c	Cartilage pre-impact Thickness T_i (mm) ^d	Magnitude used to stop loading	Rate or Duration	Max axial strain	Strain rate (1/sec)	Velocity (mm/sec)	Tissue							Release to Media											
										Cell viability ^f	AS fissures ^g	Matrix damage/deformation	H ₂ O-weight loss	Volume change	Stiffness	GAG/PG	AS Prin. strains ^g	GAG	NO	PGE ₂ , CS-846, Collagen II								
Strain rate controlled impact																												
Waters	SH	C _h	RC _w	0.55	10, 30, 50% strain	1, 100 mm/sec	0.1 to 0.5	1.8, 182	1, 100	0, 12d					0, 6, 12d	0, 12d		1.2,3, 6.9, 12d	1.2,3, 6.9, 12d	1.2,3, 6.9, 12d								
Morel ²⁵	ED	B _h	RU/SB	NR	3.5, 7, 14 (MPa)	7x10 ⁻⁵ -4. -3,-2,-1 (strain/s)	0.82 to 0.54	< 0.7	< 1.1	4d	X	X	X		X			Daily 10 days										
Quinn ²³	ED	B _s	RU	NR	3.5, 7, 14 (MPa)	3 x 10 ⁻⁵ (strain/s)	0.83 to 0.93	3x10 ⁻⁵	4.5x10 ⁻⁵ Ti=1.5	4d	X		X	X		P		Daily 4 days										
						0.3, 0.5, 0.7 (strain/s)	0.43 to 0.68	0.3, 0.5, 0.7	0.45 to 1.05 Ti=1.5	4d	X		X	X		P		Daily 4 days										
Stress rate controlled impact																												
Ewers ²¹	SH	B _m	RU	NR	40 (MPa)	40 (MPa/s)	0.476	0.44	0.7 Ti=1.5	4d	X	X						Daily 4 days	Daily 4 days									
					40 (MPa)	930 (MPa/s)	0.409	8.38	12.6 Ti=1.5	4d	X	X								Daily 4 days	Daily 4 days							
Milentijevic ⁵	SP	B _k	RC _w -Por _{wb}	1.46	10-60 (MPa)	350 (MPa/s)	0.02 to 0.23	< 1.2	< 1.5	1h		X	X		X	P												
Milentijevic ⁶	SP	B _k	RC _w -Por _{wb}	1.26	10, 20, 30, 40 (MPa)	25,50,130, 1000 (MPa/s)	0.23 to 0.11	< 1.2	< 1.5	1h		X	X		X	P												
Milentijevic ²⁹	SP	R _{fc}	RCc, <i>Viv</i>	0.7	15 to 50 (MPa) 35 (MPa)	420 (MPa/s) 420	--	--	--	15m	X	X			X													
D'Lima ²⁶	SH	B _k H _{fp}	RU	1 to 1.8	7, 14, 23 (MPa)	100 minutes to final stress	0.40, 0.67, 0.72 to 0.83	<0.09	<0.16	2d	X							Day 2										
Energy of impacting object controlled																												
Jeffrey ⁴	DT	B _m	RU	NR	12 mass-drop heights creating 0.049 to 1.96 (Joules)	1600 to 2300 initial (strain/sec) (reported for 3 of 12 mass-drop)	0.8 to 0.87 (3 example mass-drop)	--	630 _{Vi} to 3130 _{Vi}	1d	X		X		X													

Jeffrey ²⁴	Scr	H _f	RU	NR	Max strain = average from drop tower	40 (mm/s)	NR	--	40	1d or 3d	X						X	G				
	DT	H _f	RU	NR	0.12 (Joules)	1.5ms to peak load	NR	--	693 _{Vi}		X						X	G				
Bush ²⁷	DT	B _m	RU	NR	0.049, 0.098, 0.196 (Joules)	--	--	--	990 to 1400 _{Vi}	3 to 45m, 1d	X			Cell								
Duda ³⁰	DT	P _p	RC _c	NR	0.06, 0.1, 0.2 (Joule) Spheric Indentor	--	--	--	1095, 1414, 2000 _{Vi}	10h	X											
Haut ³¹	DT	R _{pf}	Viv	NR	0.9, 4.2, 6.3 (Joule)				2046, 2513, 3078 _{Vi}		X						X					
Huser ⁸	DT	E _i	RU	NR	0.123, 0.245, 0.490 (Joules)	--	--	--	701, 1008, 1400 _{Vi}	0,1, 2,5, 10, 20d	X		X				P		Day 2			
Flachsmann ²⁸	DP, ST	B _p	RC _c /SB	1.5	Strain taken at 4,10,15,20,25 (MPa) 15 (MPa)	V _{constant} = 2000 (mm/s)	<0.25 0.75	1333 "nominal"	? _{Vi}		X							X				
Ewers ²²	SH	R _{pf}	Viv	NR	590 (N)	50 ms to peak load	--	--	--		X						X					
	DT	R _{pf}	Viv	NR	630 (N)	5 ms to peak load	--	--	--		X						X					
Static (constant) load -- creep test																						
Torzilli ⁷	Cr	B _{k adult calve}	RC _w -Por _{lp}	2	0.1, 0.2, 0.3, 0.4, 0.5, 0.6, 0.7 (strain) in less than 1 second	Static stress adjusted to produce similar time to reach strain level	--	< 1.4 assuming 0.5 to 1 second to reach stress level	--	15-30m												
<p>a. Device type used for impact: DT=Drop Tower, DP=Drop Pendulum, ED=Electrodynamic, Scr=Screw, SH = Servo-Hydraulic, SP=Servo-Pneumatic, ST=Static load, Cr=Creep</p> <p>b. Explant from species: B = Bovine with subscript: h=humeral head, k=knee, s=shoulder, m=metacarpal, p=patellae C = Canine with subscript: h=humeral head E = Equine with subscript: i = interphalangeal joint H = Human with subscript: f = femoral head, ftp= femoral-tibial-patellar knee P = Porcine with subscript: p = patellae R = Rabbit with subscript: pf = patellofemoral, fc = femoral condyle</p> <p>c. Explant type/constraint: Cartilage only: RC = Radial Constrained by subscript w = well, c = surrounding cartilage RU = Radial Unconstrained, /SB = On Sub-chondral Bone -Por = Porous filter (with location subscript: wb = well bottom , lp = end of load platen) Viv = In-Vivo</p> <p>d. Initial (pre-impact trauma) thickness of cartilage: NR=Not Reported</p> <p>e. Relationship between parameters: $d\sigma/dt = (d\sigma/d\varepsilon) * d\varepsilon/dt$, $d\varepsilon/dt = V/T_i$ where: $d\varepsilon/dt$=Strain Rate, $d\sigma/dt$=Compressive stress Rate, T_i=Initial pre-impact thickness of cartilage (subscript Ti=xx is value assumed to calculate V), V=Velocity of impact tip, $d\sigma/d\varepsilon$=Slope of stress versus strain curve. For drop tower: Kinetic Energy of impact mass upon contact $E = m * g * h = 0.5 * m * V_i^2$ where: E=energy in (Joules), m=mass of weight dropped (Kg), h=height from which weight was dropped (m), g=gravitational acceleration (9.8 m/s²), V_i=Velocity of mass upon initial contact with cartilage explant (subscript Vi indicates value is initial velocity of impact mass).</p> <p>f. Time in culture from impact to cell viability evaluation: xm= x minutes, xh = x hours, xd = x days.</p> <p>g. AS = Articular Surface.</p>																						

Table 4-2. Study 1 and study 2 test groups and protocols.

Day	Action	Test Group (Velocity:Strain)	Study 1		Study 2
			Day 0 Tissue Analysis	Day 12 Tissue Analysis	Day 12 Tissue Analysis
-2	<ul style="list-style-type: none"> •Tissue harvested •Explants created and cultured 48 hrs 	--	6 dogs, 8 explants/dog (48 explants total)		4 dogs, 8 explants/dog (32 explants total)
0	<ul style="list-style-type: none"> •Put in media culture^a 	Sham (control)	--	--	n=4 _{dogs}
	<ul style="list-style-type: none"> •Thickness measured •Moduli loading test^a •Put in media culture 	0V:0ε (control)	n=6 _{dogs}	n=6 _{dogs}	n=4 _{dogs}
	<ul style="list-style-type: none"> •Pre-impact thickness measured 	1V:10ε	--	--	n=4 _{dogs}
	<ul style="list-style-type: none"> •Moduli loading test^a 	1V:30ε	--	--	n=4 _{dogs}
	<ul style="list-style-type: none"> •Impact injury 	1V:50ε	n=6 _{dogs}	n=6 _{dogs}	n=4 _{dogs}
	<ul style="list-style-type: none"> •Put in media culture 	100V:10ε	n=6 _{dogs}	n=6 _{dogs}	n=4 _{dogs}
	<ul style="list-style-type: none"> •Put in media culture 	100V:30ε	--	--	n=4 _{dogs}
0	<ul style="list-style-type: none"> •Tissue analysis^b 	--	All 4 groups	--	--
1	<ul style="list-style-type: none"> •Media changed (M) 	--	--	--	M all 8 groups
2	<ul style="list-style-type: none"> •Media analysis (M)^c 	--	--	--	M all 8 groups
3	<ul style="list-style-type: none"> •Thickness (T) measured 	--	--	M all 4 groups	M all 8 groups
6	<ul style="list-style-type: none"> •Moduli loading (L) test^a 	--	--	M all 4 groups	M all 8 groups T,L (all except sham)
9		--	--	M all 4 groups	M all 8 groups
12	<ul style="list-style-type: none"> •Moduli loading (L) test^a 	--	--	M all 4 groups	M all 8 groups T,L all 8 groups
12	<ul style="list-style-type: none"> •Tissue analysis^b 	--	--	All 4 groups	All 8 groups

a. Thickness measurement and moduli loading of sham group explants was only done on day 12 to evaluate if act of measuring thickness and moduli loading of the (0V:0ε) group created pathologic conditions.
b. Tissue analyzed for: Cell viability, GAG, Collagen
c. Media analyzed for: CS-846 (Study 1) and GAG, Collagen II, Nitric oxide, PGE₂ (Study 1 and 2)

Table 4-3. Illustration of 25 kN test machine capabilities-results: day 0 pre-impact thickness T_i , impact velocity V , stress rate, and max strain ϵ (mean \pm standard deviation).

Test groups	0V:0 ϵ	1V:10 ϵ	1V:30 ϵ	1V:50 ϵ	100V:10 ϵ	100V:30 ϵ	100V:50 ϵ
Study 1 (n = 12 explants per group)							
T_i (mm)	0.51 \pm 0.048	--	--	0.48 \pm 0.079	0.58 \pm 0.111	--	0.58 \pm 0.111
V (mm/s) ^a	0	--	--	0.99 \pm 0.004	75.0 \pm 3.7	--	95.0 \pm 2.8
Stress rate (MPa/s) ^b	0	--	--	23.2 \pm 2.7	1633 \pm 613	--	2700 \pm 482
Max strain ϵ (%)	0	--	--	48.5 \pm 1.4	12.6 \pm 0.9	--	45.1 \pm 2.1
Study 2 (n = 4 explants per group)							
T_i (mm)	0.53 \pm 0.102	0.57 \pm 0.088	0.52 \pm 0.099	0.53 \pm 0.091	0.58 \pm 0.064	0.58 \pm 0.045	0.57 \pm 0.054
V (mm/s) ^a	0	0.98 \pm 0.022	0.98 \pm 0.013	0.99 \pm 0.003	79.6 \pm 12.0	88.3 \pm 6.8	86.4 \pm 3.3
Stress rate (MPa/s) ^b	0	24.8 \pm 2.8	25.8 \pm 1.8	25.8 \pm 1.9	2380 \pm 528	2610 \pm 350	2992 \pm 269
Max strain ϵ (%)	0	9.8 \pm 0.4	29.7 \pm 0.9	52.2 \pm 4.8	9.3 \pm 2.8	25.1 \pm 1.3	47.7 \pm 1.2
^a 1V group velocity = slope of impact punch position-time data from 10N compressive force to 1 st peak strain indication. 100V group velocity = slope of impact punch position-time data from 10N compressive force to reaching half of nominal maximum strain: i.e. to reaching 5, 15, and 25% for group nominal maximum strains of 10, 30 and 50% respectively. At initial contact with cartilage $V = 99.6$ to $100.7 \pm (\leq 1.0)$. ^b Stress rate = slope of stress-time data from 10 to 30N applied compressive impact force, with exception of 10 ϵ groups to peak compressive force some being ≤ 30 N.							

Table 4-4. Summary of tissue biomarker results at day 12 (mean \pm standard deviation).

Test group (# samples)	0V:0ε (n=4)	1V:10ε (n=4)	1V:30ε (n=4)	1V:50ε (n=4)	100V:10ε (n=4)	100V:30ε (n=4)	100V:50ε (n=4)	Sham (n=4)
GAG ($\mu\text{g}/\text{mg}$)	143.39 \pm 32.37	101.31 ^A \pm 22.98	141.77 \pm 33.37	138.06 \pm 9.32	121.89 \pm 15.31	158.01 \pm 19.28	193.2 ^A \pm 58.75	143.81 \pm 32.80
HP ($\mu\text{g}/\text{mg}$)	40.04 \pm 1.48	49.26 \pm 23.46	49.50 \pm 12.05	42.99 \pm 5.20	39.70 \pm 3.38	37.60 \pm 6.36	46.72 \pm 12.09	50.20 \pm 4.16

GAG = glycosaminoglycan, HP = hydroxyproline. Values sharing a similar letter are significantly different ($p < 0.05$)

References

1. Lawrence RC, Helmick CG, Arnett FC, et al. Estimates of the prevalence of arthritis and selected musculoskeletal disorders in the United States. *Arthritis Rheum.* 1998;41:778-799.
2. Brown TD, Johnston RC, Saltzman CL, et al. Posttraumatic osteoarthritis: a first estimate of incidence, prevalence, and burden of disease. *J Orthop Trauma.* 2006;20:739-744.
3. Buckwalter JA, Brown TD. Joint injury, repair, and remodeling: roles in post-traumatic osteoarthritis. *Clin Orthop Relat Res.* 2004;423:7-16.
4. Jeffrey JE, Gregory DW, Aspden RM. Matrix damage and chondrocyte viability following a single impact load on articular cartilage. *Arch Biochem Biophys.* 1995;322:87-96.
5. Milentijevic D, Helfet DL, Torzilli PA. Influence of stress magnitude on water loss and chondrocyte viability in impacted articular cartilage. *J Biomech Eng.* 2003;125:594-601.
6. Milentijevic D, Torzilli PA. Influence of stress rate on water loss, matrix deformation and chondrocyte viability in impacted articular cartilage. *J Biomech.* 2005;38:493-502.
7. Torzilli PA, Deng XH, Ramcharan M. Effect of compressive strain on cell viability in statically loaded articular cartilage. *Biomech Model Mechanobiol.* 2006;5:123-132.
8. Huser CA, Davies ME. Validation of an in vitro single-impact load model of the initiation of osteoarthritis-like changes in articular cartilage. *J Orthop Res.* 2006;24:725-732.
9. Loening AM, James IE, Levenston ME, et al. Injurious mechanical compression of bovine articular cartilage induces chondrocyte apoptosis. *Arch Biochem Biophys.* 2000;381:205-212.
10. Torzilli PA, Grigiene R, Borrelli J, Jr., et al. Effect of impact load on articular cartilage: cell metabolism and viability, and matrix water content. *J Biomech Eng.* 1999;121:433-441.
11. Kurz B, Jin M, Patwari P, et al. Biosynthetic response and mechanical properties of articular cartilage after injurious compression. *J Orthop Res.* 2001;19:1140-1146.

12. DiMicco MA, Patwari P, Siparsky PN, et al. Mechanisms and kinetics of glycosaminoglycan release following in vitro cartilage injury. *Arthritis Rheum.* 2004;50:840-848.
13. Natoli RM, Scott CC, Athanasiou KA. Temporal effects of impact on articular cartilage cell death, gene expression, matrix biochemistry, and biomechanics. *Ann Biomed Eng.* 2008;36:780-792.
14. Borrelli J, Jr., Silva MJ, Zaegel MA, et al. Single high-energy impact load causes posttraumatic OA in young rabbits via a decrease in cellular metabolism. *J Orthop Res.* 2009;27:347-352.
15. Mrosek EH, Lahm A, Erggelet C, et al. Subchondral bone trauma causes cartilage matrix degeneration: an immunohistochemical analysis in a canine model. *Osteoarthritis Cartilage.* 2006;14:171-178.
16. Jeffrey JE, Aspden RM. Cyclooxygenase inhibition lowers prostaglandin E2 release from articular cartilage and reduces apoptosis but not proteoglycan degradation following an impact load in vitro. *Arthritis Res Ther.* 2007;9:R129.
17. Joos H, Hogrefe C, Rieger L, et al. Single impact trauma in human early-stage osteoarthritic cartilage: implication of prostaglandin D2 but no additive effect of IL-1beta on cell survival. *Int J Mol Med.* 2011;28:271-277.
18. Green DM, Noble PC, Bocell JR, Jr., et al. Effect of early full weight-bearing after joint injury on inflammation and cartilage degradation. *J Bone Joint Surg Am.* 2006;88:2201-2209.
19. Borrelli J, Jr. Chondrocyte apoptosis and posttraumatic arthrosis. *J Orthop Trauma.* 2006;20:726-731.
20. Garner BC, Stoker AM, Kuroki K, et al. Using animal models in osteoarthritis biomarker research. *The journal of knee surgery.* 2011;24:251-264.
21. Ewers BJ, Dvoracek-Driksna D, Orth MW, et al. The extent of matrix damage and chondrocyte death in mechanically traumatized articular cartilage explants depends on rate of loading. *J Orthop Res.* 2001;19:779-784.
22. Ewers BJ, Jayaraman VM, Banglmaier RF, et al. Rate of blunt impact loading affects changes in retropatellar cartilage and underlying bone in the rabbit patella. *J Biomech.* 2002;35:747-755.
23. Quinn TM, Allen RG, Schalet BJ, et al. Matrix and cell injury due to sub-impact loading of adult bovine articular cartilage explants: effects of strain rate and peak stress. *J Orthop Res.* 2001;19:242-249.

24. Jeffrey JE, Brodie JP, Aspden RM. The effects of a single fast impact load compared with slow severe loading on articular cartilage in vitro. *Osteoarthritis Cartilage*. 2006;14:S81-S82.
25. Morel V, Quinn TM. Cartilage injury by ramp compression near the gel diffusion rate. *J Orthop Res*. 2004;22:145-151.
26. D'Lima DD, Hashimoto S, Chen PC, et al. Impact of mechanical trauma on matrix and cells. *Clin Orthop Relat Res*. 2001;S90-99.
27. Bush PG, Hodkinson PD, Hamilton GL, et al. Viability and volume of in situ bovine articular chondrocytes-changes following a single impact and effects of medium osmolarity. *Osteoarthritis Cartilage*. 2005;13:54-65.
28. Flachsmann R, Broom ND, Hardy AE. Deformation and rupture of the articular surface under dynamic and static compression. *J Orthop Res*. 2001;19:1131-1139.
29. Milentijevic D, Rubel IF, Liew AS, et al. An in vivo rabbit model for cartilage trauma: a preliminary study of the influence of impact stress magnitude on chondrocyte death and matrix damage. *J Orthop Trauma*. 2005;19:466-473.
30. Duda GN, Eilers M, Loh L, et al. Chondrocyte death precedes structural damage in blunt impact trauma. *Clin Orthop Relat Res*. 2001;302-309.
31. Haut RC, Ide TM, De Camp CE. Mechanical responses of the rabbit patello-femoral joint to blunt impact. *J Biomech Eng*. 1995;117:402-408.
32. Anderson DD, Chubinskaya S, Guilak F, et al. Post-traumatic osteoarthritis: improved understanding and opportunities for early intervention. *J Orthop Res*. 2011;29:802-809.
33. Potter HG, Jain SK, Ma Y, et al. Cartilage injury after acute, isolated anterior cruciate ligament tear: immediate and longitudinal effect with clinical/MRI follow-up. *Am J Sports Med*. 2012;40:276-285.
34. Shepherd DE, Seedhom BB. Thickness of human articular cartilage in joints of the lower limb. *Ann Rheum Dis*. 1999;58:27-34.
35. Robinovitch SN, Chiu J. Surface stiffness affects impact force during a fall on the outstretched hand. *J Orthop Res*. 1998;16:309-313.
36. King AI. Fundamentals of impact biomechanics: Part 2--Biomechanics of the abdomen, pelvis, and lower extremities. *Annu Rev Biomed Eng*. 2001;3:27-55.
37. Gosset M, Berenbaum F, Levy A, et al. Mechanical stress and prostaglandin E2 synthesis in cartilage. *Biorheology*. 2008;45:301-320.

38. Gosset M, Berenbaum F, Levy A, et al. Prostaglandin E2 synthesis in cartilage explants under compression: mPGES-1 is a mechanosensitive gene. *Arthritis Res Ther*. 2006;8:R135.
39. Farndale RW, Buttle DJ, Barrett AJ. Improved quantitation and discrimination of sulphated glycosaminoglycans by use of dimethylmethylene blue. *Biochim Biophys Acta*. 1986;883:173-177.
40. Reddy GK, Enwemeka CS. A simplified method for the analysis of hydroxyproline in biological tissues. *Clin Biochem*. 1996;29:225-229.
41. Anz A, Smith MJ, Stoker A, et al. The effect of bupivacaine and morphine in a coculture model of diarthrodial joints. *Arthroscopy*. 2009;25:225-231.
42. Chrisman OD, Ladenbauer-Bellis IM, Panjabi M, et al. 1981 Nicolas Andry Award. The relationship of mechanical trauma and the early biochemical reactions of osteoarthritic cartilage. *Clin Orthop Relat Res*. 1981;275-284.
43. Attur M, Statnikov A, Aliferis CF, et al. Inflammatory genomic and plasma biomarkers predict progression of symptomatic knee osteoarthritis (SKOA). *Osteoarthritis Cartilage*. 2012;20:S34-S35.
44. Young AA, Appleyard RC, Smith MM, et al. Dynamic biomechanics correlate with histopathology in human tibial cartilage: a preliminary study. *Clin Orthop Relat Res*. 2007;462:212-220.
45. Franz T, Hasler EM, Hagg R, et al. In situ compressive stiffness, biochemical composition, and structural integrity of articular cartilage of the human knee joint. *Osteoarthritis Cartilage*. 2001;9:582-592.
46. Niederauer GG, Niederauer GM, Cullen LC, Jr., et al. Correlation of cartilage stiffness to thickness and level of degeneration using a handheld indentation probe. *Ann Biomed Eng*. 2004;32:352-359.
47. Thomas TP, Anderson DD, Mosqueda TV, et al. Objective CT-based metrics of articular fracture severity to assess risk for posttraumatic osteoarthritis. *J Orthop Trauma*. 2010;24:764-769.
48. Anderson DD, Van Hofwegen C, Marsh JL, et al. Is elevated contact stress predictive of post-traumatic osteoarthritis for imprecisely reduced tibial plafond fractures? *J Orthop Res*. 2011;29:33-39.
49. Kos P, Varga F, Handl M, et al. Correlation of dynamic impact testing, histopathology and visual macroscopic assessment in human osteoarthritic cartilage. *Int Orthop*. 2011;35:1733-1739.

50. Kleemann RU, Krockner D, Cedraro A, et al. Altered cartilage mechanics and histology in knee osteoarthritis: relation to clinical assessment (ICRS Grade). *Osteoarthritis Cartilage*. 2005;13:958-963.

CHAPTER 5

BIOMARKERS AFFECTED BY IMPACT SEVERITY

DURING OSTEOCHONDRAL INJURY

Introduction

Osteoarthritis (OA) is the most common painful, debilitating disease that is projected to affect 59 million Americans by 2020.¹ Joint injury has been shown to increase the risk of developing post-traumatic osteoarthritis (PTOA) resulting in 12% of all OA cases, costing over 3 billion dollars annually in the United States.² Joint injuries often involve force dissipation throughout the joint organ: synovium, fat, ligaments/tendons, fibrocartilage, articular cartilage, and/or subchondral bone. If these tissues are unable to remodel and repair, then pathological changes such as cartilage degradation, bone sclerosis, osteophyte formation, or synovitis may implicate PTOA.

A similarity among all injuries resulting in PTOA is that there is mechanical insult(s) to the articular cartilage.³ These types of mechanical injuries have been previously categorized:⁴ (I) Damage to chondral matrix/cells (no cartilage disruption), (II) Cartilage disruption, (III) Cartilage-bone (osteocondral) disruption. Each joint injury initiates a unique response depending on the tissues damaged, injury severity, and a host of other factors.⁴ Mild injury (I) of the articular surface may elicit cartilage cell (chondrocyte) proliferation and/or matrix synthesis. Yet, excessive mechanical loading and/or pathobiological conditions may lead to fibrillation of the articular surface. Further, fibrillation increases the shear stress in the collagen network at the articular surface making it susceptible to additional degradation and upregulation in matrix

metalloproteinases (MMPs) and interleukins.⁵ Moderate injury (II) results in chondral ruptures or fractures. This injury may initiate chondrocyte proliferation and matrix synthesis, yet new tissue may be unable to fill and adequately repair the cartilage defect. Severe injury (III) evokes cell proliferation, formation of a fibrin clot, and production of new tissue. The tissue may remodel and sufficiently repair to restore functionality or it may degenerate. Degeneration is evident by demarcation loss between cartilage and bone at the osteochondral junction which may increase osteoclastic activity to remove damaged molecules within non-calcified cartilage.⁶ Further, excessive loading and/or joint inflammation may exacerbate fragmentation of the osteochondral junction and cartilage fissuring. As the calcified cartilage encroaches upon non-calcified cartilage, perivascular ossification and thickening of the subchondral plate may occur. Eventually, the bone may become sclerotic and stiff which can lead to secondary cartilage softening and irreversible degradation.⁷ Thus, prevention of primary cartilage injury, subchondral bone sclerosis, and secondary cartilage softening is warranted to reduce the accelerating number of patients that develop PTOA.

It is challenging to develop a clinically-relevant PTOA model since a clinical joint injury may be multi-classified (I-III). For example, force sustained during rupture of the anterior cruciate ligament (ACL) may also damage other ligaments, menisci, articular cartilage, or subchondral bone.⁸ Although typically ligament/meniscal tears are due to low-moderate energy injuries (I-II), whereas articular fractures result from high-energy injuries (III).⁹ Since early chondrocyte death has been discovered within articular fracture fragments from clinical cases,¹⁰ many experimental cartilage injury models have been created and demonstrated comparable results.¹¹⁻²¹ Likewise, we have discovered with our

in vitro cartilage injury model temporal/spatial mechanisms of chondrocyte death at early (day 0/superficial zone cell death) and later (day 12/superficial/middle/deep zones cell death) time points.²² There is a positive correlation between chondrocyte death and impact energy,²³ peak stress,¹⁷ rate of loading,^{19,22} strain,^{22,24} and location of peak load.²⁵⁻²⁷ Yet, the severity of trauma needed to initiate chondrocyte death in osteochondral explants with correlation to clinically-measurable biomarkers has not been fully established. Ultimately, these types of translatable correlations between biomechanical injury and biochemical responses may allow clinicians to improve therapies and treatments for patients who may be at acute and/or chronic risk for PTOA.

Therefore, the objective of this study was to evaluate the early effects of impact severity (i.e. maximum compression) on energy absorbed, chondrocyte viability, and biomarkers following osteochondral impact. Our hypothesis was there would be a direct relationship between impact severity and energy absorbed, cell viability, PGE₂ release from osteochondral explants.

Methods

The animals used were euthanatized for reasons unrelated to this study. All procedures were approved by the institutional animal care and use committee.

Normal osteochondral explants (n=72) were harvested under sterile conditions from the femoral condyles of euthanatized adult dogs (N=6) using a 6mm diameter Osteochondral Autograft Transfer System tool (Arthrex, Naples, Florida) and were trimmed to approximately 3.6mm total thickness using a diamond blade (IsoMet Low Speed Saw, Buehler, Lake Bluff, Illinois). Explants were cultured in 1ml Dulbecco's modified Eagle's medium (DMEM) high glucose supplemented with 1X insulin-

transferrin-selenium (ITS), penicillin, streptomycin, amphotericin B, L-glutamine, sodium pyruvate, L-ascorbic acid, and non-essential amino acids and incubated at 37°C, 95% humidity, and 6% CO₂ for six days prior to impact.

Explants were radially constrained in a stainless steel well (6.0mm diameter by 2.54mm deep) while a flat punch (3.9mm diameter) attached to the ram of a servohydraulic test machine (model 8821S, Canton, Massachusetts) was lowered at 0.01mm/sec and stopped at 10N compression (Fig. 5-1). Explant thickness was calculated as the difference in ram position with and without explants in well at day 0.

While still in well on day 0, each explant (except in the *No Impact* group) was subjected to a single impact load using a 2.25mm relative displacement ramp function with impact velocity ($V=100\text{mm/sec}$) with ram raised to an initial position that would result in the desired maximum compression ($D=0.25, 0.50, 0.75, 1.00, \text{ or } 1.25\text{mm}$ designated as *Low, Low-Mod, Moderate, Mod-High, High* impact groups, respectively) on the explants at peak ram travel. Impact force was measured using a 1000N load cell (model 3173, Lebow, Troy, Michigan) attached to the test table. Displacement, force, and time data was simultaneously collected at a frequency of 5000Hz. Displacement and force values were plotted in a force-displacement graph and the slope from 20-80% maximum force was calculated as the stiffness. Stress was calculated as force divided by cross-sectional area of the explant. Strain was calculated as displacement divided by explant initial length (thickness). Similarly, the slope of the stress-strain graph from 20-80% maximum stress was calculated as the modulus. Energy absorbed during impact injury was calculated by summing the average area of each force, F , and displacement, D , segment up to the maximum force, n , according to Eq. 5-1:

$$E = \sum_{i=1}^{n-1} \frac{F_{i+1} + F_i}{2} \times (D_{i+1} - D_i) \quad (5-1)$$

No Impact (0V:0D) group served as a control. Explants in the day 0 group (n=36) were analyzed immediately for chondrocyte viability and stored at -20°C for further analysis. Explants in the Day 12 group (n=36) were cultured in supplemented-DMEM as described above for 12 days. Media was changed at days 1, 3, 6, 9, 12 and stored at -20°C for further analysis.

After 12 days of culture, explants were assessed for total glycosaminoglycan (GAG) content using the 1,9-dimethylmethylene blue dye-binding (DMMB) assay,²⁸ hydroxyproline content indicative of cumulative collagen levels,²⁹ and double-stranded DNA. Assay values were normalized to tissue dry weight (mg). Chondrocyte viability was assessed via microscopy (model BX51, Olympus, Center Valley, Pennsylvania) through the depth of the tissue using a fluorescent calcien AM (CellTracker Green CMFDA) and ethidium bromide that stains live and dead cells, respectively (Invitrogen, Carlsbad, California). An in-house developed computer algorithm was developed to automatically count live and dead cells, respectively. Total percent cell viability was calculated as the number of live cells divided by the number of total cells within the cartilage multiplied by 100. Area percent cell viability was calculated as the area of live cells divided by the area of cartilage multiplied by 100.

GAG content of the media was assessed using the aforementioned DMMB assay. Nitric oxide (NO) concentration was determined using the Griess assay (Promega, Madison, Wisconsin). Prostaglandin E₂ (PGE₂) concentration was determined using an EIA assay (Cayman Chemical, Ann Arbor, Michigan). The cytokine/chemokine (GM-

CSF; IFN γ ; IL-2, -4, -6, -7, -8, -10, -15, -18; IP-10; KC; MCP-1; TNF α) and matrix metalloproteinase (MMP-2, -3, -8, -9, -13) concentration of the media were measured using multiplex xMAP assays (Luminex, Millipore, Billerica, Massachusetts).

Treatment comparisons for cartilage were analyzed by one-way analysis of variance with Tukey post-hoc group comparisons. Time comparisons were conducted using a two-tailed, t-test. Treatment comparisons for media biomarkers were analyzed by repeated measures analysis of variance with Holm-Sidak post-hoc group comparisons. Significance was set at $p < 0.05$ using SigmaPlot (San Rafael, California) for all statistical tests.

Results

Sample thickness for all osteochondral explants prior to impact were not significantly different (Table 5-1). Maximum displacement (compression) and strain increased with greater osteochondral impact ($p < 0.001$). Maximum compressive force was increased for *Moderate, Mod-High, High* versus *Low-Mod, Low* ($p \leq 0.002$); *Low-Mod* versus *Low* ($p = 0.007$). There were no significant differences in maximum compressive force among *Moderate, Mod-High, High* impact groups. Maximum compressive stress (force/area) followed similar trends such that *Moderate, Mod-High, High* were increased versus *Low-Mod, Low* ($p \leq 0.002$); *Low-Mod* versus *Low* ($p = 0.007$). Impact stiffness of *Moderate, Mod-High* was increased versus *Low* ($p \leq 0.034$). Impact modulus was increased for *Moderate, Mod-High, High* versus *Low* ($p \leq 0.026$). Impact time was significantly different ($p < 0.001$) among all groups with the exception of *Moderate* versus *Mod-High* ($p = 0.055$). Energy absorbed increased with greater osteochondral impact (Fig. 5-2). For

example, energy absorbed increased for *Low* versus *Low-Mod* versus *Moderate* versus *Mod-High* versus *High* ($p=0.709, 0.008, 0.048, 0.011$, respectively).

As impact increased, the amount of chondrocyte death increased at the superficial zone of the articular cartilage at day 0. At day 0, there was reduced area cell viability for *High* versus *Low-Mod* ($p=0.035$, Table 5-2). Total and area percent cell viability decreased with time from day 0 to day 12 for *Low-Mod* ($p=0.0426, 0.018$, respectively). For *Mod-High* and *High* explants that fractured, chondrocyte death appeared to be localized along the edges of the fracture site for all time points. However, the lower impact groups exhibited increased chondrocyte death within the middle and deep zones of the articular cartilage by day 12 (Fig. 5-3).

From day 0 to day 12, there was increased double-stranded DNA concentration for *Low-Mod* and *Moderate* ($p=0.002, 0.041$, respectively, Table 5-3). From day 0 to day 12, there was increased glycosaminoglycan (GAG) concentration for *Moderate* and *High* ($p=0.021, 0.022$, respectively). At day 12, hydroxyproline (HP) concentration was increased for *Moderate* versus *No Impact*, *Low*, *Mod-High*, *High* ($p<0.001, p=0.037, p<0.001, p<0.001$, respectively) and *Low-Mod* versus *No Impact*, *Mod-High*, *High* ($p=0.013, p=0.001, p=0.002$, respectively). From day 0 to day 12, there was decreased HP for *Mod-High* ($p=0.01$).

PGE₂ demonstrated the greatest sensitivity to osteochondral impact for all time points (Day 1-12). At day 1, PGE₂ concentration in the media (Fig. 5-4) was increased for *High* versus *Moderate*, *Low-Mod*, *Low*, *No Impact* ($p\leq 0.01$); *Mod-High* versus *Low-Mod*, *Moderate*, *No Impact* ($p<0.001$); *Moderate* versus *Low*, *No Impact* ($p=0.014, 0.02$, respectively). At day 3, PGE₂ was increased for *Mod-High* versus *Low-Mod*, *Low*, *No*

Impact ($p=0.003, 0.002, 0.001$, respectively). At day 6, PGE_2 was increased for *High* versus *Moderate, Low-Mod, Low, No Impact* ($p\leq 0.002$; *Mod-High* versus *Moderate, Low-Mod, Low, No Impact* ($p\leq 0.009$). At day 9, PGE_2 was increased for *Mod-High* versus *Low-Mod, Low, No Impact* ($p=0.032, 0.018, 0.032$, respectively). At day 12, PGE_2 was increased for *High* versus *Low* ($p=0.034$). Cumulatively, PGE_2 was increased for *High, Mod-High* versus *Moderate, Low-Mod, Low, No Impact* ($p\leq 0.036$).

Additional inflammatory (cytokine/chemokine) biomarkers were increased due to osteochondral impact. At day 1, MCP-1 was increased for *High, Mod-High* versus *Low, No Impact* ($p\leq 0.032$). At day 6, MCP-1 was increased for *High* versus *Low* ($p=0.036$). Cumulatively, MCP-1 was increased for *Mod-High* versus *Low* ($p=0.027$). Delayed biomarker response was evident at day 6 such that KC was increased for *High, Mod-High* versus *Low* ($p\leq 0.023$). Similarly at day 6, IL-8 was increased for *Mod-High* versus *Low* ($p=0.022$). This trend for IL-8 continued at day 9 where *Mod-High* was increased versus *Low* ($p=0.046$). At day 6, IL-6 was increased for *Mod-High* versus *Moderate, Low* ($p\leq 0.029$). This trend for IL-6 continued at day 9 where *Mod-High* was increased versus *Moderate, Low* ($p\leq 0.045$). Cumulatively, IL-6 was increased for *Mod-High* versus *Low* ($p=0.018$).

At day 3, there was increased nitric oxide (NO) for *High* versus *Low* ($p=0.037$, Table 5-4). At day 6, there was increased NO for *High, Mod-High* versus *Low* ($p=0.009, 0.014$, respectively).

Collagen degradation biomarkers were elevated later (Day 9, 12) due to osteochondral impact. Cumulatively, MMP-3 (stromelysin-1) was increased for *High* versus *Low* ($p=0.040$). At day 9, the amount of MMP-13 (collagenase 3) was increased for *High*,

Mod-High versus *Low-Mod, Low* ($p \leq 0.042$). At day 12, MMP-13 was increased for *Mod-High* versus *Low* ($p = 0.04$). Significant differences among other biomarkers were not detected.

Discussion

Impact to osteochondral explants resulted in various levels of energy absorbed corresponding to *Low, Low-Mod, Moderate, Mod-High, and High* impact groups. Clinically, the amount of energy absorbed and fragment displacement during fracture correlates to trauma severity³⁰ and has been quantified via computed tomography to estimate the risk of PTOA.³¹ In our study, there was no evidence of additional cell death or elevated biomarkers in the explants within the *Mod-High, High* impact groups that sustained fracture of the subchondral bone. Whether fracture may mitigate sustained cartilage trauma via cartilage force dissipation and/or cell progenitor activation requires further investigation.

Although there were no significant differences for total percent cell viability among groups, it was apparent that there was focal loss of cell viability within the superficial zone for *Mod, Mod-High, High* impact groups as well as along fracture edges at day 0. Similarly, Backus *et al.* reported reduced cell viability along the fractured edge of a porcine knee following transarticular impact loading.²⁶ The intrinsic load sharing between cartilage and bone within the osteochondral explant may determine the location and extent of chondrocyte death in response to impact. The reduced area percent cell viability of *High* versus *Low-Mod* in the present study suggests that energy absorbed for *Low-Mod, Low* impact groups may not be pathologic nor initiate catabolic responses. We suspect that a significant factor in determining if a patient develops PTOA is the amount

of energy absorbed specifically within cartilage during injury. Currently, the clinical measurement of cartilage energy absorbed during injury is not possible. Yet, in this study we measured osteochondral energy absorbed during impact; ideally, we also would have measured cartilage energy absorbed. However, this would require additional microscopic optical tracking of cartilage. Alternatively, a translational approach for estimating cartilage energy absorbed is to correlate the response of impact severity to clinically-measurable biomarkers that are sensitive to mechanical forces such as PGE₂.

Elevation of plasma PGE₂ has been associated with disease severity in symptomatic knee OA patients.^{32,33} Similar to our previous studies,^{22,34} PGE₂ release was highly dependent on maximum compression during high velocity (100mm/sec) impact to cartilage explants albeit the maximum amount produced in the present study was 100 times greater for osteochondral explants. Likewise, Joos et al. reported increased PGE₂ in human early OA cartilage 24 hours after impact injury.³⁵ Gosset et al. have described PGE₂ as a “mechanosensitive” biomarker and attribute this to the upstream enzyme microsomal prostaglandin E synthase type 1 (mPGES-1) gene which is highly sensitive to dynamic loading in cartilage explants.^{36,37} It is plausible that there may be a homeostatic threshold level of PGE₂ that is necessary for cartilage repair and bone remodeling. Yet, once this level of PGE₂ is surpassed and/or is sustained for long periods of time the initiation of early or post-traumatic osteoarthritis (PTOA) may begin. Further study is warranted to explore the relationship between PGE₂ response to cartilage injury and PTOA especially regarding clinical use of non-steroidal anti-inflammatory drugs (NSAIDs) that mitigate PGE₂ via the cyclooxygenase pathway.

Recently, our lab discovered a potential diagnostic OA biomarker panel for canines consisting of monocyte chemoattractant protein 1 (MCP-1), interleukin 8 (IL-8), keratinocyte-derived chemoattractant (KC), and matrix metalloproteinases (MMP-2, MMP-3).³⁸ Although this panel was derived from canine symptomatic OA samples, we similarly discovered elevations in MCP-1, IL-8, KC, and MMP-3 in the present study. Out of these biomarkers, MCP-1 demonstrated the most immediate and sustained response throughout the 12-day period following osteochondral impact. Specifically, at day 1 we discovered increased MCP-1 for *Mod-High*, *High* versus *Low*, *No Impact*. Cumulatively, MCP-1 was increased for *Mod-High* versus *Low*. MCP-1 is a cysteine-cysteine chemokine that may regulate migration of common monocyte osteoclast progenitor cells from blood/bone marrow to sites of osteoclast development at the bone surface.³⁹ Thus, it is plausible that increased MCP-1 indicates immediate remodeling of the osteochondral interface in response to impact of osteochondral explants.

Other chemokines such as KC and IL-8 demonstrated a delayed response to osteochondral impact. For instance, at day 6 KC was increased for *Mod-High*, *High* versus *Low* but not *No Impact*. Phylogenetic analysis has shown that canine KC/CXCL1 is similar to human growth regulated oncogene-alpha (GRO α).⁴⁰ As such, GRO α has been shown to induce the synthesis of tissue inhibitor of metalloproteinases (TIMP).⁴¹ Thus, the increase of KC in the present study may suggest an anabolic response to impact whereas later and sustained release of KC may promote cartilage hypertrophy present in OA.⁴² Also, the reduced amount of KC for *Low* may indicate an anabolic response to minimal impact. Further, this phenomenon implies that the free-swelling, *No Impact* control group may benefit (i.e. increased cell viability) with the addition of physiological

loading. Similar to KC, IL-8 is a cysteine-X-cysteine chemokine that demonstrates neutrophil chemotactic activity. Likewise, IL-8 appears to respond to osteochondral impact in a differential and temporal manner. Specifically, we found increased IL-8 for *Mod-High* versus *Low* at days 6 and 9 but not for *High* versus *No Impact*. Again, this response suggests that *Low* may not drive catabolism of osteochondral explants following impact but may indicate a reparative, anabolic response. Similar to others reporting increased IL-6 after experimental cartilage impact injury^{35,43} as well as clinical joint injury⁴⁴ we found that IL-6 elevation was a delayed response occurring at day 6 in the present study. Nevertheless, there was a cumulative increase of IL-6 for *Mod-High* versus *Low*.

Since we measured protein-level of biomarkers, it is plausible that we may have seen alterations of gene expression (increased mRNA levels) of these biomarkers at earlier time points. For example, others have reported increased MMP-3 gene expression immediately (1-24 hours) following experimental cartilage injury^{45,46} with elevated protein levels measured ~15 days following clinical joint injury.⁴⁷ In the present study, we measured increased cumulative amount of MMP-3 for *High* versus *Low*. Patwari et al.⁴⁵ reported increased MMP-3 but no alteration in MMP-13 gene expression following injury of juvenile bovine explants. In contrast, Ding et al.⁴⁸ reported increased MMP-13 gene expression following injury of mature bovine explants. In the present study, we detected increased MMP-13 concentration for *Mod-High* versus *Low* at day 9 and 12 following impact of mature canine osteochondral explants. Therefore, the aforementioned results may suggest that the role of MMP-3 and MMP-13 following cartilage injury may be dependent upon tissue maturity such that MMP-3 has a more

dominant role in juvenile tissue. Clinically, the number of teenage females that suffer anterior cruciate ligament (ACL) injury is increasing. Thus, many of these individuals may be skeletally-immature and at risk for PTOA. Further study is warranted to evaluate if treatment of MMP-3 or -13 inhibitors may have beneficial effects on joint health following cartilage injury depending on skeletal maturity. These translational studies may provide evidence for personalizing therapies for young patients at risk for PTOA.

Current studies in our laboratory are aimed at evaluating the effect of impact severity to both cartilage and osteochondral explants in the presence of additional joint tissues affected during injury. Further, the relationship among PTOA, impact, and post-injury loading with controlled intensity, frequency, and duration during physiological “exercise” programs or pathological loading conditions are being investigated through translational studies.



Figure 5-1. Custom made stainless steel fixtures consisting of the impactor ($\phi = 3.9\text{mm}$) attached to test machine ram (A), well ($\phi = 6.01\text{mm}$) (B), and base fixture (C) attached to test machine table used to measure the thickness and deliver impact injury of an osteochondral explant ($\phi = 6\text{mm}$, thickness= $3.6\pm 0.29\text{mm}$) (D).

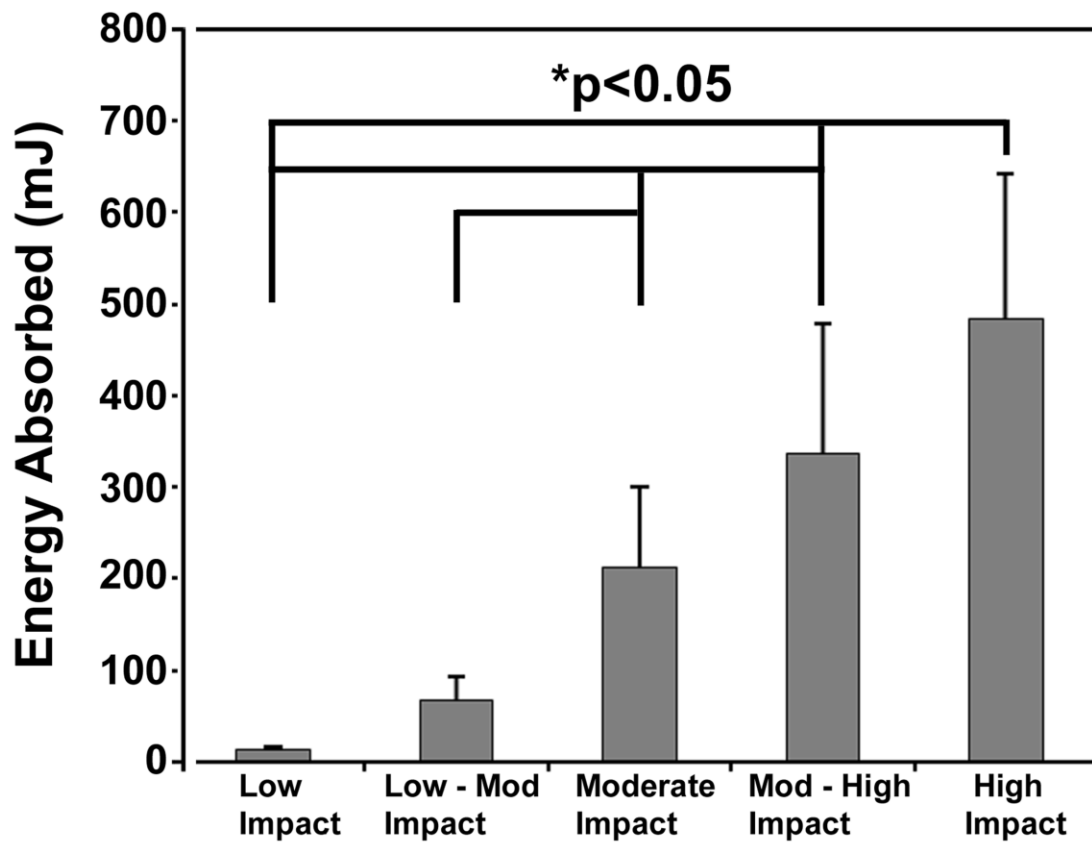


Figure 5-2. Energy absorbed by integrating the area under the force-displacement curve during 100mm/sec impact resulting in max compression of 0.25mm (Low), 0.5mm (Low-Mod), 0.75mm (Moderate), 1mm (Mod-High), or 1.25mm(High) of the osteochondral explant.

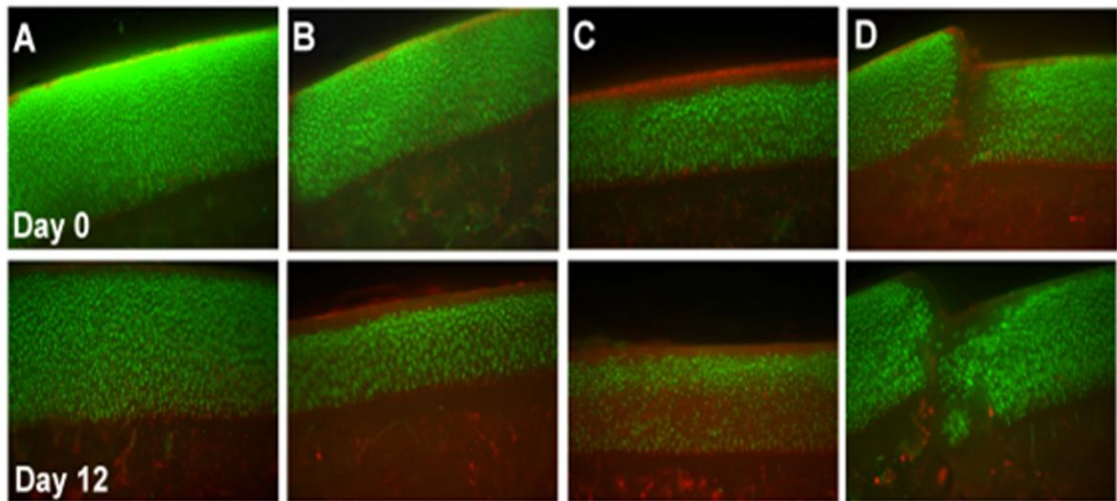


Figure 5-3. Representative fluorescent images of live (green) and dead (red) cells within cartilage of osteochondral explants from Control – no impact (A), Low Impact – 0.25mm max compression (B), Moderate Impact – 0.75mm max compression (C), and High Impact – 1.25mm max compression groups after impact on day 0 and day 12 after culture (D).

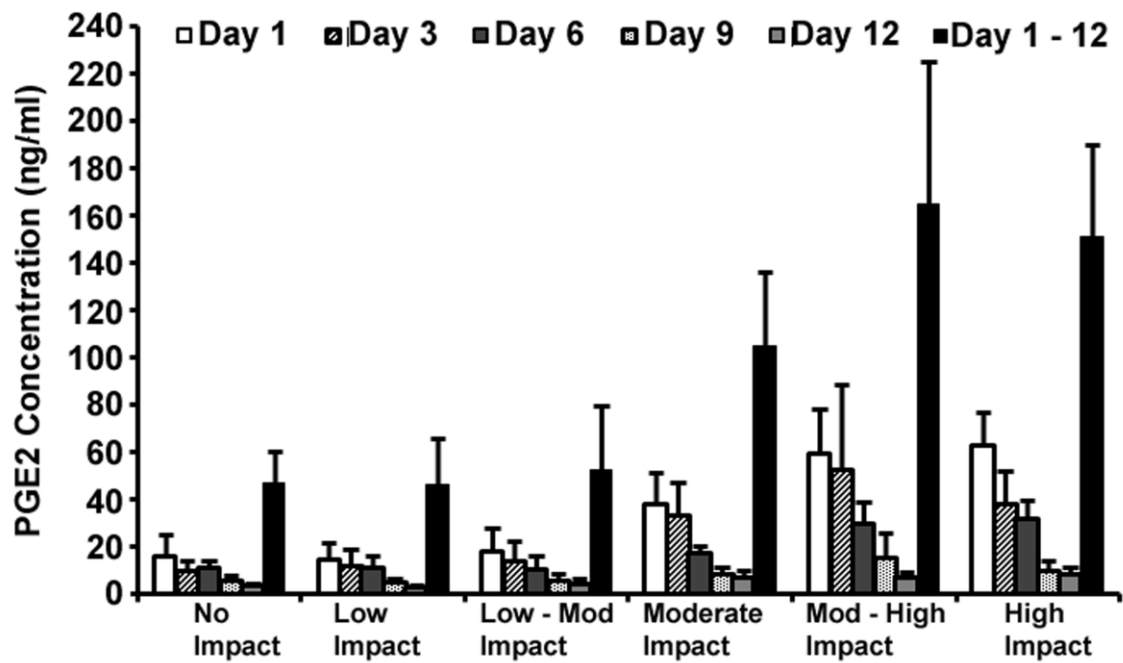


Figure 5-4. Prostaglandin E2 (PGE2) released by the osteochondral explants into the media.

Table 5-1. Biomechanical properties during day 0 testing of osteochondral explants.

Biomechanical Properties	Study Groups					
	No ¹	Low ²	Low-Mod ³	Moderate ⁴	Mod-High ⁵	High ⁶
Sample Thickness (mm)	3.599 ± 0.2613	3.666 ± 0.2454	3.592 ± 0.2138	3.592 ± 0.1626	3.689 ± 0.5037	3.730 ± 0.3106
Max Compression (mm)		0.2539 ^A ± 0.0035	0.4903 ^A ± 0.0067	0.7370 ^A ± 0.0096	1.001 ^A ± 0.0129	1.262 ^A ± 0.0124
Max Compressive Strain (mm/mm)		0.0695 ^A ± 0.0042	0.1360 ^A ± 0.0059	0.2056 ^A ± 0.0096	0.2766 ^A ± 0.0440	0.3405 ^A ± 0.0299
Max Compressive Force (N)		106.3 ^{A-C} ± 33.37	370.4 ^{A-C} ± 151.5	696.8 ^A ± 256.8	682.8 ^B ± 220.5	738.6 ^C ± 174.1
Max Compressive Stress (MPa)		8.901 ^{A-C} ± 2.794	31.01 ^{A-C} ± 12.68	58.33 ^A ± 21.49	57.16 ^B ± 18.46	61.83 ^C ± 14.57
Stiffness (N/mm)		380.8 ^{A,B} ± 92.87	549.9 ± 230.9	775.5 ^A ± 307.6	692.3 ^B ± 290.8	658.5 ± 247.1
Compressive Modulus (MPa)		115.9 ^{A-C} ± 24.99	162.8 ± 64.89	230.6 ^A ± 88.32	206.0 ^B ± 77.14	201.8 ^C ± 70.33
Impact Time (msec)		6.500 ^{A,B} ± 1.415	8.933 ^{A,B} ± 1.237	12.03 ^A ± 1.477	13.40 ^B ± 0.5578	16.13 ^{A,B} ± 0.5929

¹No = Control, non-injured osteochondral explant group

²Low Trauma = Impact at 100 mm/sec to 0.25mm compression of explant group

³Low-Mod Trauma = Impact at 100 mm/sec to 0.50mm compression of explant group

⁴Moderate Trauma = Impact at 100 mm/sec to 0.75mm compression of explant group

⁵Mod-High Trauma = Impact at 100 mm/sec to 1.00mm compression of explant group

⁶High Trauma = Impact at 100 mm/sec to 1.25mm compression of explant group

Groups within each row sharing a letter are significantly different (p<0.05)

Table 5-2. Cell viability of chondrocytes within osteochondral explants.

Cell Viability	Day 0						Day 12					
	No ¹	Low ²	Low-Mod ³	Mod ⁴	Mod-High ⁵	High ⁶	No	Low	Low-Mod	Mod	Mod-High	High
Area (%)	90.78 ± 3.967	89.37 ± 4.603	91.92 ^A ± 1.308	85.47 ± 4.172	80.49 ± 2.965	74.9 ^A ± 20.94	90.52 ± 0.9508	86.23 ± 5.533	87.78 ± 3.340	84.13 ± 6.649	80.81 ± 6.122	78.29 ± 6.571
Total (%)	88.31 ± 3.964	85.27 ± 7.332	94.69 ± 1.793	84.79 ± 7.701	90.96 ± 4.655	90.89 ± 10.08	79.09 ± 11.86	89.35 ± 8.872	89.25 ± 5.453	91.63 ± 4.333	85.85 ± 4.312	90.02 ± 6.134

¹No = Control, non-injured osteochondral explant group

²Low Trauma = Impact at 100 mm/sec to 0.25mm compression of explant group

³Low-Mod Trauma = Impact at 100 mm/sec to 0.50mm compression of explant group

⁴Moderate Trauma = Impact at 100 mm/sec to 0.75mm compression of explant group

⁵Mod-High Trauma = Impact at 100 mm/sec to 1.00mm compression of explant group

⁶High Trauma = Impact at 100 mm/sec to 1.25mm compression of explant group

Groups within each row sharing a letter are significantly different (p<0.05)

Table 5-3. Cartilage double-stranded DNA, glycosaminoglycan (GAG), and hydroxyproline (HP) concentration of osteochondral explants.

Cartilage Bio-marker	Day 0						Day 12					
	No ¹	Low ²	Low-Mod ³	Mod ⁴	Mod-High ⁵	High ⁶	No ¹	Low ²	Low-Mod ³	Mod ⁴	Mod-High ⁵	High ⁶
dsDNA (ng/mg)	32.50 ± 4.620	30.08 ± 12.98	26.82 ^A ± 5.639	27.49 ^B ± 3.590	27.98 ± 3.117	25.30 ± 4.603	34.59 ± 8.231	34.12 ± 6.399	45.48 ^A ± 4.287	36.24 ^B ± 7.397	33.35 ± 7.060	37.62 ± 14.12
GAG (µg/mg)	73.70 ± 20.25	70.99 ± 36.58	77.92 ± 18.29	65.75 ^A ± 15.52	73.48 ± 10.30	61.26 ^B ± 17.19	91.15 ± 35.25	88.65 ± 9.257	101.45 ± 24.58	90.95 ^A ± 16.47	66.97 ± 20.17	89.88 ^B ± 19.21
HP (µg/mg)	23.91 ± 7.912	22.78 ± 10.98	24.12 [±] 11.39	28.36 ± 11.31	26.79 ^H ± 2.073	13.97 ± 2.637	16.79 ^{A,E} ± 5.128	23.94 ^B ± 9.756	33.76 ^{E,G} ± 14.19	38.90 ^{A,D} ± 7.593	12.64 ^{C,F} ±	13.20 ^{D,G} ± 3.856

¹No = Control, non-injured osteochondral explant group

²Low Trauma = Impact at 100 mm/sec to 0.25mm compression of explant group

³Low-Mod Trauma = Impact at 100 mm/sec to 0.50mm compression of explant group

⁴Moderate Trauma = Impact at 100 mm/sec to 0.75mm compression of explant group

⁵Mod-High Trauma = Impact at 100 mm/sec to 1.00mm compression of explant group

⁶High Trauma = Impact at 100 mm/sec to 1.25mm compression of explant group

Groups within each row and time point sharing a letter are significantly different (p<0.05)

Table 5-4. Biomarkers released by osteochondral explants into the media.

Media Bio-marker	Day 1						Day 3					
	No ¹	Low ²	Low-Mod ³	Mod ⁴	Mod-High ⁵	High ⁶	No	Low	Low-Mod	Mod	Mod-High	High
MCP-1 (pg/ml)	2439 ^{A,B} ± 741.5	3025 ^C ± 1285	3472 ± 1976	3670 ± 1016	5930 ^{A,C} ± 2176	5172 ^B ± 1772	3193 ± 1402	2432 ± 1359	4720 ± 4575	4363 ± 1320	6343 ± 3247	5237 ± 1145
KC (pg/ml)	1967 ± 935.4	2199 ± 679.6	2823 ± 1054	2353 ± 648.3	2411 ± 831.1	2626 ± 850.8	1425 ± 740.9	965.4 ± 228.3	1539 ± 909.9	1596 ± 955.6	2077 ± 1182	2248 ± 488.2
IL-8 (pg/ml)	4794 ± 2601	4432 ± 1985	8317 ± 5508	4953 ± 1283	7628 ± 6895	7474 ± 5179	4092 ± 2762	2043 ± 964.5	4285 ± 3236	3854 ± 2110	7603 ± 7621	6483 ± 2840
IL-6 (pg/ml)	44.67 ± 32.66	44.91 ± 28.69	103.9 ± 133.0	60.47 ± 14.69	108.1 ± 46.18	105.1 ± 35.40	42.66 ± 26.26	23.11 ± 16.18	77.23 ± 101.5	58.81 ± 24.49	115.7 ± 89.60	82.74 ± 33.17
Media Bio-marker	Day 6						Day 9					
	No	Low	Low-Mod	Mod	Mod-High	High	No	Low	Low-Mod	Mod	Mod-High	High
MCP-1 (pg/ml)	5122 ± 1773	4436 ^A ± 1856	4952 ± 3463	5779 ± 1864	11298 ± 5390	12348 ^A ± 8050	6953 ± 2472	5706 ± 2204	9090 ± 6989	7648 ± 1337	15096 ± 10770	10050 ± 7143
KC (pg/ml)	952.0 ± 471.9	757.7 ^{A,B} ± 835.7	1154 ± 835.7	1151 ± 548.2	2068 ^A ± 967.6	1997 ^B ± 480.5	1222 ± 504.0	834.5 ± 273.6	1393 ± 911.0	980.8 ± 280.5	1647 ± 879.4	1273 ± 643.4
IL-8 (pg/ml)	2975 ± 2053	1841 ^A ± 1061	3447 ± 3002	2772 ± 1275	9286 ^A ± 7936	6598 ± 2810	3146 ± 1285	2054 ^A ± 1025	3932 ± 2950	2535 ± 616.0	6141 ^A ± 3590	4229 ± 2390
IL-6 (pg/ml)	49.35 ± 32.25	27.50 ^A ± 20.75	65.27 ± 65.87	38.88 ^B ± 19.15	172.7 ^{A,B} ± 139.6	120.1 ± 61.95	39.42 ± 14.63	23.60 ^A ± 20.89	64.37 ± 54.03	32.77 ^B ± 13.09	109.6 ^{A,B} ± 53.58	82.34 ± 59.63
Media Bio-marker	Day 12						Cumulative (Day 1 - 12)					
	No	Low	Low-Mod	Mod	Mod-High	High	No	Low	Low-Mod	Mod	Mod-High	High
MCP-1 (pg/ml)	8095 ± 5540	5922 ± 2941	10508 ± 9100	9479 ± 2920	16468 ± 12964	12163 ± 10723	25802 ± 6707	21522 ^A ± 9026	32741 ± 23810	30938 ± 4730	55136 ^A ± 29981	44969 ± 25627
KC (pg/ml)	1121 ± 862.7	665.7 ± 297.5	1290 ± 851.5	806.8 ± 216.0	1280 ± 703.9	992.0 ± 322.9	6687 ± 808.9	5422 ± 1576	8200 ± 4141	6887 ± 2294	9482 ± 3634	9136 ± 1389
IL-8 (pg/ml)	2904 ± 1708	1487 ± 737.2	3403 ± 2435	1908 ± 388.5	4563 ± 3116	2931 ± 1528	17911 ± 6931	11857 ± 5276	23384 ± 14521	16022 ± 5226	35222 ± 26565	27714 ± 9306
IL-6 (pg/ml)	32.50 ± 29.78	7.890 ± 8.718	43.73 ± 44.48	12.28 ± 10.59	64.80 ± 42.84	43.48 ± 34.16	208.6 ± 53.33	127.0 ^A ± 83.70	354.5 ± 340.3	203.2 ± 58.50	570.9 ^A ± 355.5	433.7 ± 168.6

Table 5-4 (continued). Biomarkers released by osteochondral explants into the media.

Media Bio-marker	Day 1						Day 3					
	No ¹	Low ²	Low-Mod ³	Mod ⁴	Mod-High ⁵	High ⁶	No	Low	Low-Mod	Mod	Mod-High	High
GAG (µg/ml)	92.41 ± 35.28	73.47 ± 35.34	71.16 ± 13.55	71.46 ± 14.62	71.78 ± 36.53	119.46 ± 74.93	94.56 ± 35.03	74.50 ± 26.40	73.55 ± 6.997	71.20 ± 14.49	67.32 ± 28.35	90.26 ± 24.83
NO (uM/ml)	4.738 ± 0.7765	4.655 ± 1.127	4.655 ± 1.137	5.127 ± 0.3230	5.043 ± 1.423	4.960 ± 1.464	4.361 ± 2.540	2.765 ^A ± 2.195	3.794 ± 1.953	4.754 ± 1.166	5.500 ± 1.341	6.410 ^A ± 1.448
MMP2 (ng/ml)	0.6263 ± 0.4075	0.8600 ± 0.6807	0.9521 ± 0.6607	1.121 ± 0.6008	1.395 ± 0.7225	0.8854 ± 0.6992	1.429 ± 0.7045	1.648 ± 0.8998	1.683 ± 0.7536	2.078 ± 0.6643	2.027 ± 0.5849	1.817 ± 0.8818
MMP3 (ng/ml)	1.857 ± 0.2241	1.747 ± 0.1435	2.021 ± 0.2858	1.858 ± 0.0925	1.863 ± 0.1346	1.891 ± 0.1286	1.747 ± 0.3319	1.584 ± 0.1476	1.711 ± 0.2576	1.690 ± 0.1173	1.745 ± 0.2103	1.824 ± 0.1466
MMP13 (ng/ml)	2.557 ± 1.588	2.103 ± 1.366	2.813 ± 2.086	2.557 ± 0.7544	3.191 ± 1.552	3.369 ± 1.650	2.912 ± 2.162	2.584 ± 1.759	2.813 ± 1.943	3.955 ± 1.557	4.406 ± 1.966	4.734 ± 1.863
Media Bio-marker	Day 6						Day 9					
	No	Low	Low-Mod	Mod	Mod-High	High	No	Low	Low-Mod	Mod	Mod-High	High
GAG (µg/ml)	82.73 ± 31.02	91.67 ± 18.18	104.7 ± 4.198	103.5 ± 11.00	64.34 ± 35.47	85.32 ± 38.83	80.72 ± 34.05	77.33 ± 27.47	83.42 ± 22.50	78.42 ± 25.25	68.51 ± 31.99	73.84 ± 12.84
NO (uM/ml)	4.800 ± 1.022	1.986 ^{A,B} ± 2.207	3.552 ± 1.932	4.885 ± 1.199	5.508 ^A ± 1.291	5.692 ^B ± 1.423	3.664 ± 0.2720	2.861 ± 1.407	3.511 ± 1.874	4.730 ± 0.9127	4.753 ± 0.5869	4.639 ± 0.7408
MMP2 (ng/ml)	2.656 ± 0.5667	2.592 ± 0.7389	2.635 ± 0.7696	3.161 ± 0.6609	3.409 ± 0.5955	3.354 ± 0.6866	3.537 ± 0.4119	3.534 ± 0.5867	3.591 ± 0.6316	4.101 ± 0.6104	4.122 ± 0.7411	3.968 ± 0.7830
MMP3 (ng/ml)	1.837 ± 0.2957	1.642 ± 0.1777	1.763 ± 0.2738	1.720 ± 0.0998	1.928 ± 0.2006	1.991 ± 0.1231	1.808 ± 0.1014	1.639 ± 0.2156	1.809 ± 0.2613	1.771 ± 0.1645	1.842 ± 0.2282	1.871 ± 0.1700
MMP13 (ng/ml)	5.223 ± 3.111	4.705 ± 2.990	4.589 ± 2.775	7.117 ± 3.095	8.668 ± 2.392	8.892 ± 2.226	8.285 ± 3.135	6.623 ^{A,D} ± 3.618	6.899 ^{B,C} ± 3.384	9.011 ± 2.301	11.47 ^{A,C} ± 1.852	11.68 ^{B,D} ± 1.169
Media Bio-marker	Day 12						Cumulative (Day 1 - 12)					
	No	Low	Low-Mod	Mod	Mod-High	High	No	Low	Low-Mod	Mod	Mod-High	High
GAG (µg/ml)	66.58 ± 26.92	66.70 ± 20.68	73.09 ± 21.10	55.53 ± 16.41	49.42 ± 27.10	63.54 ± 21.04	417.0 ± 149.4	383.7 ± 105.4	405.9 ± 35.07	380.1 ± 56.21	321.4 ± 157.7	432.4 ± 155.9
NO (uM/ml)	3.952 ± 0.3957	3.122 ± 1.590	2.731 ± 2.174	4.211 ± 0.4465	4.623 ± 0.9373	4.280 ± 0.6597	21.51 ± 3.845	15.39 ± 7.272	18.24 ± 7.311	23.71 ± 3.303	25.43 ± 4.766	25.98 ± 3.723
MMP2 (ng/ml)	3.665 ± 0.3684	3.655 ± 0.5094	3.763 ± 0.7244	4.461 ± 0.7147	4.437 ± 0.8236	3.969 ± 0.6545	11.91 ± 2.196	12.29 ± 3.298	12.62 ± 3.349	14.92 ± 2.988	15.39 ± 3.084	14.00 ± 3.369
MMP3 (ng/ml)	1.696 ± 0.1343	1.492 ± 0.0683	1.768 ± 0.2761	1.687 ± 0.1777	1.717 ± 0.2100	1.699 ± 0.1412	8.945 ± 0.7825	8.104 ^A ± 0.6205	9.073 ± 1.174	8.725 ± 0.5552	9.095 ± 0.6341	9.276 ^A ± 0.3129
MMP13 (ng/ml)	8.214 ± 2.334	6.781 ^A ± 3.023	7.806 ± 4.064	9.041 ± 2.200	11.76 ^A ± 2.600	10.997 ± 0.8172	27.19 ± 11.84	22.80 ± 12.25	24.92 ± 13.28	31.68 ± 9.026	39.49 ± 8.638	39.67 ± 5.884

¹No = Control, non-injured osteochondral explant group

²Low Trauma = Impact at 100 mm/sec to 0.25mm compression of explant group

³Low-Mod Trauma = Impact at 100 mm/sec to 0.50mm compression of explant group

⁴Moderate Trauma = Impact at 100 mm/sec to 0.75mm compression of explant group

⁵Mod-High Trauma = Impact at 100 mm/sec to 1.00mm compression of explant group

⁶High Trauma = Impact at 100 mm/sec to 1.25mm compression of explant group

Groups within each row and time point sharing a letter are significantly different (p<0.05)

References

1. Lawrence RC, Helmick CG, Arnett FC, et al. Estimates of the prevalence of arthritis and selected musculoskeletal disorders in the United States. *Arthritis Rheum.* 1998;41:778-799.
2. Brown TD, Johnston RC, Saltzman CL, et al. Posttraumatic osteoarthritis: a first estimate of incidence, prevalence, and burden of disease. *J Orthop Trauma.* 2006;20:739-744.
3. Buckwalter JA. Articular cartilage injuries. *Clin Orthop Relat Res.* 2002;21-37.
4. Buckwalter JA, Brown TD. Joint injury, repair, and remodeling: roles in post-traumatic osteoarthritis. *Clin Orthop Relat Res.* 2004;423:7-16.
5. Chaudhari AM, Briant PL, Bevill SL, et al. Knee kinematics, cartilage morphology, and osteoarthritis after ACL injury. *Med Sci Sports Exerc.* 2008;40:215-222.
6. Suri S, Walsh DA. Osteochondral alterations in osteoarthritis. *Bone.* 2012;51:204-211.
7. Haut RC, Ide TM, De Camp CE. Mechanical responses of the rabbit patellofemoral joint to blunt impact. *J Biomech Eng.* 1995;117:402-408.
8. Lohmander LS, Englund PM, Dahl LL, et al. The long-term consequence of anterior cruciate ligament and meniscus injuries: osteoarthritis. *Am J Sports Med.* 2007;35:1756-1769.
9. Buckwalter JA, Saltzman C, Brown T. The impact of osteoarthritis: implications for research. *Clin Orthop Relat Res.* 2004;S6-15.
10. Kim HT, Lo MY, Pillarisetty R. Chondrocyte apoptosis following intraarticular fracture in humans. *Osteoarthritis Cartilage.* 2002;10:747-749.
11. Borrelli J, Jr., Tinsley K, Ricci WM, et al. Induction of chondrocyte apoptosis following impact load. *J Orthop Trauma.* 2003;17:635-641.
12. D'Lima DD, Hashimoto S, Chen PC, et al. Human chondrocyte apoptosis in response to mechanical injury. *Osteoarthritis Cartilage.* 2001;9:712-719.
13. D'Lima DD, Hashimoto S, Chen PC, et al. Impact of mechanical trauma on matrix and cells. *Clin Orthop Relat Res.* 2001;S90-99.
14. Huser CA, Peacock M, Davies ME. Inhibition of caspase-9 reduces chondrocyte apoptosis and proteoglycan loss following mechanical trauma. *Osteoarthritis Cartilage.* 2006;14:1002-1010.

15. Krueger JA, Thisse P, Ewers BJ, et al. The extent and distribution of cell death and matrix damage in impacted chondral explants varies with the presence of underlying bone. *J Biomech Eng.* 2003;125:114-119.
16. Loening AM, James IE, Levenston ME, et al. Injurious mechanical compression of bovine articular cartilage induces chondrocyte apoptosis. *Arch Biochem Biophys.* 2000;381:205-212.
17. Milentijevic D, Helfet DL, Torzilli PA. Influence of stress magnitude on water loss and chondrocyte viability in impacted articular cartilage. *J Biomech Eng.* 2003;125:594-601.
18. Milentijevic D, Rubel IF, Liew AS, et al. An in vivo rabbit model for cartilage trauma: a preliminary study of the influence of impact stress magnitude on chondrocyte death and matrix damage. *J Orthop Trauma.* 2005;19:466-473.
19. Milentijevic D, Torzilli PA. Influence of stress rate on water loss, matrix deformation and chondrocyte viability in impacted articular cartilage. *J Biomech.* 2005;38:493-502.
20. Natoli RM, Scott CC, Athanasiou KA. Temporal effects of impact on articular cartilage cell death, gene expression, matrix biochemistry, and biomechanics. *Ann Biomed Eng.* 2008;36:780-792.
21. Patwari P, Gaschen V, James IE, et al. Ultrastructural quantification of cell death after injurious compression of bovine calf articular cartilage. *Osteoarthritis Cartilage.* 2004;12:245-252.
22. Waters NP, Stoker AM, Carson WL, et al. Effects of impact velocity and maximum strain on articular cartilage matrix composition, cell viability, and culture media. *55th Annual Meeting of the Orthopaedic Research Society.* Las Vegas, NV. 2009;Paper 1088.
23. Jeffrey JE, Gregory DW, Aspden RM. Matrix damage and chondrocyte viability following a single impact load on articular cartilage. *Arch Biochem Biophys.* 1995;322:87-96.
24. Torzilli PA, Deng XH, Ramcharan M. Effect of compressive strain on cell viability in statically loaded articular cartilage. *Biomech Model Mechanobiol.* 2006;5:123-132.
25. Waters NP, Stoker AM, Pfeiffer FM, et al. Biological effects of impact maximum compression on osteochondral explants. *58th Annual Meeting of the Orthopaedic Research Society.* San Francisco, CA. 2012;Paper 829.

26. Backus JD, Furman BD, Swimmer T, et al. Cartilage viability and catabolism in the intact porcine knee following transarticular impact loading with and without articular fracture. *J Orthop Res*. 2011;29:501-510.
27. Hembree WC, Ward BD, Furman BD, et al. Viability and apoptosis of human chondrocytes in osteochondral fragments following joint trauma. *J Bone Joint Surg Br*. 2007;89:1388-1395.
28. Farndale RW, Buttle DJ, Barrett AJ. Improved quantitation and discrimination of sulphated glycosaminoglycans by use of dimethylmethylene blue. *Biochim Biophys Acta*. 1986;883:173-177.
29. Reddy GK, Enwemeka CS. A simplified method for the analysis of hydroxyproline in biological tissues. *Clin Biochem*. 1996;29:225-229.
30. Anderson DD, Mosqueda T, Thomas T, et al. Quantifying tibial plafond fracture severity: absorbed energy and fragment displacement agree with clinical rank ordering. *J Orthop Res*. 2008;26:1046-1052.
31. Thomas TP, Anderson DD, Mosqueda TV, et al. Objective CT-based metrics of articular fracture severity to assess risk for posttraumatic osteoarthritis. *J Orthop Trauma*. 2010;24:764-769.
32. Attur M, Statnikov A, Aliferis CF, et al. Inflammatory genomic and plasma biomarkers predict progression of symptomatic knee osteoarthritis (SKOA). *Osteoarthritis Cartilage*. 2012;20:S34-S35.
33. Nemirovskiy O, Buck R, Sunyer T, et al. Predicting radiographic joint space narrowing (JSN) using biomarkers for osteoarthritis (OA) clinical trials. *Osteoarthritis and Cartilage*. 2008;16:S56-S57.
34. Waters NP, Stoker AM, Pfeiffer FM, et al. Effects of impact velocity and maximum strain on articular cartilage material properties, extracellular matrix, and tissue inflammation. *56th Annual Meeting of the Orthopaedic Research Society*. New Orleans, LA. 2010;Paper 942.
35. Joos H, Hogrefe C, Rieger L, et al. Single impact trauma in human early-stage osteoarthritic cartilage: implication of prostaglandin D2 but no additive effect of IL-1beta on cell survival. *Int J Mol Med*. 2011;28:271-277.
36. Gosset M, Berenbaum F, Levy A, et al. Mechanical stress and prostaglandin E2 synthesis in cartilage. *Biorheology*. 2008;45:301-320.
37. Gosset M, Berenbaum F, Levy A, et al. Prostaglandin E2 synthesis in cartilage explants under compression: mPGES-1 is a mechanosensitive gene. *Arthritis Res Ther*. 2006;8:R135.

38. Garner BC, Stoker AM, Kuroki K, et al. Using animal models in osteoarthritis biomarker research. *The journal of knee surgery*. 2011;24:251-264.
39. Bilezikian JP, Raisz LG, Martin TJ. *Principles of bone biology*. 3rd ed. San Diego, Calif.: Academic Press/Elsevier; 2008.
40. Modi WS, Yoshimura T. Isolation of novel GRO genes and a phylogenetic analysis of the CXC chemokine subfamily in mammals. *Mol Biol Evol*. 1999;16:180-193.
41. Unemori EN, Marsters JC, Bauer EA, et al. The product of the gro gene regulates collagen turnover by inducing tissue inhibitor of metalloproteinases. *Arthritis Rheum*. 1991;34:S117.
42. Merz D, Liu R, Johnson K, et al. IL-8/CXCL8 and growth-related oncogene alpha/CXCL1 induce chondrocyte hypertrophic differentiation. *J Immunol*. 2003;171:4406-4415.
43. Sui Y, Lee JH, DiMicco MA, et al. Mechanical injury potentiates proteoglycan catabolism induced by interleukin-6 with soluble interleukin-6 receptor and tumor necrosis factor alpha in immature bovine and adult human articular cartilage. *Arthritis Rheum*. 2009;60:2985-2996.
44. Sward P, Frobell R, Englund M, et al. Cartilage and bone markers and inflammatory cytokines are increased in synovial fluid in the acute phase of knee injury (hemarthrosis) - a cross-sectional analysis. *Osteoarthritis Cartilage*. 2012;
45. Patwari P, Cook MN, DiMicco MA, et al. Proteoglycan degradation after injurious compression of bovine and human articular cartilage in vitro: interaction with exogenous cytokines. *Arthritis Rheum*. 2003;48:1292-1301.
46. Lee JH, Fitzgerald JB, Dimicco MA, et al. Mechanical injury of cartilage explants causes specific time-dependent changes in chondrocyte gene expression. *Arthritis Rheum*. 2005;52:2386-2395.
47. Catterall JB, Stabler TV, Flannery CR, et al. Changes in serum and synovial fluid biomarkers after acute injury (NCT00332254). *Arthritis Res Ther*. 2010;12:R229.
48. Ding L, Heying E, Nicholson N, et al. Mechanical impact induces cartilage degradation via mitogen activated protein kinases. *Osteoarthritis Cartilage*. 2010;18:1509-1517.

CHAPTER 6

BIOMARKERS AFFECTED BY OSTEOCHONDRAL IMPACT

WITH POST-INJURY LOADING

Introduction

Acute joint injury has been shown to increase the risk of developing post-traumatic osteoarthritis (PTOA) resulting in 12% of all OA cases, afflicting 5.6 million Americans, and costing over 3 billion dollars annually in the United States.¹ These statistics are estimated to dramatically increase since OA is projected to affect 59 million Americans by 2020.² At this time, there are no disease-modifying osteoarthritis drugs (DMOADs), and all treatments currently available are palliative. Further, there are no tests available to differentiate between patients that will develop PTOA after injury from those that will not. The inability to differentiate between patients that will develop PTOA from patients that will not, or even to identify patients in the early phase 1 (silent molecular phase), has hindered the development of DMOADs because a suitable treatment population cannot be identified for clinical trials. Therefore, it is important to identify biomarkers involved early in the disease sequelae to diagnose patients with the potential for developing PTOA. Once these patients can be identified during the early stages of OA (Phase 1:silent molecular stage),³ potential DMOADs can be evaluated based on their ability to prevent PTOA development in this patient population. To identify new potential biomarkers for PTOA development, we have developed an *in vitro* osteochondral impact injury model that applies post-injury loading to mimic activities of daily living such as walking that may lead to early onset of PTOA.

Recently, MRI was used to detect “mild” chondral defects and bone bruising immediately after anterior cruciate injury.⁴ This suggests that immediately after clinical injury alteration to the osteochondral junction may exist. If so, then it is plausible that there will be mechanical adaptations and biological cross-talk between tissues especially at the tidemark between non-calcified and calcified cartilage. For instance, if there is demarcation loss at the tidemark junction, then there may be increased osteoclastic activity to permit the removal of “damaged” molecules within the non-calcified cartilage. If there is continued compromised joint health (excessive mechanical loading, synovial inflammation, etc.), then fragmentation of the tidemark and additional cartilage fissuring can continue. As the calcified front encroaches upon non-calcified cartilage, perivascular ossification and thickening of the subchondral plate can occur.⁵ Eventually, the bone may become sclerotic and stiff which can lead to secondary cartilage softening.⁶ Further, it has been demonstrated that subchondral bone exacerbates the synthesis of pro-inflammatory cytokines and MMPs in osteoarthritis.⁷

In previous studies, we identified a potential canine OA biomarker panel (IL-8, KC, MCP-1, MMP-2, MMP-3)⁸ as well as biomarkers (PGE₂, GAG, MCP-1) increased by impact severity to osteochondral explants.⁹ Expanding upon this work, we sought to evaluate the effect of post-injury loading designed to mimic walking (1MPa, 1Hz, for 30min, 3X/day)^{10,11} after a moderate impact injury on tissue health and biomarker production. Our hypothesis was that post-injury loading following impact to osteochondral explants would result in lower cell viability and higher biomarker (IL-8, KC, MCP-1, MMP-2, MMP-3, PGE₂, GAG) release.

Methods

Tissues were harvested from one canine euthanized for reasons unrelated to this study. All procedures were approved by the institutional animal care and use committee. Normal osteochondral explants (n=11) were harvested under sterile conditions from the humeral heads using a 6mm diameter cannulated coring reamer (Arthrex, Naples, Florida, Fig. 6-1A) and were trimmed to approximately 3.6mm total thickness using a diamond blade saw (IsoMet Low Speed Saw, Buehler, Lake Bluff, Illinois, Fig. 6-1B). Explants were cultured in 6ml Dulbecco's modified Eagle's medium (DMEM) high glucose supplemented with 1X insulin-transferrin-selenium (ITS), penicillin, streptomycin, amphotericin B, L-glutamine, sodium pyruvate, L-ascorbic acid, and non-essential amino acids and incubated at 37°C, 95% humidity, and 6% CO₂ for two days prior to treatment.

Explants were placed in a stainless steel well (6.0mm diameter by 2.54mm deep) while a 3.9mm diameter flat punch attached to the ram of a servohydraulic test machine (model 8821S, Canton, Massachusetts) was lowered at 0.01mm/sec and stopped at 10N compression (Fig. 6-1C). Explant thickness was calculated as the difference in ram position with and without explants in well at day 0.

Explants were randomly assigned into four groups: 1) *No Impact – No Load*, 2) *No Impact – Load*, 3) *Impact – No Load*, 4) *Impact – Load*. Each explant in the impact groups was subjected to an impact velocity of 100mm/sec to 0.75mm compression (mean 20.8±1.49% strain) of the osteochondral explants to produce a moderate injury. Impact force was measured using a 880N load cell (model 3173, Lebow, Troy, Michigan) attached to the test machine table. Approximately four hours later, each explant was transferred individually to sterile, 6-well, culture plates (BioPress, Flexcell International

Corporation, Hillsborough, North Carolina) and a known volume (3-4ml) of supplemented DMEM was added to immerse each explant.

Plates containing explants in the load groups were connected to a computer-controlled, pneumatic bioreactor system (model FX-4000C, Flexcell International Corporation, Hillsborough, North Carolina, Fig. 6-1D) that applied dynamic, compressive loading using a haversine waveform (max pressure = 1MPa, frequency = 1Hz, duration = 30 min, thrice a day) to mimic walking for the 7-day culture period within the incubator. Culture media was collected 1 hour post-injury at day 0, 1, 3, 6 and stored at -20°C for further analysis.

Explants were assessed for cell activity using a resazurin sodium salt (199303, Sigma-Aldrich, St. Louis, Missouri) assay¹² to detect fluorescence of resorufin before (day -1) and after (day 1) treatment. On Day 7, explants viability was determined using fluorescent calcein AM (CellTracker Green CMFDA) and sytox blue that stains live and dead cells, respectively (Invitrogen, Carlsbad, California) and images of live and dead cells were collected via fluorescent microscopy (model BX51, Olympus, Center Valley, Pennsylvania, Fig. 6-2A). Live and dead cells were counted using a computer algorithm and percent cell viability ($\frac{\text{\#live cells}}{\text{\#total cells}} \times 100$) was quantified (Fig. 6-2B). Number of viable cells/tissue area was measured ($\frac{\text{area live cells}}{\text{total cartilage area}} \times 100$).

Culture media from each explant was assessed for PGE₂ concentration (pg/ml) using an EIA assay (Cayman Chemical, Ann Arbor, Michigan) analyzed by a multi-detection microplate reader (Synergy HT, Bio-Tek, Winooski, Vermont). PGE₂ released from each explant to the culture media was adjusted to media volume (ml) and normalized by initial

explant volume, V (mm^3) where $V = A \cdot h$, cross-sectional area, πr^2 , of explant multiplied by initial height. PGE_2 release per hour from each explant was reported in units of pg/mm^3 . GAG concentration of the culture media was assessed using the 1,9-dimethylmethylene blue (DMMB) assay¹³ and reported in release per hour from each explant in units of ng/mm^3 . Multiplex analysis was used to measure media cytokine/chemokine (IL-6, -8, KC, MCP-1, Millipore, Billerica, Massachusetts) and matrix metalloproteinase (MMP-2, -3, -8, -13, R&D Systems, Minneapolis, Minnesota) concentration using xMAP software (LUMINEX, Billerica, Massachusetts) in conjunction with a multiple, bead-based interaction assay analyzer (LiquiChip 200, Qiagen, Valencia, CA) and release per day from each explant was reported in units of pg/mm^3 .

Treatment comparisons for cartilage were analyzed by one-way analysis of variance with Holm-Sidak post-hoc group comparisons with significance set at $p < 0.05$ using SigmaPlot (San Rafael, California).

Results

All explants had reduced cell viability around the periphery due to harvesting associated trauma. Impact injury resulted in a peak force of $736.93 \pm 252.89\text{N}$. At day 7, the total percent cell viability was significantly higher for *No Impact – Load* versus *No Impact – No Load* ($p=0.04$, Fig. 6-2B). While the number of viable cells/tissue area was higher for the *No Impact* groups compared to the *Impact* groups, the difference was not statistically significant.

Within an hour after injury, PGE_2 release was significantly higher for *Impact* groups versus *No Impact* groups ($p=0.009$, Fig. 6-3A). At day 1, the concentration of GAG

released to the media was significantly higher in the *Impact – No Load* and *Impact – Load* group compared to the *No Impact – No Load* ($p=0.026$; $p=0.015$) and *No Impact – Load* ($p=0.046$, $p=0.031$) groups; At day 3, the concentration of GAG released to the media was significantly higher for *Impact – No Load* group compared to *No Impact – No Load* and *No Impact – Load* groups ($p=0.041$, 0.045). At day 6, the concentration of GAG released to the media was significantly higher for *Impact – No Load* group compared to all other groups ($p \leq 0.008$).

At day 1, the *Impact – Load* group released significantly more MMP-2 to the media compared to the *Impact – No Load* group and the *No Impact – Load* group ($p=0.015$, 0.034 , Table 6-1). At day 3, for the *Impact – Load* group released significantly more IL-8 to the media compared to the *No Impact – Load* and *No Impact – No Load* groups ($p=0.009$, 0.009). No other significant differences for other biomarkers were detected.

Discussion

We accepted the part of our hypothesis that post-injury loading following impact to osteochondral explants would result in lower cell viability and higher IL-8, MMP-2, PGE₂, and GAG release but we rejected that this would lead to higher KC, MCP-1, or MMP-3 based on our results. We demonstrated that physiological loading was associated with beneficial effects on chondrocyte viability in non-injured osteochondral explants. This phenomenon was similar to others who have reported the benefits of dynamic hydrostatic pressure on cartilage.¹⁴

Similar to our previous studies,^{9,15} impact injury to cartilage was associated with significant increases in PGE₂ as early as one hour post-injury. This effect dissipated in the present study such that there were no significant differences in PGE₂ at later time

points through day 6 for impact and/or loading groups. It has been previously shown that later in the disease sequelae of osteoarthritis, plasma PGE₂ was elevated in symptomatic knee OA patients.^{16,17} This suggests that an ideal PTOA model would involve impact injury with supraphysiological loading that would result in sustained PGE₂ release. In this study, we attempted to model an impact injury with physiological loading to mimic walking which may explain why there was not extended PGE₂ release for *Impact-Load*. PGE₂ has been previously shown to be involved in bone remodeling.¹⁸ Thus, following cartilage-bone injury it appears that there may be a minimum threshold of PGE₂ that is needed for acute joint repair as well as a maximum threshold that exists for chronic joint osteoarthritis. Therefore, measuring the concentration of PGE₂ immediately after traumatic joint injury and checking if this level increases at later time points may be a relevant measure to assess for PTOA risk in clinical patients.

In the present study, we observed elevated GAG release after impact injury which others have previously reported.¹⁹⁻²¹ Release of GAG may be due to mechanical rupture of collagen II fibrils within the cartilage tissue extracellular matrix during impact injury since it has been previously shown that inhibitors of biosynthesis or MMP activity are unable to mitigate this phenomenon.²¹ Previously, we observed that GAG release was dependent upon impact severity of osteochondral explants.⁹ In the present study, GAG release of *Impact-No Load* was significantly greater than all other groups (including *Impact-Load*) at day 6. This finding implies that post-injury loading may mitigate GAG release suggesting an anabolic role for joint loading after cartilage-bone impact.

There was a significant increase of MMP-2 at day 1 for the *Impact – Loading* group compared to the *Impact – No Load* and *No Impact – Load* groups and approached

significance for the *No Impact – No Load* group ($p=0.051$). Similarly, Mansell et al. reported increased concentration of both pro- and active-forms of MMP-2 in OA subchondral bone suggesting altered collagen turnover.²² Further, Tang et al. measured increased MMP-2 within the synovial fluid as well as within cartilage and subchondral bone following ACL injury.²³ In contrast, serum MMP-2 levels were lower in individuals who developed OA²⁴ as well as pre-surgery OA canine patients recently reported by our laboratory.²⁵ These contradictory results of MMP-2 levels may be due to the activity of other MMPs. It is well-established that MMP-2 (gelatinase A) is a 72-kDa, Type IV collagenase that is involved in proteolysis of basement membranes by degradation of type IV, V, and denatured collagens.²⁶ Yet, unlike the regulation of other MMPs, MMP-2 does not have an AP-1 site or TATA box in the 5' promoter region but does have a potential AP-2 binding site.²⁷ Tissue inhibitor of metalloproteinase (TIMP-2) has been shown to inactivate MMP-2,²⁸ whereas membrane-type 1 matrix metalloproteinase (MMP-14) has been shown to activate MMP-2.²⁹ For future work, a high ratio of local MMP-2 to TIMP-2 concentration may implicate pathological remodeling despite low levels of serum MMP-2. Alternatively, the ratio of local MMP-2 to MMP-14 may corroborate trends between local and systemic MMP-2 levels.

IL-8 is a chemokine (cysteine-X-cysteine motif), inflammatory mediator that has been shown to be elevated after ACL injury,³⁰⁻³² early OA²⁵ and late OA.³³ It functions as a neutrophil chemoattractant as well as angiogenic factor to regulate cell migration to sites of inflammation.²⁶ Further, IL-8 increases motility but decreases resorptive rate of osteoclasts.³⁴ IL-8 induces chondrocyte hypertrophic differentiation which may ultimately lead to cartilage dysfunction and pathologic calcification in OA.³⁵ Chauffier et

al. reported increased IL-8 in response to compressive loading of cartilage explants.³⁶ Attur et al. reported increased IL-8 in response to $\alpha 5\beta 1$ integrin receptor activation thus confirming its role in chondrocyte mechanotransduction signaling pathway.³⁷ Similar to this loading response, we measured elevated IL-8 at day 3 for the *Impact –Load* group as compared to either *No Impact* groups in the present study. A plausible mechanism for higher IL-8 in the present study may involve chondrocyte $\alpha 5\beta 1$ activation and/or perhaps another mechano-receptor such as osteocyte $\alpha V\beta 3$ activation that occurred in the subchondral bone. This phenomenon may explain why IL-8 was significantly higher in the *Impact-Load* group compared to the *No Impact* groups but not for the *Impact-No Load* group. Thus, the additional loading following impact may activate additional mechano-coupling, biochemical coupling, signal transmission, and/or effector cell response.³⁸

Despite the small sample size of this pilot study, we suspect that the elevated biomarkers (PGE₂, GAG, MMP-2, IL-8) in this impact-loading model provides evidence that the tidemark junction was damaged and that these aforementioned biomarkers are involved in the remodeling process. It is unknown what the specific effects of NSAIDs administered immediately after this type of injury may have with respect to mitigating biomarker release, delaying the reparative response, and/or accelerating the onset of PTOA. Therefore, future studies are required to assess the effects of pathological, controlled loading regimens (i.e. increased pressure, frequency, duration) after osteochondral injury comparable to conditions that may occur during a sporting event, dance performance, or other strenuous physical activity.

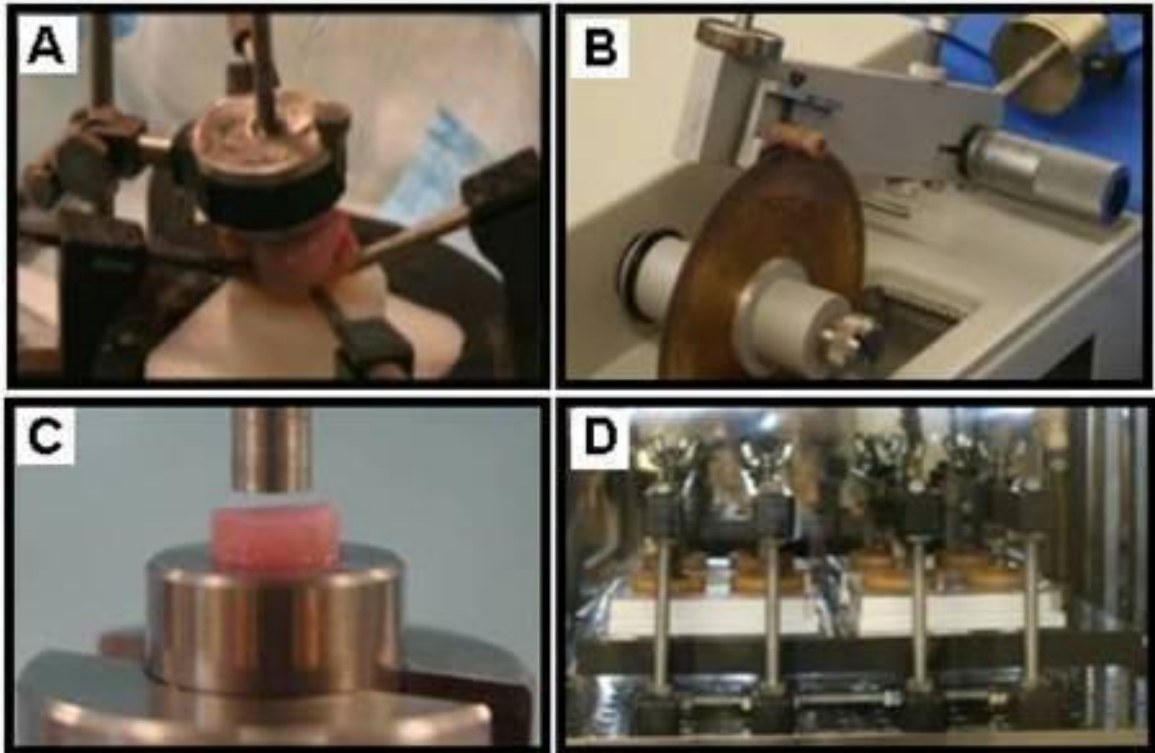


Figure 6-1. Harvest of osteochondral explants using a 6mm-diameter coring reamer and jig to stabilize humeral head (A). Trimming of bone using a diamond blade saw to ~3.6mm total thickness of explant (B). Delivery of impact ($v = 100\text{mm/sec}$) injury using a 3.9mm-diameter impactor attached to ram of test machine (C). Dynamic compressive loading ($P=1\text{MPa}$, $f=1\text{Hz}$, $d=30\text{min}$, 3x/day for 7 days) of explants in four, 6-well plates using a bioreactor device (D).

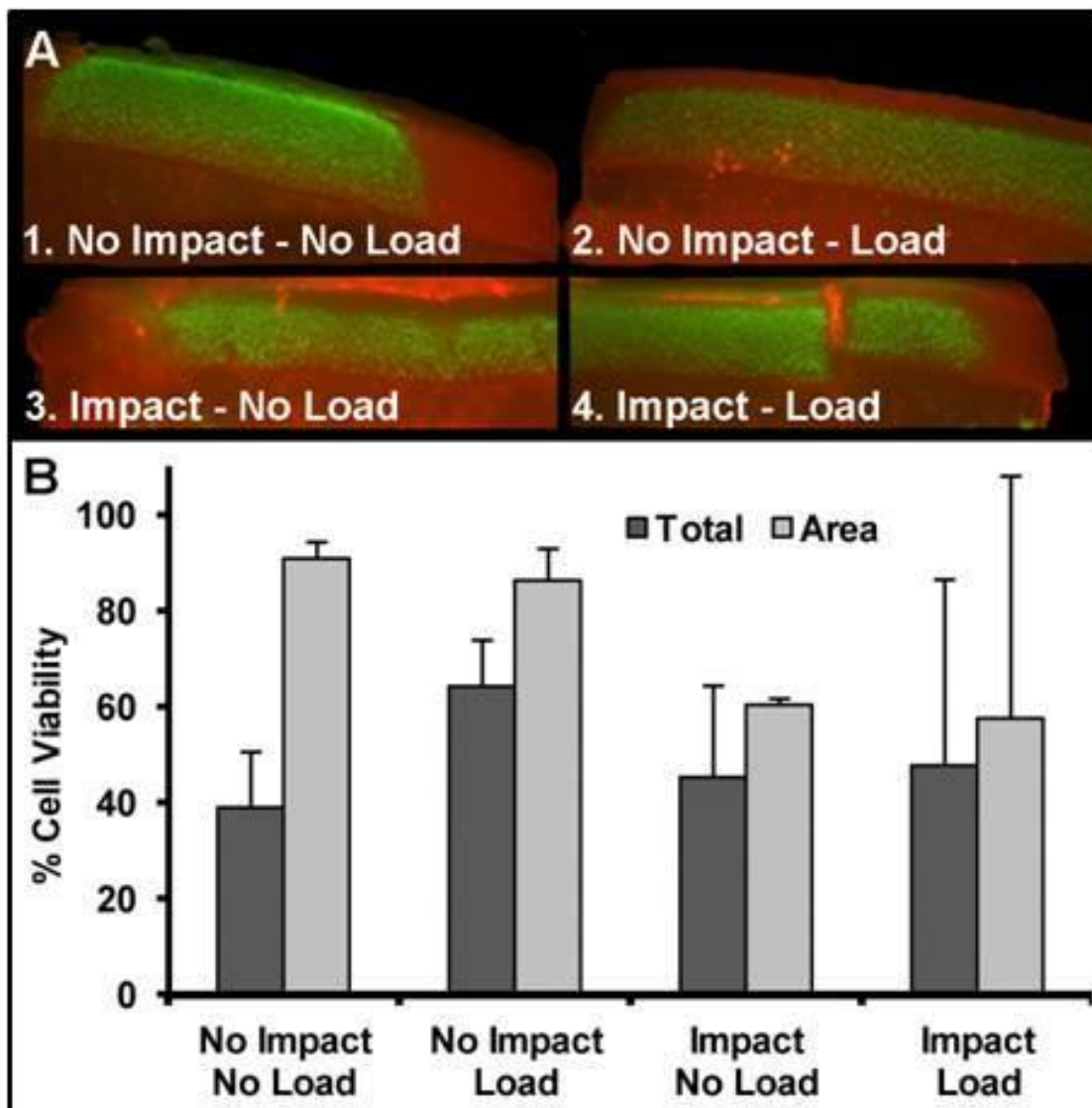


Figure 6-2. Representative images of fluorescent live (green) and dead (red) cells from test groups after 7 days of culture (A). Total percent cell viability (live/total cells x 100) and area percent cell viability (live area/total area x 100) of chondrocytes within explants after 7 days of culture (B).

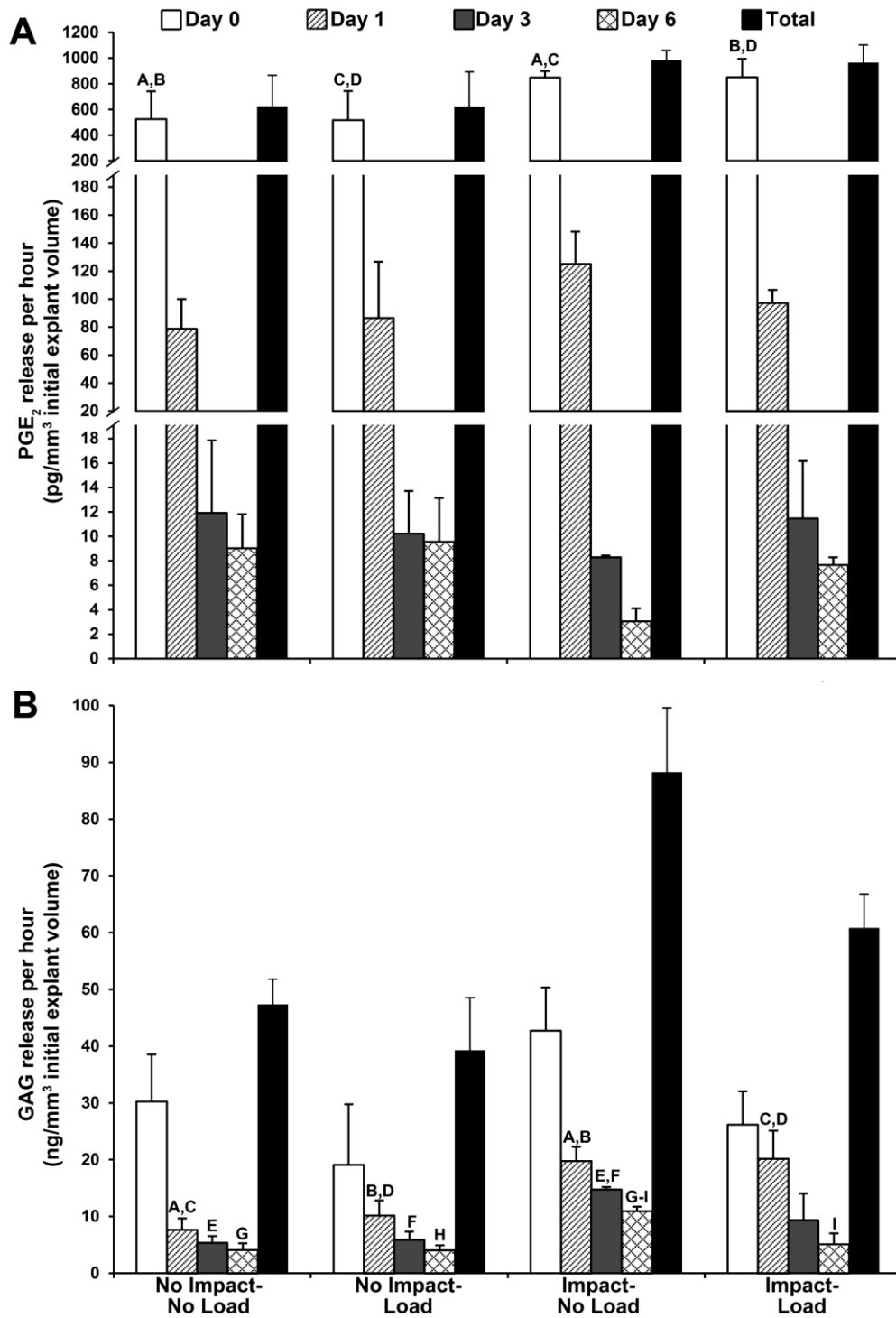


Figure 6-3. Prostaglandin E₂, PGE₂, (A) and Glycosaminoglycan, GAG, (B) release from osteochondral explants into culture media. Groups within each time point sharing a letter are significantly different ($p < 0.05$).

Table 6-1. Biomarkers released by osteochondral explants into the media.

Media Biomarker Per Day	Day 1				Day 3			
	No Impact No Load	No Impact Load	Impact No Load	Impact Load	No Impact No Load	No Impact Load	Impact No Load	Impact Load
IL-6 (pg/mm ³)	2.145 ± 2.089	2.234 ± 1.052	4.404 ± 0.294	6.000 ± 3.139	0.799 ± 0.787	0.266 ± 0.461	1.855 ± 0.406	2.623 ± 2.632
IL-8 (pg/mm ³)	13.323 ± 9.570	23.228 ± 12.362	24.807 ± 11.856	99.062 ± 105.103	17.046 ^A ± 11.817	17.256 ^B ± 4.242	61.035 ± 4.672	76.688 ^{A,B} ± 25.975
KC (pg/mm ³)	10.063 ± 6.965	17.062 ± 12.469	27.176 ± 8.941	50.880 ± 48.022	8.557 ± 7.110	4.078 ± 1.452	19.462 ± 9.916	49.331 ± 35.730
MCP-1 (pg/mm ³)	8.974 ± 11.372	4.012 ± 1.828	6.206 ± 2.017	12.566 ± 16.470	11.319 ± 13.700	2.457 ± 1.390	13.664 ± 12.752	14.757 ± 21.529
MMP-2 (pg/mm ³)	6.162 ± 6.260	4.899 ^A ± 5.003	0.265 ^B ± 0.374	19.199 ^{A,B} ± 4.211	9.390 ± 2.408	4.817 ± 4.453	7.510 ± 3.178	10.249 ± 1.409
MMP-3 (pg/mm ³)	9.016 ± 15.617	25.224 ± 15.240	29.517 ± 11.268	37.212 ± 21.458	10.458 ± 4.139	14.123 ± 12.369	14.125 ± 6.386	20.783 ± 8.690
MMP-8 (pg/mm ³)	0.844 ± 1.462	346.981 ± 479.590	231.051 ± 230.282	492.456 ± 736.240	126.090 ± 204.956	219.209 ± 241.137	214.653 ± 251.303	234.405 ± 281.825
MMP-13 (pg/mm ³)	2.983 ± 5.167	8.599 ± 7.597	4.984 ± 2.113	12.972 ± 13.620	7.014 ± 3.670	7.001 ± 6.066	9.883 ± 1.548	10.316 ± 4.795
Media Biomarker Per Day	Day 6				Day 1-6			
	No Impact No Load	No Impact Load	Impact No Load	Impact Load	No Impact No Load	No Impact Load	Impact No Load	Impact Load
IL-6 (pg/mm ³)	0.095 ± 0.165	0 ± 0	0 ± 0	0 ± 0	4.029 ± 4.019	2.767 ± 1.926	8.114 ± 0.519	11.246 ± 7.230
IL-8 (pg/mm ³)	7.728 ± 5.081	4.742 ± 0.564	5.975 ± 1.809	5.459 ± 2.395	70.600 ± 48.127	71.967 ± 20.072	164.802 ± 2.914	268.816 ± 142.512
KC (pg/mm ³)	4.249 ± 3.859	0.998 ± 0.413	2.945 ± 1.587	2.811 ± 0.795	39.923 ± 32.660	28.211 ± 16.559	74.936 ± 15.651	157.976 ± 120.346
MCP-1 (pg/mm ³)	7.401 ± 7.616	1.420 ± 1.052	4.335 ± 5.433	3.562 ± 5.945	53.814 ± 61.383	13.187 ± 7.641	46.540 ± 43.820	52.766 ± 77.211
MMP-2 (pg/mm ³)	1.294 ± 1.121	14.156 ± 20.356	0 ± 0	2.541 ± 4.401	28.823 ± 13.043	57.001 ± 63.395	15.284 ± 5.982	47.319 ± 15.755
MMP-3 (pg/mm ³)	2.860 ± 2.667	6.591 ± 11.416	0 ± 0	9.096 ± 10.275	38.512 ± 26.239	73.242 ± 20.067	57.767 ± 24.041	106.065 ± 55.142
MMP-8 (pg/mm ³)	20.621 ± 31.732	65.866 ± 114.083	0 ± 0	74.071 ± 128.295	314.886 ± 504.315	982.996 ± 490.647	660.357 ± 732.888	1183.481 ± 1676.800
MMP-13 (pg/mm ³)	5.526 ± 2.885	9.008 ± 15.603	0 ± 0	4.853 ± 6.151	33.589 ± 16.022	49.627 ± 40.170	24.751 ± 0.982	48.162 ± 39.734

Values sharing a letter are significantly different (p<0.05)

References

1. Brown TD, Johnston RC, Saltzman CL, et al. Posttraumatic osteoarthritis: a first estimate of incidence, prevalence, and burden of disease. *J Orthop Trauma*. 2006;20:739-744.
2. Lawrence RC, Helmick CG, Arnett FC, et al. Estimates of the prevalence of arthritis and selected musculoskeletal disorders in the United States. *Arthritis Rheum*. 1998;41:778-799.
3. Kraus VB. Waiting for action on the osteoarthritis front. *Curr Drug Targets*. 2010;11:518-520.
4. Potter HG, Jain SK, Ma Y, et al. Cartilage injury after acute, isolated anterior cruciate ligament tear: immediate and longitudinal effect with clinical/MRI follow-up. *Am J Sports Med*. 2012;40:276-285.
5. Suri S, Walsh DA. Osteochondral alterations in osteoarthritis. *Bone*. 2012;51:204-211.
6. Haut RC, Ide TM, De Camp CE. Mechanical responses of the rabbit patellofemoral joint to blunt impact. *J Biomech Eng*. 1995;117:402-408.
7. Hulejova H, Baresova V, Klezl Z, et al. Increased level of cytokines and matrix metalloproteinases in osteoarthritic subchondral bone. *Cytokine*. 2007;38:151-156.
8. Garner BC, Stoker AM, Kuroki K, et al. Using animal models in osteoarthritis biomarker research. *J Knee Surg*. 2011;24:251-264.
9. Waters NP, Stoker AM, Pfeiffer FM, et al. Biological effects of impact maximum compression on osteochondral explants. *58th Annual Meeting of the Orthopaedic Research Society*. Paper 829. San Francisco, CA, 2012.
10. Seedhom BB, Takeda T, Tsubuku M, et al. Mechanical factors and patellofemoral osteoarthrosis. *Ann Rheum Dis*. 1979;38:307-316.
11. Waters RL, Lunsford BR, Perry J, et al. Energy-speed relationship of walking: standard tables. *J Orthop Res*. 1988;6:215-222.
12. Perrot S, Dutertre-Catella H, Martin C, et al. Resazurin metabolism assay is a new sensitive alternative test in isolated pig cornea. *Toxicol Sci*. 2003;72:122-129.
13. Farndale RW, Buttle DJ, Barrett AJ. Improved quantitation and discrimination of sulphated glycosaminoglycans by use of dimethylmethylene blue. *Biochim Biophys Acta*. 1986;883:173-177.

14. Parkkinen JJ, Ikonen J, Lammi MJ, et al. Effects of cyclic hydrostatic pressure on proteoglycan synthesis in cultured chondrocytes and articular cartilage explants. *Arch Biochem Biophys*. 1993;300:458-465.
15. Waters NP, Stoker AM, Pfeiffer FM, et al. Effects of impact velocity and maximum strain on articular cartilage material properties, extracellular matrix, and tissue inflammation. *56th Annual Meeting of the Orthopaedic Research Society*. Paper 942. New Orleans, LA, 2010.
16. Attur M, Statnikov A, Aliferis CF, et al. Inflammatory genomic and plasma biomarkers predict progression of symptomatic knee osteoarthritis (SKOA). *Osteoarthritis Cartilage*. 2012;20:S34-S35.
17. Nemirovskiy O, Buck R, Sunyer T, et al. Predicting radiographic joint space narrowing (JSN) using biomarkers for osteoarthritis (OA) clinical trials. *Osteoarthritis and Cartilage*. 2008;16:S56-S57.
18. Xie C, Ming X, Wang Q, et al. COX-2 from the injury milieu is critical for the initiation of periosteal progenitor cell mediated bone healing. *Bone*. 2008;43:1075-1083.
19. Loening AM, James IE, Levenston ME, et al. Injurious mechanical compression of bovine articular cartilage induces chondrocyte apoptosis. *Arch Biochem Biophys*. 2000;381:205-212.
20. Torzilli PA, Deng XH, Ramcharan M. Effect of compressive strain on cell viability in statically loaded articular cartilage. *Biomech Model Mechanobiol*. 2006;5:123-132.
21. DiMicco MA, Patwari P, Siparsky PN, et al. Mechanisms and kinetics of glycosaminoglycan release following in vitro cartilage injury. *Arthritis Rheum*. 2004;50:840-848.
22. Mansell JP, Tarlton JF, Bailey AJ. Biochemical evidence for altered subchondral bone collagen metabolism in osteoarthritis of the hip. *Br J Rheumatol*. 1997;36:16-19.
23. Tang Z, Yang L, Wang Y, et al. Contributions of different intraarticular tissues to the acute phase elevation of synovial fluid MMP-2 following rat ACL rupture. *J Orthop Res*. 2009;27:243-248.
24. Ling SM, Patel DD, Garnero P, et al. Serum protein signatures detect early radiographic osteoarthritis. *Osteoarthritis Cartilage*. 2009;17:43-48.
25. Garner BC, Stoker AM, Kuroki K, et al. Using animal models in osteoarthritis biomarker research. *The journal of knee surgery*. 2011;24:251-264.

26. Bilezikian JP, Raisz LG, Martin TJ. *Principles of bone biology*. 3rd ed. San Diego, Calif.: Academic Press/Elsevier; 2008.
27. Huhtala P, Chow LT, Tryggvason K. Structure of the human type IV collagenase gene. *J Biol Chem*. 1990;265:11077-11082.
28. Stetler-Stevenson WG, Kruttsch HC, Liotta LA. Tissue inhibitor of metalloproteinase (TIMP-2). A new member of the metalloproteinase inhibitor family. *J Biol Chem*. 1989;264:17374-17378.
29. Sato H, Takino T, Okada Y, et al. A matrix metalloproteinase expressed on the surface of invasive tumour cells. *Nature*. 1994;370:61-65.
30. Bigoni M, Sacerdote P, Turati M, et al. Acute and late changes in intraarticular cytokine levels following anterior cruciate ligament injury. *J Orthop Res*. 2013;31:315-321.
31. Sward P, Frobell R, Englund M, et al. Cartilage and bone markers and inflammatory cytokines are increased in synovial fluid in the acute phase of knee injury (hemarthrosis)--a cross-sectional analysis. *Osteoarthritis Cartilage*. 2012;20:1302-1308.
32. El-Hadi M, Charavaryamath C, Aebischer A, et al. Expression of interleukin-8 and intercellular cell adhesion molecule-1 in the synovial membrane and cranial cruciate ligament of dogs after rupture of the ligament. *Can J Vet Res*. 2012;76:8-15.
33. Remick DG, DeForge LE, Sullivan JF, et al. Profile of cytokines in synovial fluid specimens from patients with arthritis. Interleukin 8 (IL-8) and IL-6 correlate with inflammatory arthritides. *Immunol Invest*. 1992;21:321-327.
34. Fuller K, Owens JM, Chambers TJ. Macrophage inflammatory protein-1 alpha and IL-8 stimulate the motility but suppress the resorption of isolated rat osteoclasts. *J Immunol*. 1995;154:6065-6072.
35. Merz D, Liu R, Johnson K, et al. IL-8/CXCL8 and growth-related oncogene alpha/CXCL1 induce chondrocyte hypertrophic differentiation. *J Immunol*. 2003;171:4406-4415.
36. Chauffier K, Laiguillon MC, Bougault C, et al. Induction of the chemokine il-8/kc by the articular cartilage: possible influence on osteoarthritis. *Joint Bone Spine*. 2012;79:604-609.
37. Attur MG, Dave MN, Clancy RM, et al. Functional genomic analysis in arthritis-affected cartilage: yin-yang regulation of inflammatory mediators by alpha 5 beta 1 and alpha V beta 3 integrins. *J Immunol*. 2000;164:2684-2691.

38. Duncan RL, Turner CH. Mechanotransduction and the functional response of bone to mechanical strain. *Calcif Tissue Int.* 1995;57:344-358.

CHAPTER 7

BIOMARKERS AFFECTED BY HUMERAL HEAD IMPACT INJURY

Introduction

Impact injury to articular cartilage has been shown to elevate the risk of developing post-traumatic osteoarthritis (PTOA). However, the exact sequelae involved in the pathogenesis of PTOA remains unknown but are assumed to be dependent upon both biochemical and biomechanical changes. These pathologic changes are more than likely due to intrinsic, reparative capabilities of the individual as well as environmental factors such as post-injury physiological/excessive loading. Our objective was to isolate immediate changes due to impact injury by analyzing chondrocyte viability, extracellular matrix, and tissue inflammatory markers after delivering an *in situ* impact injury to the humeral heads of adult canines.

Methods

All procedures were approved by the internal animal care and use committee. Animals were euthanatized for reasons unrelated to this study.

Humeral heads of the left shoulders (n=4) of normal adult canines (m=21.45±5.00kg) were impacted using a custom fabricated, spring-driven impactor (Fig. 7-1 - stainless steel impactor tip, d = 8mm). The right humeral heads served as controls. An additional set of normal adult canines (n=3) with impacted (left) and non-impacted (right) shoulders were used for day 0 cartilage analyses.

Immediately after, humeral heads were surgically removed post-impact and were cultured in 60ml supplemented Dulbecco's modified Eagle's medium (DMEM) high

glucose (Gibco, Invitrogen, Carlsbad, CA) and incubated at 37°C, 95% humidity, and 6% CO₂ for 12 days. At days 1, 2, 3 post-impact, 2ml of media was removed and stored at -20°C for further analysis. After 6 days post-impact, all media was replaced and 2ml of media removed at days 9 and 12 post-impact and stored at -20°C for further analysis.

Live/dead staining of chondrocytes was assessed using fluorescent microscopy to attain surface and depth views as previously described in Ch. 4-6. India ink staining of each humeral head was used to analyze gross surface changes.

After twelve days of culture, cartilage was assessed for total glycosaminoglycan (GAG) content using the 1,9-dimethylmethylene blue dye-binding (DMMB) assay, total collagen content by measuring hydroxyproline (HP) content, and double-stranded DNA content as previously described in Ch. 4-6.

GAG content of the media was assessed using the DMMB assay. Nitric oxide (NO) concentration was determined using the Griess assay (Promega). Prostaglandin E₂ (PGE₂) concentration was determined using an EIA assay (Cayman Chemical). Data were analyzed by one-way ANOVA with Tukey post-hoc group comparisons with significance set at p<0.05 (Sigma Stat, San Rafael, CA).

Results

The area of the focal defect was significantly larger for the impact group as compared to the control at Day 0 and 12 (Fig. 7-2). However, there appeared to be no difference for the impact group from Day 0 to Day 12.

There were no significant differences for any of the tissue biomarkers compared to controls (Fig. 7-3).

There were no significant differences for any of the media biomarkers compared to controls (Fig. 7-4).

Discussion

Although there was gross observation of focal defects of the articular surface due to impact injury, we did not observe any significant changes from the biomarkers analyzed in this study. Furthermore, the region of chondrocyte death due to impact injury of the humeral head remained relatively localized after 12 days of free-swelling culture. It is reasonable to assume that some type of physiological loading occurs after *in vivo*, traumatic joint injury, albeit this study was designed to analyze the aforementioned biomarkers due to isolated injury. The fabrication of a portable, impactor device has enabled us to deliver a clinically-relevant, mechanical injury to articular cartilage within a canine, shoulder joint. Experimentally, the use of this device during arthroscopic surgery will further develop our *in vivo* PTOA model for pre-clinical trials.

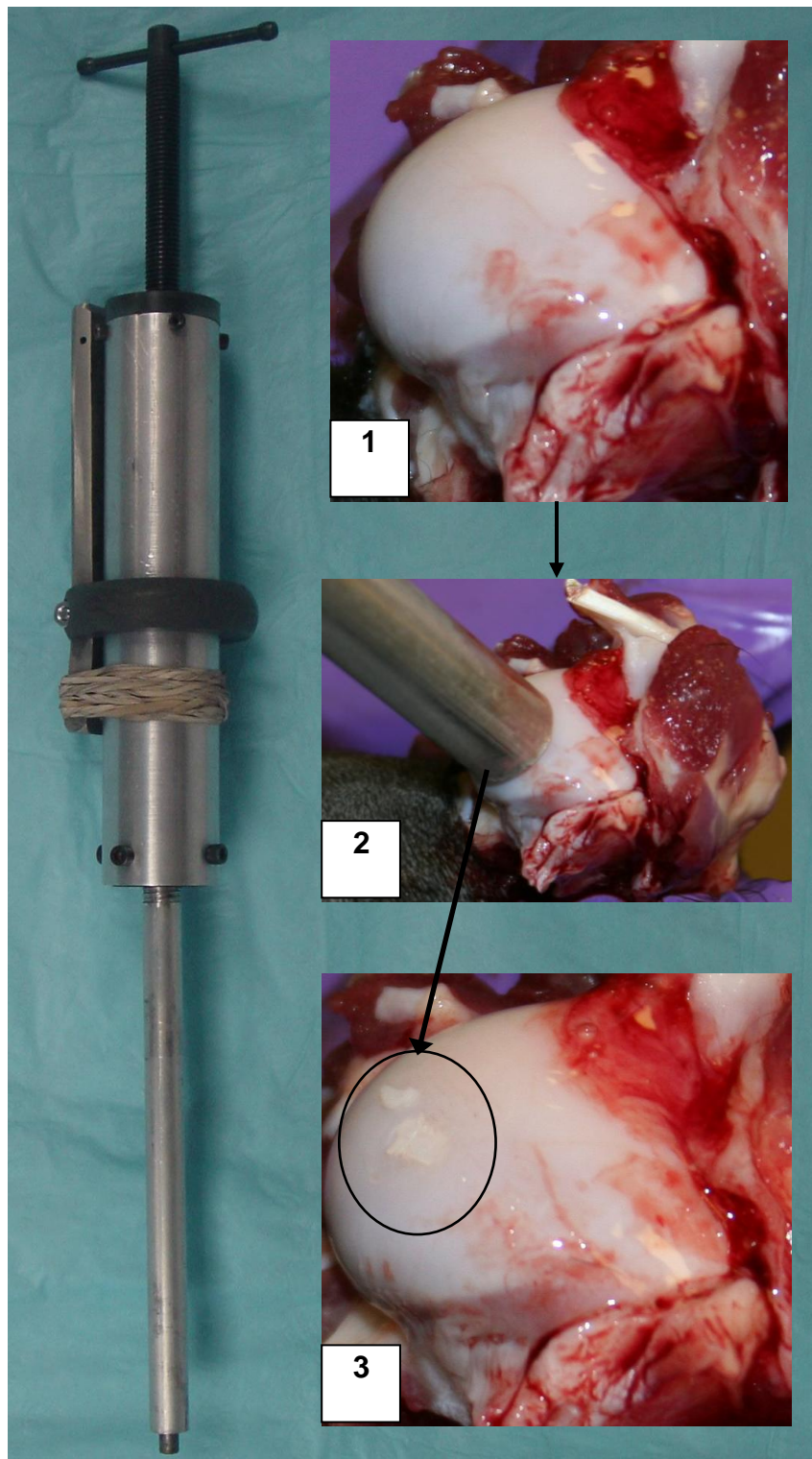


Figure 7-1. Custom-made impactor used to deliver impact injury on humeral head.

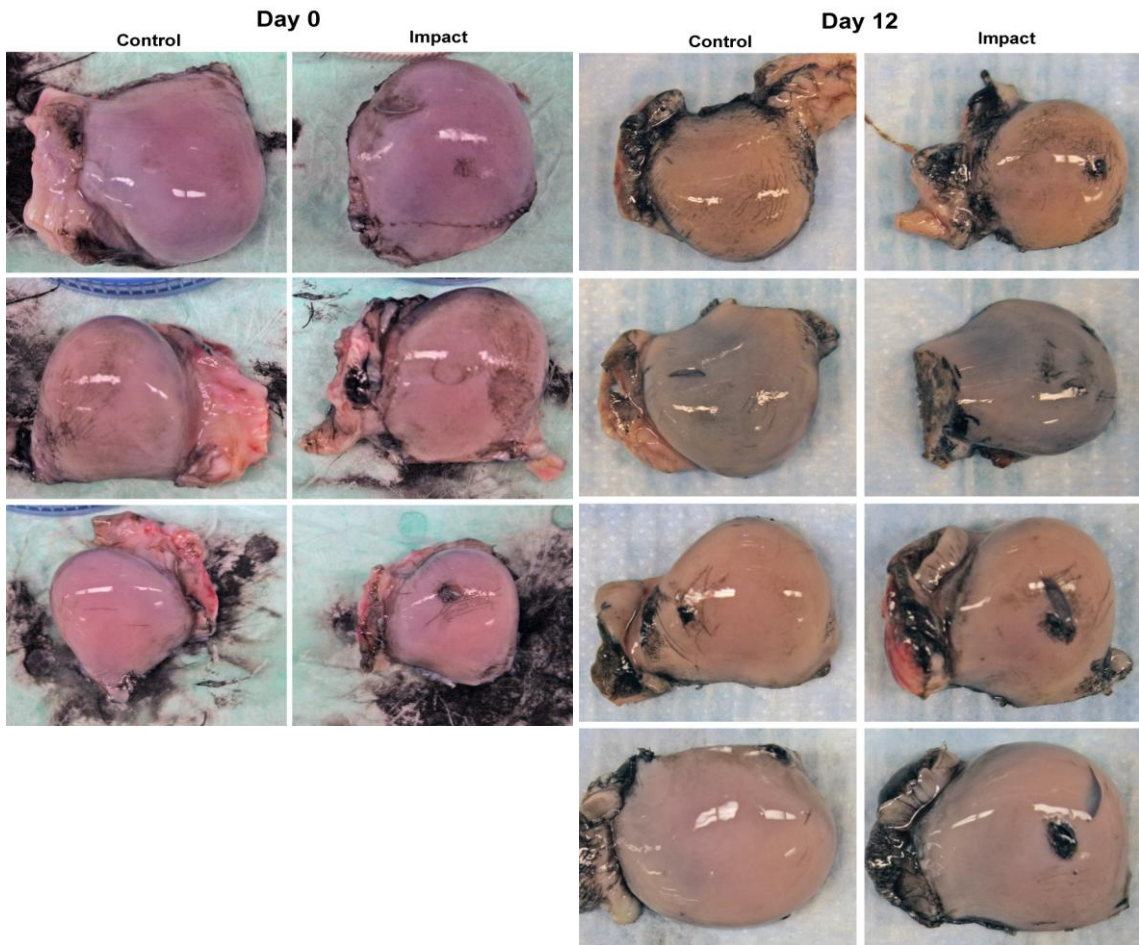


Figure 7-2. Gross observation using india ink staining of humeral heads at Day 0 and Day 12 post-injury.

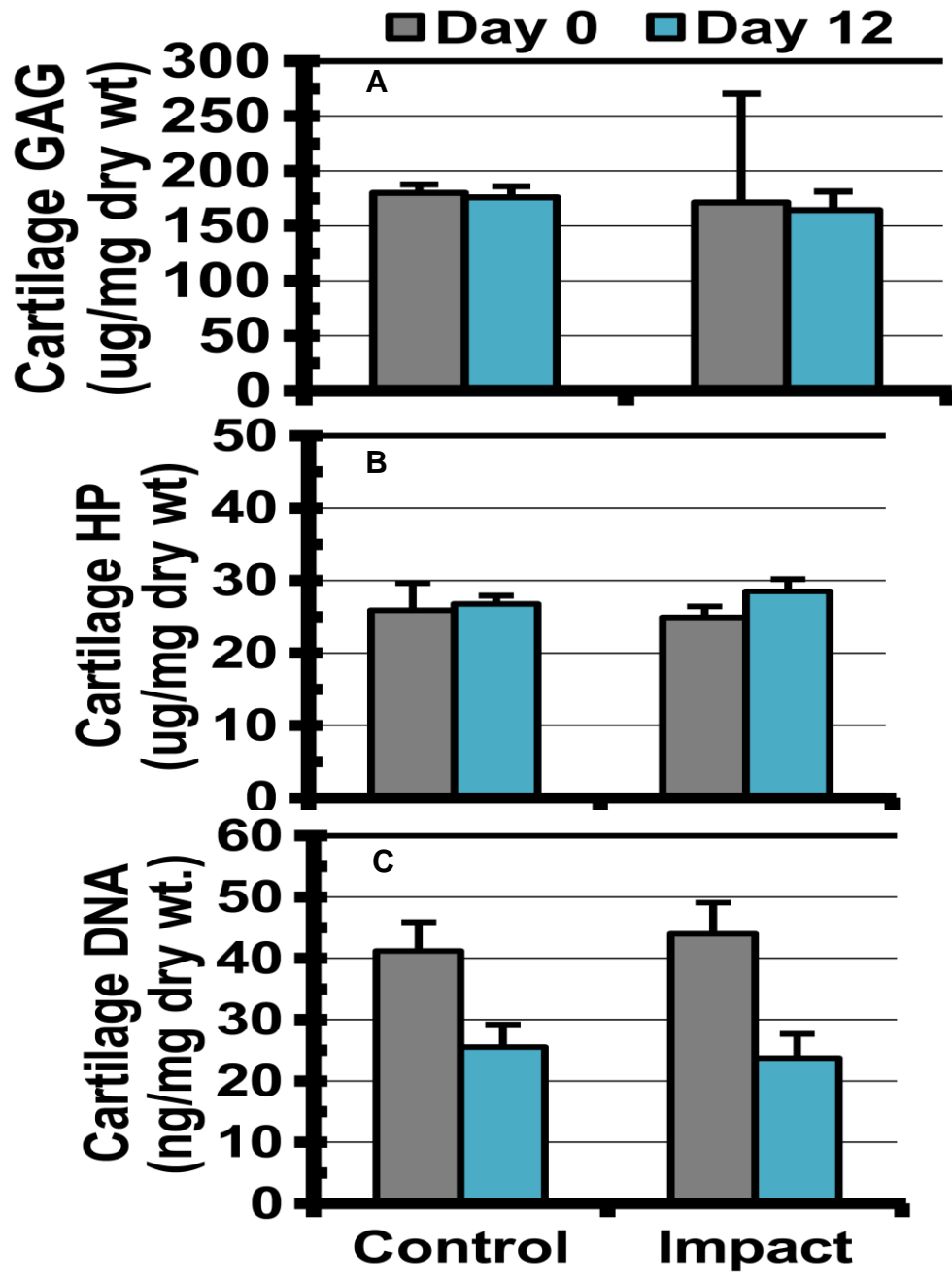


Figure 7-3. Cartilage analysis: A) Glycosaminoglycan (GAG), B) Hydroxyproline (HP), C) DNA content.

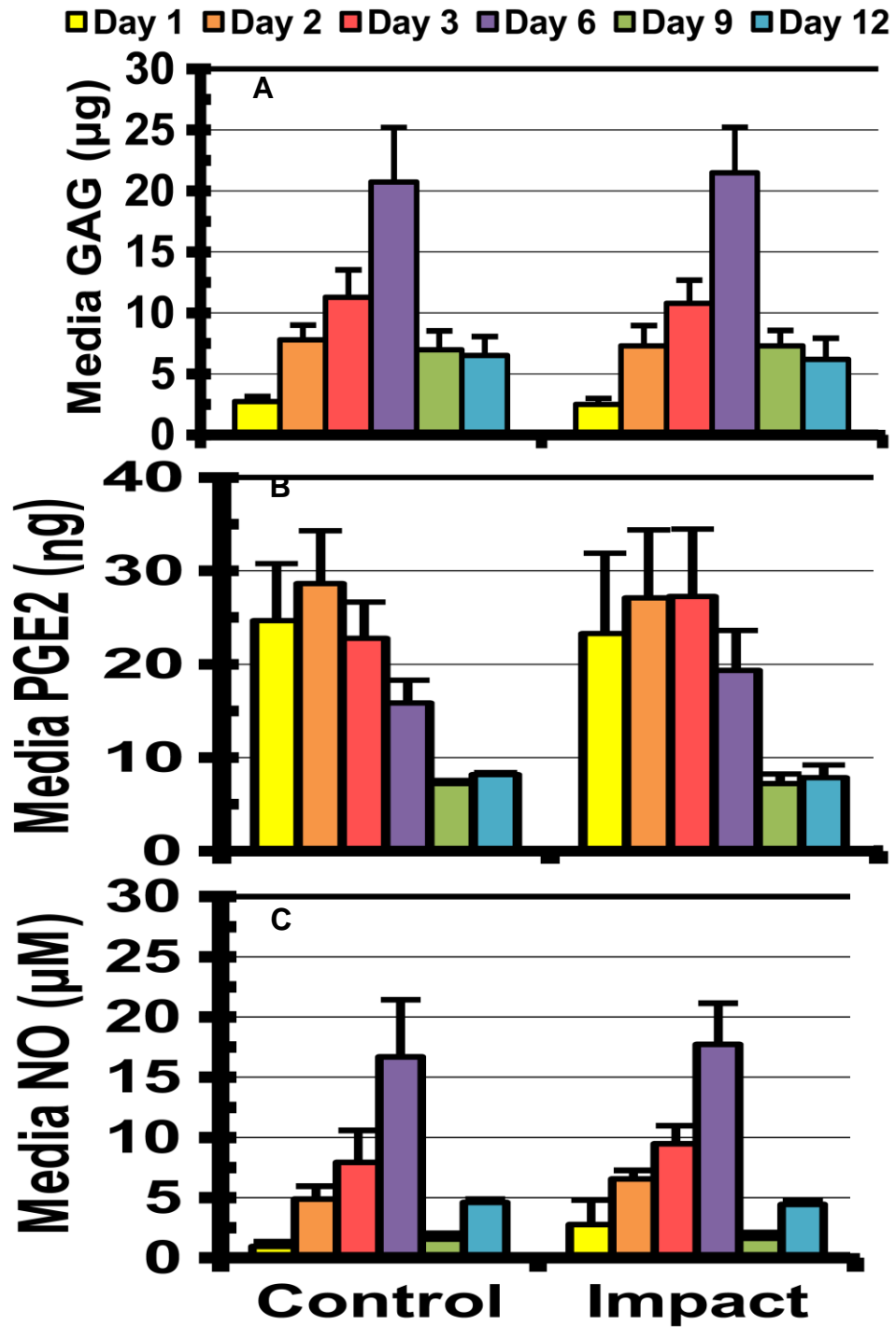


Figure 7-4. Media analysis: A) Glycosaminoglycan (GAG), B) Prostaglandin E2 (PGE2), C) Nitric oxide (NO) released into culture media from humeral head during 12 days of culture.

CHAPTER 8

DEVELOPMENT OF A DEVICE TO DELIVER IMPACT INJURY FOR PRE-CLINICAL MODELS OF OSTEOARTHRITIS

Introduction

Impact injury to articular cartilage has been shown to elevate the risk of developing post-traumatic osteoarthritis (PTOA). Yet, the mechanisms that distinguish PTOA from *in vivo* reparative responses remain unknown. Thus, pre-clinical animal models that involve acute, joint impact are warranted for further disease investigation. Therefore, our objective was to develop an arthroscopic device with controlled low or high impact to the articular cartilage of femoral condyles. Our hypothesis was that high impact energy would produce greater surface damage to articular cartilage.

Methods

Impactor Design

A custom-made, spring-driven impactor (Fig. 8-1) was fabricated to deliver an impact injury. Specific shop drawings of all components are included in Appendix C. Briefly, the device consisted of a stainless steel, 2-mm diameter, flat circular impactor tip (89325K11, McMaster-Carr, Atlanta, Georgia) enclosed within a stainless steel tube (8457K28, McMaster-Carr, Atlanta, Georgia). The spring (1986K151, McMaster Carr, Atlanta, Georgia) had the following manufacturer's characteristics: overall length = 101.6 mm (4 inches), outer diameter = 23.83 mm (0.938 inches), wire diameter = 3.76 mm (0.148 inches), compressed length = 60.20 mm (2.37 inches), max load = 680.58 N (153 lbf), rate = 1.678 kg/mm (93.75 lbs/in). Compression of the spring was controlled by

attaching it to a handle (89965K395, McMaster-Carr, Atlanta, Georgia) that contained a crank that was turned at various increments ranging from 1 to 20 turns. Therefore, force applied at the impactor tip was directly proportional to the turns of the crank mechanism.

Impactor Calibration

A pendulum device (Fig. 8-2) was fabricated to quantify the force applied by the impactor device. The apparatus consisted of support pieces (8982K21, McMaster-Carr, Atlanta, Georgia), pendulum rod (6750K163, McMaster-Carr, Atlanta, Georgia), stainless steel weight (89415K371, McMaster-Carr, Atlanta, Georgia), attached by a ½” shaft dia., 1-1/8” outer dia. double sealed and double shielded bearings (6384K49 and 6384K61, McMaster-Carr, Atlanta, Georgia).

The following physical measurements were made in order to calculate the moment of inertia, I_p , of the pendulum device: distance from center of pivot to rod, $d_{rod} = 0.0127$ m (0.5 inches), mass of rod, $m_{rod} = 0.1295$ kg, length of rod, $l_{rod} = 0.5842$ m (23 inches), mass of weight, $m_{weight} = 0.4428$ kg, base of cubic weight, $b = 0.0381$ m (1.5 inches).

The moment of inertia, I_p , was calculated using Eq. 8-1, 8-2, 8-3:

$$I_p = (I_{rod} + m_{rod}d_{rod}^2) + (I_{weight} + m_{weight}d_{weight}^2) \quad (8-1)$$

$$I_{rod} = 1/3ml^2 \quad (8-2)$$

$$I_{weight} = 1/12m(b^2 + h^2) \quad (8-3)$$

Using the appropriate physical measurements for Eq. 8-2 yields:

$$I_{rod} = 1/3(0.1295 \text{ kg})(0.5842 \text{ m})^2 = 0.01473 \text{ kg-m}^2$$

Using the appropriate physical measurements for Eq. 8-3 yields:

$$I_{weight} = 1/12(0.4428 \text{ kg})[(0.0381 \text{ m})^2 + (0.0381 \text{ m})^2] = 0.0001071 \text{ kg-m}^2$$

Thus, using the appropriate physical measurements and substituting the values of I_{rod} and I_{weight} into Eq. 8-1 yields:

$$I_p = [0.01473 \text{ kg}\cdot\text{m}^2 + (0.1295 \text{ kg})(0.0127 \text{ m} + 0.2921 \text{ m})^2] + [0.0001071 \text{ kg}\cdot\text{m}^2 + (0.4428 \text{ kg})(0.0127 \text{ m} + 0.5842 \text{ m} + 0.01905 \text{ m})^2]$$

$$I_p = (0.01473 \text{ kg}\cdot\text{m}^2 + 0.01203 \text{ kg}\cdot\text{m}^2) + (0.0001071 \text{ kg}\cdot\text{m}^2 + 0.1680 \text{ kg}\cdot\text{m}^2)$$

$$I_p = \mathbf{0.195 \text{ kg}\cdot\text{m}^2}$$

By solving for the pendulum moment of inertia, I_p , it was possible to calculate using Newtonian laws of motion for kinetic energy, KE, and the force, F, of the impactor using Eq. 8-4 and 8-5:

$$KE = 1/2 I_p \omega^2 \quad (8-4)$$

$$F = I_p \alpha / d \quad (8-5)$$

where ω , is the angular velocity, α , is the angular acceleration, and d, is the distance of the pendulum from the point of impact to the point of rotation.

An optical tracking system (Optotrak Certus, Northern Digital, Inc., Waterloo, Ontario, Canada) with light-emitting diodes, LEDs, placed on the pendulum device center of rotation (LED 1) and the weight (LED 2) was used to measure the static and dynamic position of the weight. Specifically, the static, initial weight position was used to create vector₁₋₂, whereas the dynamic weight position during impact was used to create vector₁₋₃. During impact, the angle (radians) between vector₁₋₂ and vector₁₋₃ was measured at a collection frequency of 300 Hz (every 0.003333 sec). The results were plotted to create a linear and angular position (radians) versus time (sec) graphs including the first 20 points. The derivative or slope, m, of the line ($y = mx + b$) of the linear and angular position-time graph yielded linear and angular velocity, respectively. Angular velocity (rad/sec)

versus time (sec) graph was used to calculate the angular acceleration in a similar manner. The force applied with ≤ 3 turns of the impactor, was not sufficient to displace the weight. Therefore, data was collected at 5, 10, 15, 20 turns of the impactor.

Impactor Validation

According to institutional animal care and use committee protocol, Adult New Zealand White rabbits ($n = 3$) were euthanized for reasons unrelated to this study. The hind limbs were removed, exposed areas covered with saline-soaked gauze, placed in a freezer bag, and stored in a -80°C freezer for several months prior to study. Hind limbs were thawed at room temperature and then placed in a machine vise to maintain $\sim 120^{\circ}$ flexion. The limb was dissected to expose the femoral condyle (Fig. 8-4). The central region of the medial and lateral, right femoral condyle received a Low Impact (10 turns of impactor) blow, whereas the left femoral condyle received a High Impact (20 turns of impactor) blow. Immediately after, india ink stain was applied to the impacted surface for gross observation.

Results

The results of calibration from 5, 10, 15, and 20 turns of the impactor are shown in Table 8-1. The average max stress from 5, 10, 15, and 20 turns of the impactor was 6.8 ± 0.97 , 9.9 ± 1.43 , 14.6 ± 1.24 , and 22.1 ± 1.83 MPa, respectively (Fig. 8-5). There was significantly greater stress from 20 turns vs. 15 turns ($p=0.002$) and 10 turns ($p=0.004$). Further, there was significantly greater stress from 15 turns vs. 10 turns ($p=0.017$).

Gross observation revealed that the Low and High Impact created a 2 mm diameter focal defect of the articular surface of each femoral condyle (Fig. 8-6). However, it

appeared that High Impact trauma created additional fissures migrating away from the primary defect that was not present with Low Impact.

Discussion

The 2 mm diameter impactor developed in this study appears to be a useful, device for creating focal defects of the articular surface. Additional biological outcome measures (i.e. cell viability, histology, scanning electron microscopy, etc.) would enable further validation of this device. Other groups have reported fabricating similar devices to create controlled, damage of articular cartilage.¹⁻³ Comparisons of these impactors including the ones presented in this dissertation are included in Table 8-2.

A few modifications to this impactor may improve accuracy and repeatability. First, an anchoring system would minimize rebound (energy loss) experienced while a user impacts an articular surface. Second, a more sophisticated crank mechanism to compress the spring would enable greater resolution of force applied than the current method (1 turn = 1 revolution of spring). Third, a hemi-spherical tip would mitigate edge effects of the impactor creating too much damage (i.e. fracture) of the articular cartilage.

It may be possible to use this device arthroscopically to create *in vivo*, focal defects of the distal femoral condyle in anesthetized animals. This would allow further assessment of local and systemic effects of cartilage injury and its progression to post-traumatic osteoarthritis for pre-clinical studies.



Figure 8-1. Arthroscopic impactor.



Figure 8-2. Pendulum device.

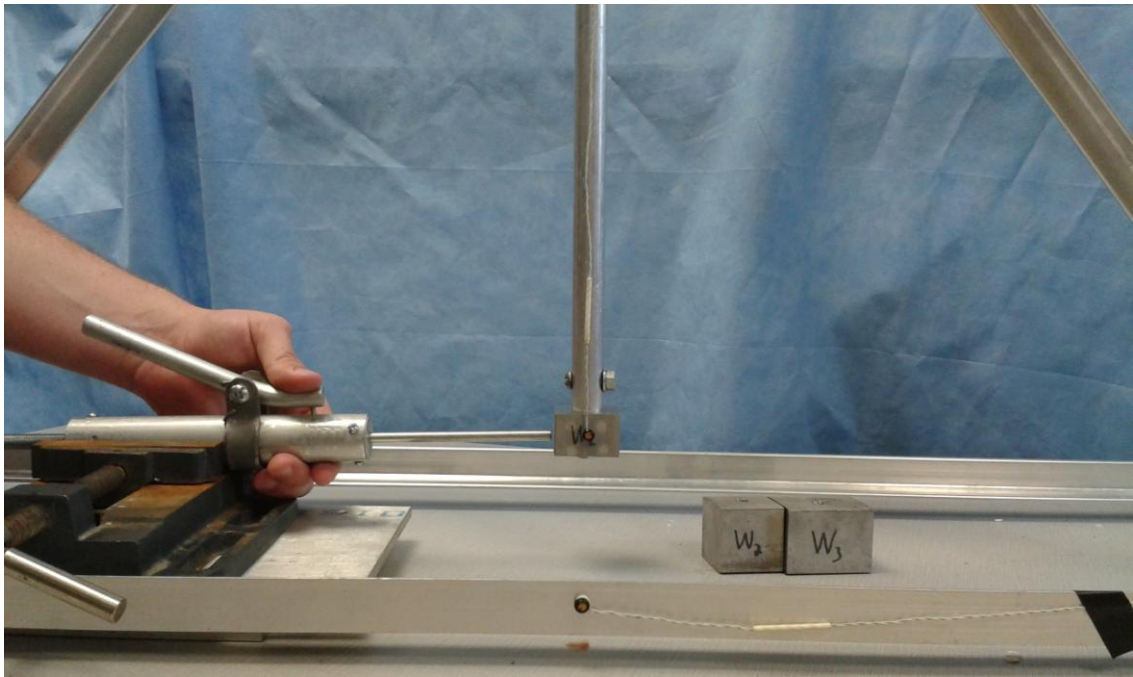


Figure 8-3. Impactor calibration.



Figure 8-4. Impactor placed upon the lateral femoral condyle prior to impact.

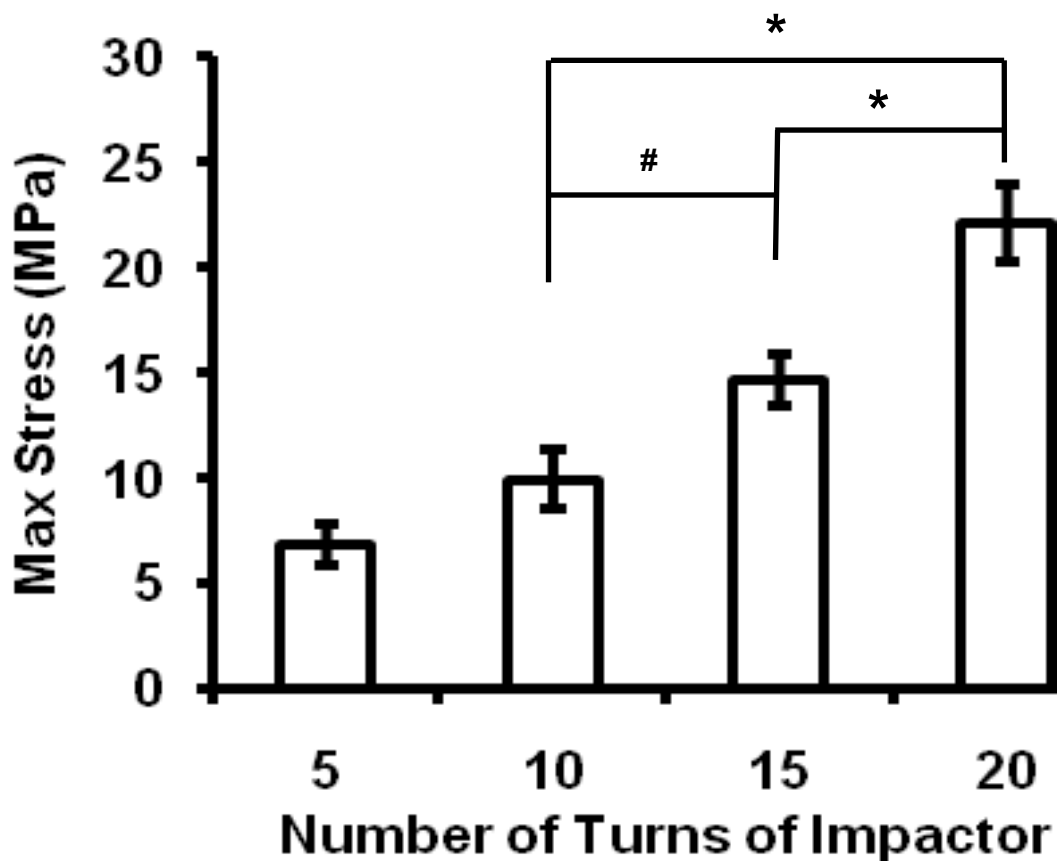


Figure 8-5. Maximum stress applied from 5, 10, 15, and 20 turns of the impactor. Statistical significance denoted by * $p < 0.001$, # $p < 0.01$.


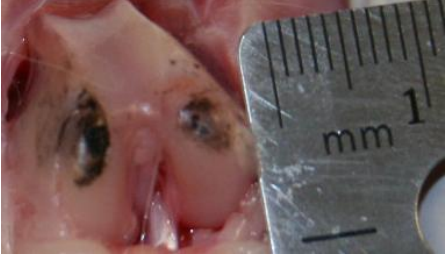
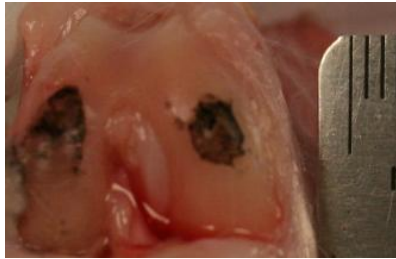
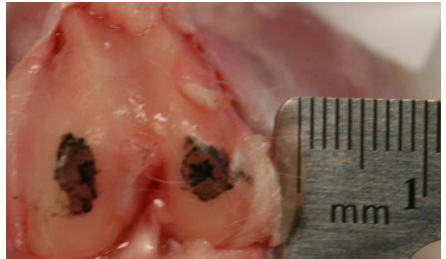

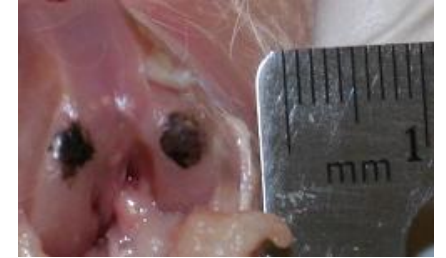
Rabbit	Low Impact	High Impact
1		
2		
3		

Figure 8-6. India ink staining of cadaveric rabbit femoral condyles (right knee = low impact, left knee = high impact).

Table 8-1. Calibration results from 5, 10, 15, and 20 turns of the impactor striking the weight at the end of the pendulum device.

#	Turns	Max Angle (rad)	Max Angle (deg)	Max Distance (mm)	Impact Velocity (mm/s)	ω (rad/s)	I (kg-m ²)	α (rad/s ²)	Force (N)	σ (MPa)
1	5	0.062	3.563	39.366	155.440	0.246	0.195	62.19	19.249	6.127
2	5	0.060	3.422	37.810	149.874	0.238	0.195	76.14	23.567	7.502
3	10	0.136	7.787	85.958	338.126	0.538	0.195	113.22	35.044	11.155
4	10	0.133	7.611	84.013	330.343	0.527	0.195	84.87	26.269	8.362
5	10	0.131	7.511	82.918	328.508	0.520	0.195	104.40	32.314	10.286
6	15	0.229	13.106	144.438	571.525	0.903	0.195	162.99	50.449	16.059
7	15	0.249	14.245	156.915	613.381	0.981	0.195	142.29	44.042	14.019
8	15	0.243	13.931	153.472	605.517	0.962	0.195	140.22	43.401	13.815
9	20	0.342	19.574	215.071	849.950	1.343	0.195	245.52	75.994	24.190
10	20	0.329	18.853	207.241	819.381	1.295	0.195	214.20	66.300	21.104
11	20	0.348	19.929	218.923	864.280	1.366	0.195	212.67	65.826	20.953

Table 8-2. Comparison of impactor devices used with various animal species, impact location, impactor type, and calibration developed for pre-clinical OA models.

Author	Species	Location	Impactor	Calibration
Bolam, 2006 ¹	Adult Equine <i>in vivo</i> N=10	Medial Femorotibial Joint: Medial Femoral Condyle (4 adjacent impacts) Medial Femoral Condyle (normal), Medial Tibial Plateau	Spring-loaded Circular tip (r=3.25mm) Impact stress = 60MPa	227.3-kg load cell connected to a computer equipped with data acquisition software (LabView) Acquisition rate of 5kHz
Leucht, 2012 ²	Adult Laprine <i>in situ</i> N=3, n=6	Medial and Lateral Femoral Condyles Right Femoral Condyle (1J "Low" Impact) Left Femoral Condyle (1.4J "High" Impact)	Spring-loaded Circular tip (r=1mm) Impact energy = 1J (Low) or 1.4J (High)	Mass = 0.5kg Spring stiffness = 0.49N/mm Spring distance = 40mm
Alexander, 2013 ³	Adult Bovine <i>in vitro</i> cartilage N=1, n=7?	Patellofemoral groove	Spring-loaded (5mm spring, 1mm compression/turn) Hemispherical tip (r=2.5mm) Impact stress = 7.7, 17.2, 27.6, 32.1, 36, or 40.1 MPa	Two (10-220lb) quartz force sensors connect to a computer equipped with data acquisition software (LabView) using a signal conditioner (200kHz) and AC/DC converter Pressure-sensitive film (impact area)
Chapter 7	Adult Canine <i>in situ</i> N=7	Humeral head	Spring-loaded Circular tip (r=4mm) Impact force = 150-200N	Cannister load cell
Chapter 8	Adult Laprine <i>cadaveric</i> N=3, n=12	Medial and Lateral Femoral Condyles Right Femoral Condyle (10MPa "Low" Impact) Left Femoral Condyle (20MPa "High" Impact)	Spring-loaded Circular tip (r=1mm) Impact stress = 10MPa (Low) or 20MPa (High)	Pendulum device with LEDs connected to a computer equipped with data acquisition software (Optotrak) Acquisition rate of 300Hz

Table 8-2 (continued). Comparison of impactor devices used at various time points, outcome measures, and results for pre-clinical OA models.

Author	Timepoints	Measures	Results
Bolam, 2006 ¹	Day 84 (n=5) Day 180 (n=5) Every 14 days (synovial fluid collected)	Radiographs, lameness, gross (India ink with ICRS and modified WORM), histo (modified Mankin and OARSI), cartilage GAG, modulus, synovial fluid GAG	↑cartilage loss and thinning (impacted cartilage) ↑COL2-3/4C _{short} (impacted cartilage) ↓sGAG (impacted cartilage)
Leucht, 2012 ²	Day 0 (immediately after impact)	Gross (India ink), radiographs, microCT, cell viability (Live/Dead), histo (Safarin O)	↑cell death, PG loss, fissuring (Low-High impact) ↑deep fissuring and shearing (High impact)
Alexander, 2013 ³	Day 1 (24 hours after impact)	Histo, cell viability, cartilage GAG media GAG, NO, PGE2 gene expression MMP1, MMP3, MMP9, MMP13, ADAM-TS5, COL2, AGG	↑NO (>7.7MPa), ↑cell death, GAG, PGE2 (>17MPa) Low Impact (17MPa) = ↑MMP13 gene, ↑MMP9 gene High Impact (36MPa) = ↑MMP3 gene, ↑MMP9 gene
Chapter 7	Day 0 (n=3), Day 12 (n=4) Day 1, 2, 3, 6, 9, 12 (media collected)	Gross, cell viability, cartilage GAG, HP, DNA, media GAG, PGE2, NO	↑impacted area
Chapter 8	Day 0 (n=12)	Gross	↑impacted area (High vs. Low)

Table 8-2 (continued). Comparison of advantages and disadvantages of impactor devices for pre-clinical OA models.

Author	Pros	Cons
Bolam, 2006 ¹	<ul style="list-style-type: none"> •Short- and long-term local and systemic effects of impact •Small amount of cartilage damaged (minor joint incongruity) 	<ul style="list-style-type: none"> •Some impact force was probably dissipated from movement during impact
Leucht, 2012 ²	<ul style="list-style-type: none"> •Sterilizable device that delivers an impact energy of 1J •Delivery of injury to lateral or medial femoral condyle •Does NOT induce bleeding or stimulation of BMSCs 	<ul style="list-style-type: none"> •Nonhomogenous cell death and matrix damage •Edge effects of impactor and use of K-wire fixation •Short-term analysis (Day 0 immediately after impact)
Alexander, 2013 ³	<ul style="list-style-type: none"> •100kHz load cell allows real-time measurement of force and duration of impact •Pressure-sensitive film allows direct measurement of impact load and maximum displacement 	<ul style="list-style-type: none"> •Short-term analysis (Day 1 or ~24 hours after impact) •No protein-level measurements of MMPs •Use of fixation device to constrain impactor
Chapter 7	<ul style="list-style-type: none"> •Sterilizable device that delivers an impact load of 150-200N 	<ul style="list-style-type: none"> •Did not create sufficient injury to result in significant differences between impacted and control tissue
Chapter 8	<ul style="list-style-type: none"> •Sterilizable device that delivers an impact load up to 20MPa 	<ul style="list-style-type: none"> •Rebound effects of impactor may result in energy loss •Spring-loaded based upon number of turns of handle •Circular tip may create too much damage at its peripheral edges

References

1. Bolam CJ, Hurtig MB, Cruz A, et al. Characterization of experimentally induced post-traumatic osteoarthritis in the medial femorotibial joint of horses. *Am J Vet Res.* 2006;67:433-447.
2. Leucht F, Durselen L, Hogrefe C, et al. Development of a new biomechanically defined single impact rabbit cartilage trauma model for in vivo-studies. *J Invest Surg.* 2012;25:235-241.
3. Alexander PG, Song Y, Taboas JM, et al. Development of a Spring-Loaded Impact Device to Deliver Injurious Mechanical Impacts to the Articular Cartilage Surface. *Cartilage.* 2013;4:52-62.

CONCLUSION

Osteoarthritis is a very complex, chronic disease. Since my parents have OA, I have seen how extraordinarily painful and debilitating the disease is. Further, I have had the opportunity to meet with hundreds of clinical patients with OA whom have shared their life stories about how the disease has affected their quality of life. It is quite easy for people to get trapped in the vicious cycle of OA where they can no longer do the activities they once loved or they no longer have the desire to do so.

Therefore, my main goal of this dissertation was to develop better research models for studying osteoarthritis. Like most major diseases, prevention is vital which is why I chose to focus on post-traumatic osteoarthritis (PTOA). By delivering a controlled, impact injury to cartilage and cartilage-bone, it was possible to measure various biomarkers released from and within these tissues.

Many significant findings were discovered through this dissertation work. Specifically, by using the proportional-integral-derivative (40, 0, 0) values, a large (25kN) servo-hydraulic materials test machine may be used to deliver a controlled impact injury to explants. Biomarkers glycosaminoglycan (GAG) and prostaglandin E₂ (PGE₂) were elevated after cartilage impact injury with PGE₂ having the highest mechanosensitivity than any other biomarker. Energy absorbed during cartilage-bone injury is dependent upon trauma severity; PGE₂ and monocyte attractant protein (MCP-1) were elevated following cartilage-bone injury. Dynamic, compressive loading to mimic walking conditions retained cell viability in non-impacted cartilage-bone explants and mitigated GAG release in impacted explants; GAG and PGE₂ were elevated due to

cartilage-bone injury whereas matrix metalloproteinase-2 (MMP-2) and interleukin-8 (IL-8) were elevated due to injury plus dynamic, compressive loading. The development of a 8mm diameter impactor does create articular cartilage damage, albeit a smaller, 2mm diameter impactor creates higher impact stresses and may be used arthroscopically for pre-clinical animal models.

Hopefully, this work will provide another step towards establishing a panel of “joint health” biomarkers that can be routinely monitored by primary care physicians especially for those with previous joint injury. Ultimately, this may encourage people to live a life that promotes better joint health.

APPENDIX

A. Thickness Measurement and Impact Protocol

The protocol for sequentially measuring thickness and impacting several specimens of cartilage with varying thicknesses, T_i , under laterally constrained conditions is as follows:

1. Load Instron 8821s BasLab software program for a desired velocity
i.e. $v_1 = 0.1$ to 100 mm/sec. (Version containing thickness measurement)
2. Place empty specimen anvil (with well facing upwards) into base support located on the test table of the Instron 8821.
3. Activate (by selecting “continue”) the first thickness measurement portion of the program to lower ram into bottom of anvil well until -10 N is detected and record this absolute ram base position, AP_b .
4. Manually raise ram to arbitrary position and place cartilage into well of anvil.
5. Activate the second thickness measurement portion of the program to lower ram towards cartilage surface until -10 N is detected and record this absolute ram position, AP_t .
6. Calculate cartilage thickness by using: $T_i = AP_t - AP_b$.
7. Determine the initial ram position, AP_i , by using equation 2-2 ($EP_1 = -2.25$ mm), overshoot T_o from Table 2, and the desired maximum strain ϵ :

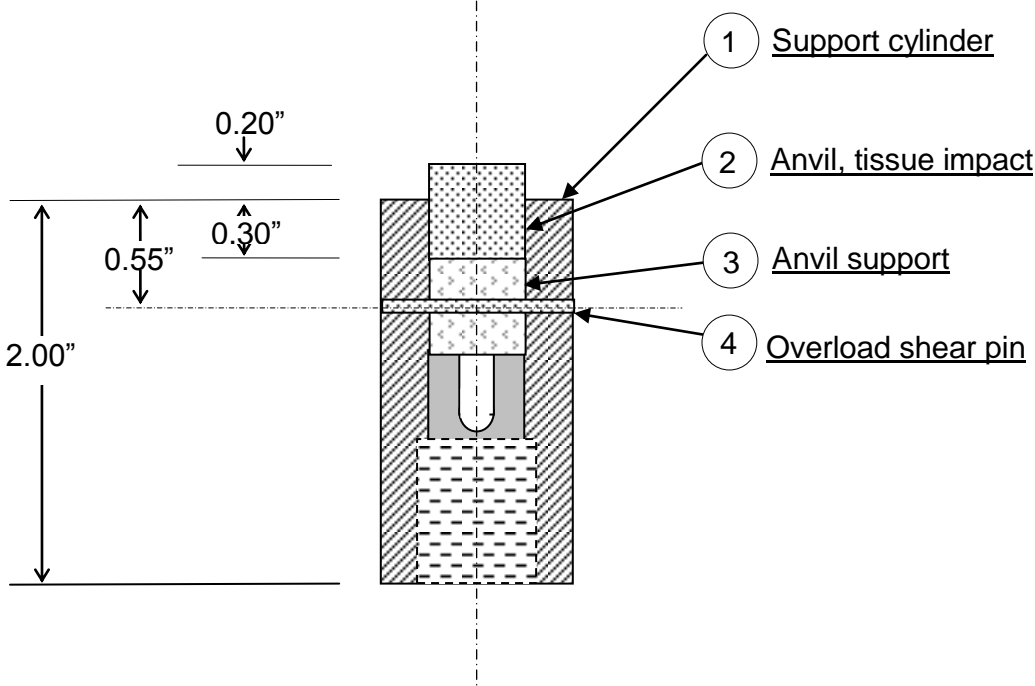
$$AP_i = AP_b + (1-\epsilon)T_i + T_o + |EP_1|$$

8. Use the Instron set point control or manually move ram to position, AP_i .

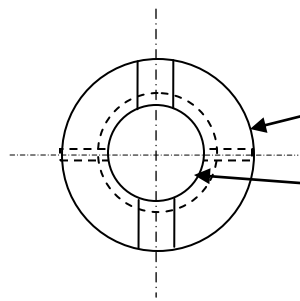
Note: If using the Instron set point control then the value of 0.02 should be added to AP_i to obtain the set point value, SAP_i to get Instron indicated ram position.

9. Run impact program.

B. Fixture Drawings

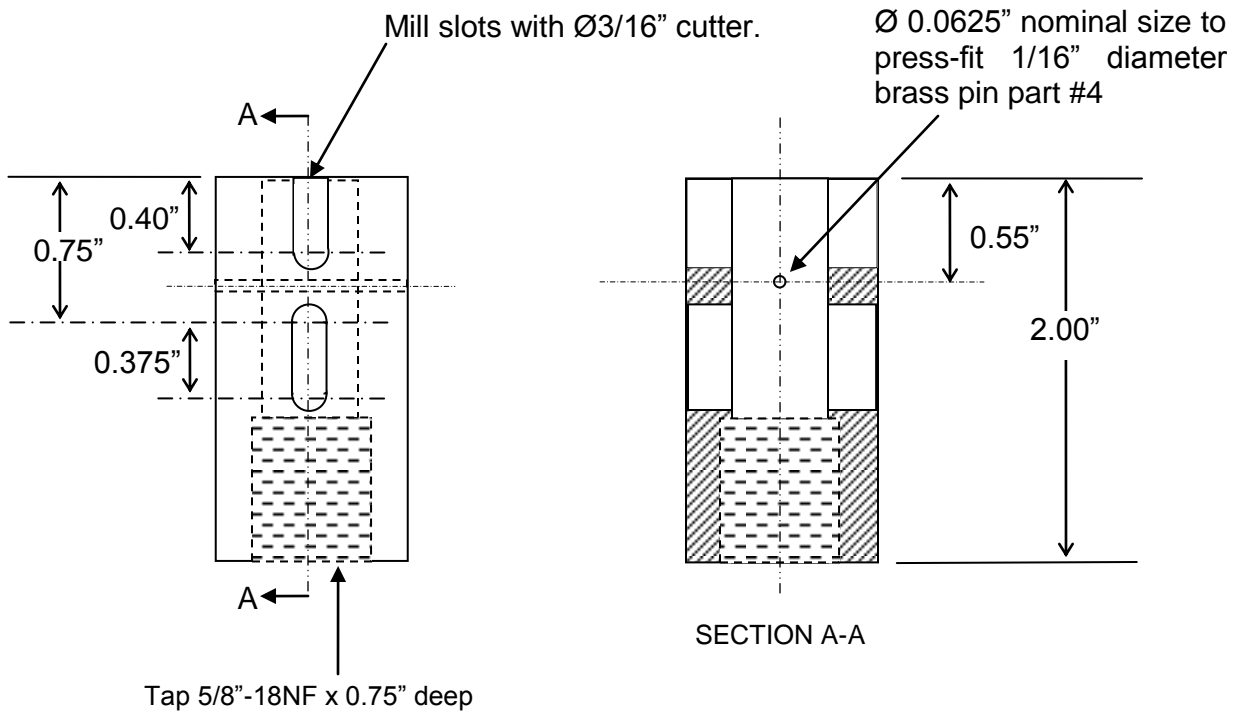


Anvil Support Assembly



1.00" nominal outer diameter to slip fit with minimal clearance into cylindrical recess in torsional base plate.

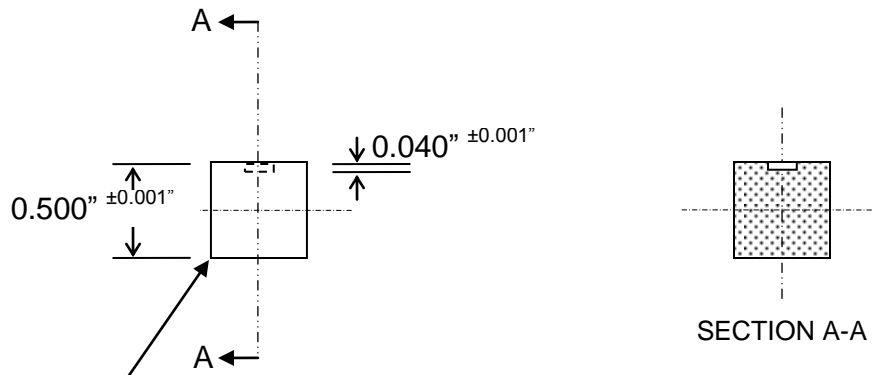
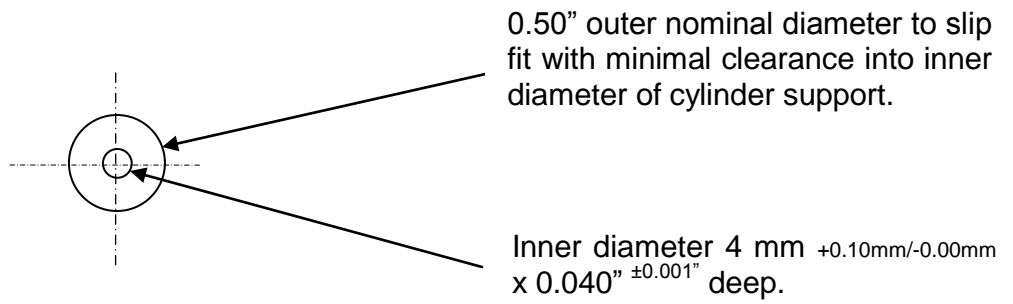
Drill-ream through 0.500" dia. +0.001"/-0.000"



Material: 1" diameter stainless steel x 2" long.

Quantity: 1

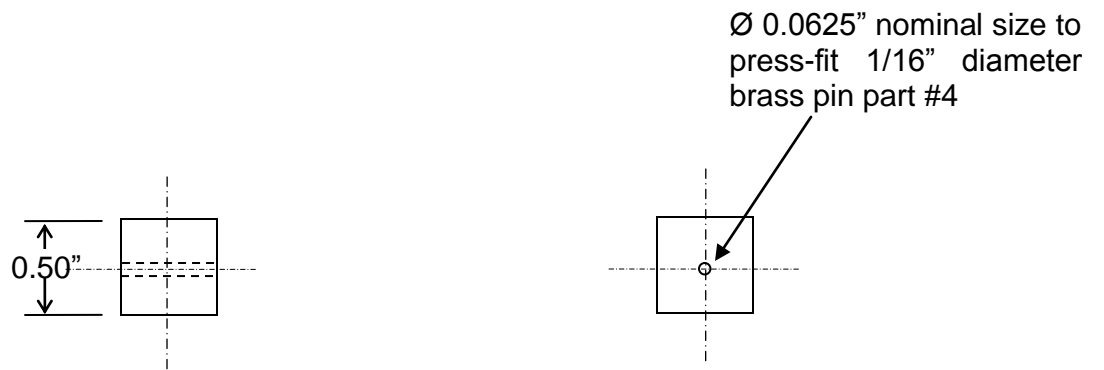
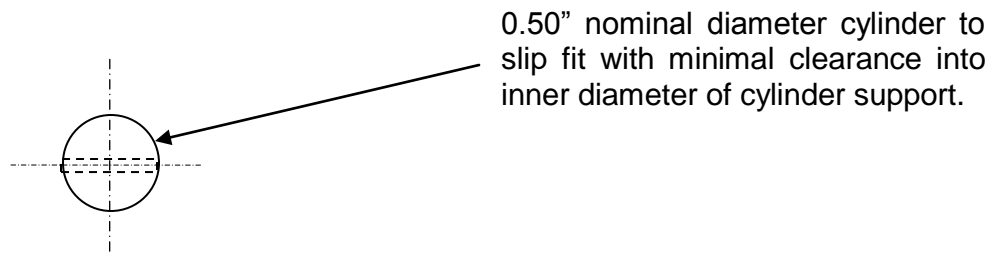
Part 1: Support Cylinder



Break both circumferences 0.025" $+0.010$ " -0.000 "

Material: 0.5" diameter stainless steel x 0.5" long.
 Quantity: 1

Part 2: Anvil, tissue impact

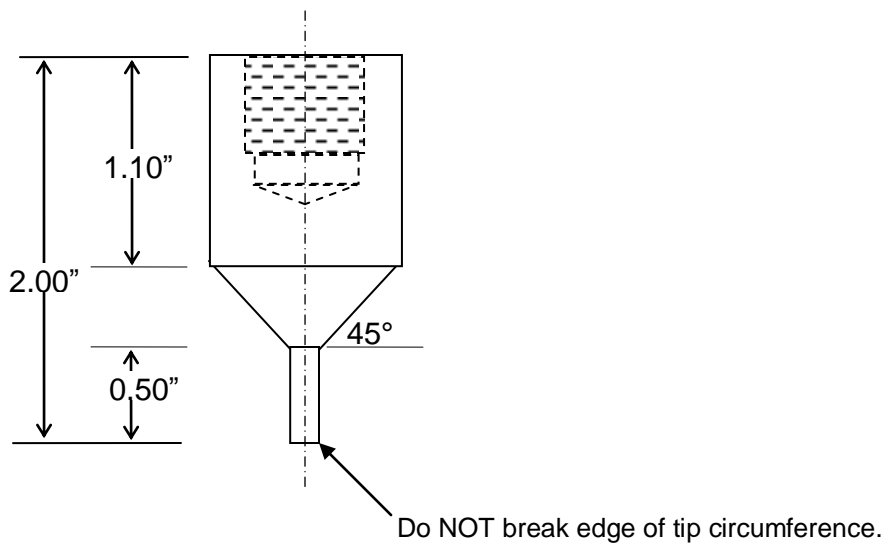
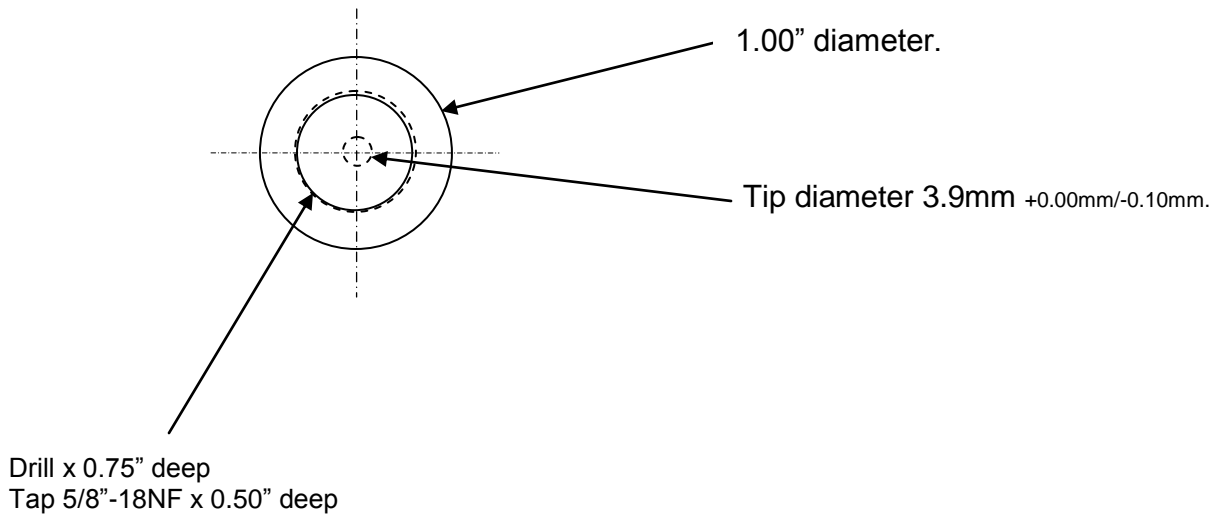


Material: 0.5" diameter stainless steel x 0.5" long.
Quantity: 1

Part 3: Anvil support

Material: McMaster Carr #97325A110 1/16" diameter brass pin x 1/2" long.
Quantity: Minimum of 25

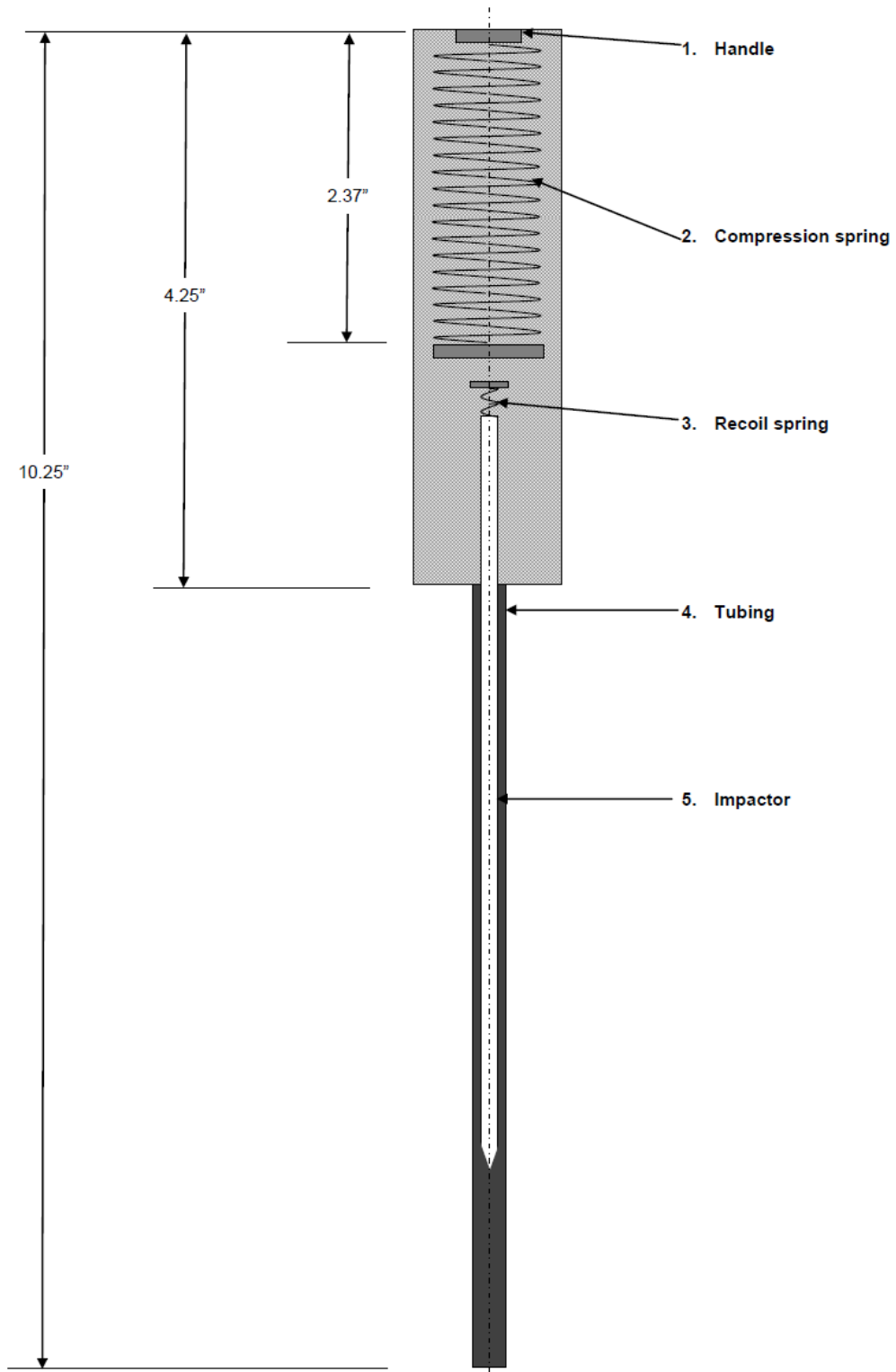
Part 4: Overload shear pin



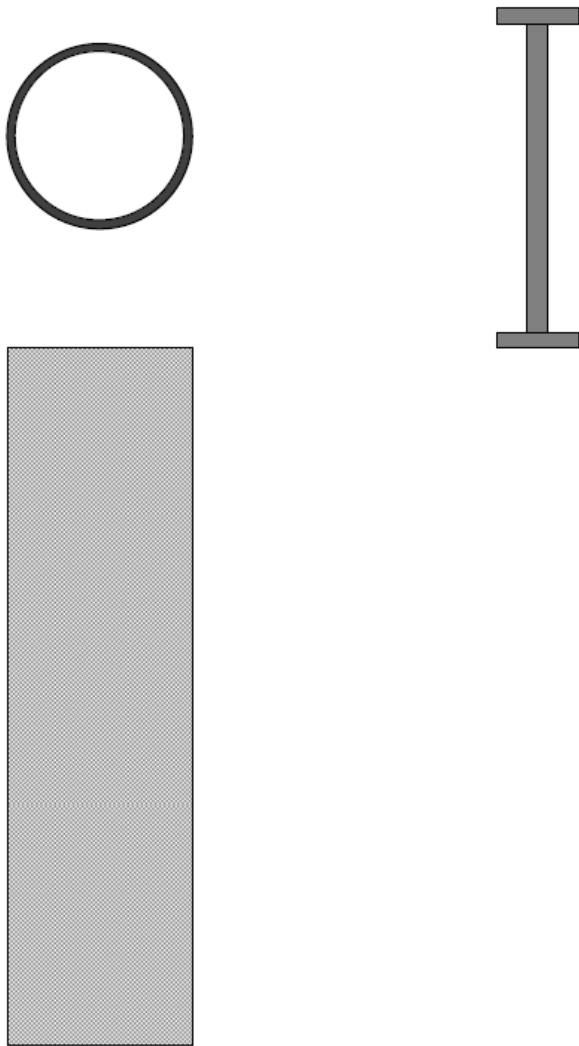
Material: 1" diameter stainless steel x 2" long.
Quantity: 1

Part 5: Impactor

C. Impactor Drawings



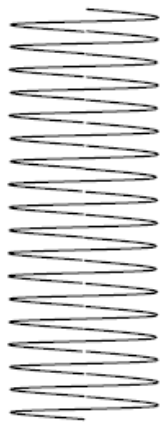
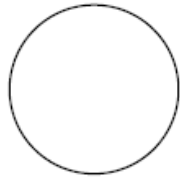
Impactor Drawing



Material: Aluminum tubing, 1.125" outer diameter, 1.027" inner diameter, x 4.25" long.

Quantity: 1

Part 1: Handle



Material: Stainless steel spring, 0.938" outer diameter x 4" long (Force_{max} = 153 lbf)

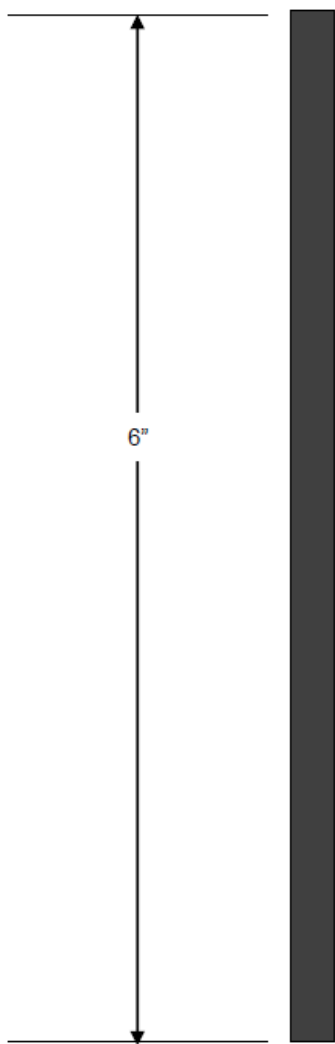
Quantity: 1

Part 2: Compression Spring

Material:

Quantity: 1

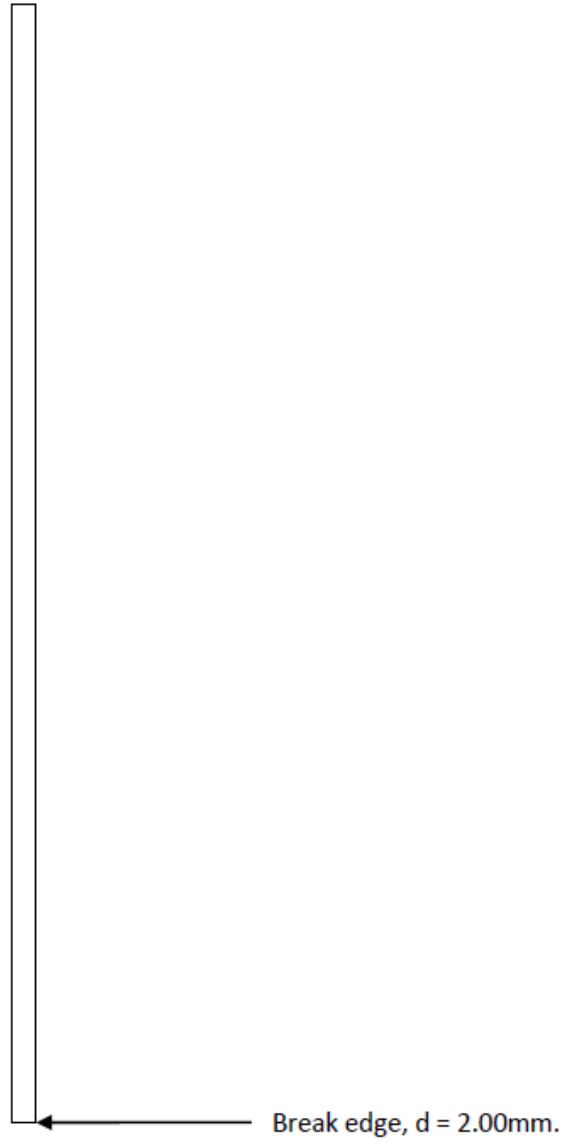
Part 3: Recoil Spring



Material: Stainless steel tubing, 0.25" outer diameter, 0.194" inner diameter, x 6" long

Quantity: 1

Part 4: Tubing

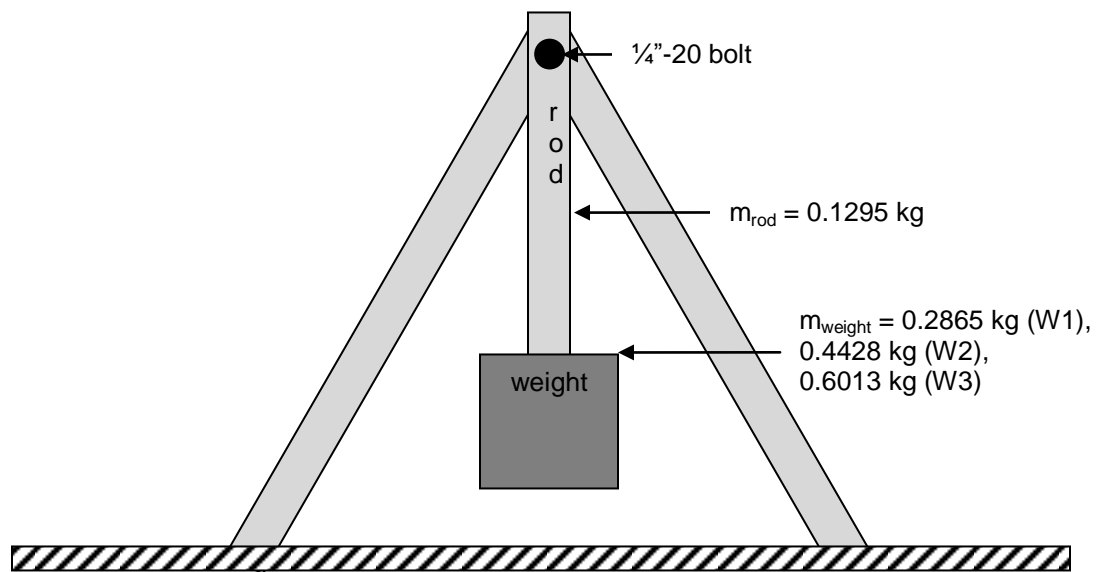


Material: Stainless steel rod, 0.125" diameter x 6" long

Quantity: 1

Part 5: Impactor

D. Pendulum Drawing



VITA

Nicole (Poythress) Waters was born May 1, 1984 in Atlanta, Georgia. She grew up the oldest of 5 children in rural, southeast Missouri. She has always been active in sports as well as performing arts in her community. After attending parochial grade school, she graduated second out of 370 students at Jackson High School in Jackson, Missouri (2002). She graduated *cum laude* with her Bachelor of Science in Biological Engineering from University of Missouri, Columbia, Missouri (2005). After completing a full-time internship as a Research Engineer at Smith & Nephew, Orthopaedics in Memphis, Tennessee (2006), she graduated with her Master of Science in Biological Engineering from University of Missouri, Columbia, Missouri (2009). Waters lives with her husband and children on their family farm in Fulton, Missouri. She hopes to pursue a career in rural, family medicine to improve the quality of life for people, especially those with or at-risk for osteoarthritis.